Supplementary table 1. Disorders that can present with bilateral basal ganglia abnormalities on MRI

3-HMG-COA LYASE DEFICIENCY
2-METHYL-3-HYDROXYBUTYRYL-COA DEHYDROGENASE DEFICIENCY
ACERULOPLASMINEMIA
ACUTE DISSEMINATED ENCEPHALOMYELITIS
ACUTE NECROTIZING ENCEPHALOPATHY
AFG3L2
ADAR1
ALEXANDER DISEASE
ALPHA MANNOSIDOSIS
AP4 DEFICIENCY
ASPARTYLGLUCOSAMINURIA (*AGA*)
AUTOIMMUNE BASAL GANGLIA ENCEPHALITIS
BETA KETOTHIOLASE DEFICIENCY
BETA PROPELLER PROTEIN ASSOCIATED NEURODEGENERATION
CANAVAN DISEASE
CARASAL
CARBON MONOXIDE POISONING
CERBROTENDINOUS XANTHOMATOSIS
CEREBRAL CREATINE DEFICIENCY SYNDROMES 1, 2, 3 (*SLC6A8, GAMT, AGAT*)
CHILDHOOD-ONSET-DYSTONIA-28
CHOLINE TRANSPORTER-LIKE 1 DEFICIENCY

(*SLC44A1*)

COCKAYNE SYNDROME TYPE A AND TYPE B (*ERCC8, ERCC6*)

CONGENITAL DISORDER OF GLYCOSYLATION, TYPE IIn (*SLC39A8*)

COPAN (*COASY*)

CRAT

CYANIDE POISONING

DNAJC19

EPHEDRONE / MANGANESE TOXICITY

ETHYLENE GLYCOL TOXICITY

FA2H ASSOCIATED NEURODEGENERATION

FUCOSIDOSIS

GANGLIOSIDOSES GM1 AND GM2

GIANT AXONAL NEUROPATHY

GLUTARIC ACIDURIA TYPE I

GTPBP2

HAEMOLYTIC URAEMIC SYNDROME

HYPERMANGANESEMIA WITH DYSTONIA 1 (*SLC30A10*)

HYPERMANGANESEMIA WITH DYSTONIA 2 (*SLC39A14*)

HYPOXIC ISCHAEMIC ENCEPHALOPATHY (TERM NEONATES)

IDIOPATHIC BASAL GANGLIA CALCIFICATION (FAHR'S DISEASE)

INFECTIOUS ENCEPHALITIS

ISOVALERIC ACIDEMIA (*IVD*)

JUVENILE HUNTINGTON'S DISEASE

KCNQ2

KEARNS SAYRE SYNDROME

KERNICTERUS

KRABBE DISEASE

KUFOR RAKEB SYNDROME (*ATP13A2*)

L-2-OH GLUTARIC ACIDURIA (*L2HGDH*)

LANGERHAN'S CELL HISTIOCYTOSIS

LEBER HEREDITARY OPTIC NEUROPATHY

MANGANESE TOXICITY

MAPLE SYRUP URINE DISEASE

MECR

3-METHYLGLUTACONIC ACIDURIA WITH SENSORI-NEURAL DEAFNESS , ENCEPHALOPATHY AND LEIGH -LIKE SYNDROME (MEGDEL)

METACHROMATIC LEUKODYSTROPHY

METHADONE TOXICITY

METHANOL TOXICITY

METHYLMALONIC ACIDEMIA

MITOCHONDRIAL COMPLEX 1 DEFICIENCY

MITOCHONDRIAL COMPLEX IV DEFICIENCY

MITOCHONDRIAL COMPLEX V DEFICIENCY

MITOCHONDRIAL MAINTAINENCE

MITOCHONDRIAL MEMBRANE PROTEIN ASSOCIATED NEURODEGENERATION

MITOCHONDRIAL THIAMINE TRANSPORTER

MITOCHONDRIAL TRANSLATION

MUCOLIPIDOSIS TYPE IV

MYELINOLYSIS

NEUROFERRITINOPATHY

NUP62

PANTOTHENATE KINASE ASSOCIATED NEURODEGENERATION

PDE8B

PDE10A

PLA2G6 ASSOCIATED NEURODEGENERATION

PRKRA

PROPIONIC ACIDEMIA

PYRUVATE DEHYDROGENASE COMPLEX DEFICIENCY

RAB39B

REPS1

SCP2

SQSTM1

SUCCINIC SEMIALDEHYDE DEHYDROGENASE DEFICIENCY

SULFITE OXIDASE AND MOLYBDENUM COFACTOR DEFICIENCY

THIAMINE RESPONSIVE BASAL GANGLIA DISEASE

TUBB4A

UFM1

VAC14

VIGABATRIN TOXICITY

VPS13A

VPS13D

WILSON'S DISEASE

WOODHOUSE SAKATI SYNDROME

Supplementary table 2. Definitions used for including patients in various diagnostic categories for BG MRI study

Group	Diagnostic Category	Definition for inclusion in the study#
Inflammation	ADEM	Patients who fulfilled criteria by Krupp et al. (Krupp *et al.*, 2007)
	ANE	"The specific neurologic presentation with bilateral symmetric thalamic, midbrain, and/or hindbrain lesions within days following acute viral illness caused by influenza A, influenza B, parainfluenza II, human herpesvirus 6 (HHV6), coxsackie virus, or an enterovirus"(Neilson, 2014)
	BGE	Presentation with acute encephalopathy, akinesia or dystonia, inflammatory findings on CSF## and the presence of anti-D2R antibodies and/or bilateral basal ganglia abnormalities on MRI(Dale *et al.*, 2012)
	Infectious encephalitis	Patients who fulfilled criteria by Granerod et al.(Granerod *et al.*, 2010) and had probable or confirmed encephalitis associated with an identified viral/bacterial agent
Injury	Hypoxic ischemic encephalopathy	Patients with a history of neonatal encephalopathy fulfilling American College of Obstetricians and Gynecologists' Task Force criteria for hypoxic ischaemic encephalopathy(Pediatrics, 2014)
	Kernicterus (Bilirubin toxicity)	Patients with a history of documented hyperbilirubinemia in the neonatal period associated with encephalopathy
	Osmotic myelinolysis	Patients with acutely evolving corticospinal and bulbar dysfunction associated with= electrolyte disturbances or rapid correction
	Vigabatrin toxicity	Acute encephalopathy associated with initiation of Vigabatrin in the preceding week(Wheless *et al.*, 2009)
Genetic – NBIA and NBIA-like disorders	BPAN	Patients with mutations in *WDR45* and a clinical syndrome with movement disorder and epilepsy(Saitsu *et al.*, 2013)

Group	Diagnostic Category	Definition for inclusion in the study#
	Fucosidosis	Patients with mutations in *FUCA1* or abnormally low alpha-L-fucosidase activity in fibroblasts (OMIM #230000)
	MPAN	Patients with mutations in *C19orf12*(OMIM #614298) (Hartig *et al.*, 2013)
	PKAN	Patients with mutations in *PANK2* (OMIM # 234200)
	PLAN	Patients with mutations In *PLA2G6* (OMIM # 256600)
	Manganese transport-*SLC30A10*	Patients with mutations in *SLC30A10* (OMIM #613280)
	Manganese transport-*SLC39A14*	Patients with mutations in *SLC39A14* (OMIM #608736)
	Wilson disease	Patients with mutations in *ATP7B* and supportive copper studies (OMIM #277900)
Genetic – Other disorders	ADAR1	Patients with mutations in *ADAR1* (OMIM #615010)
	Huntington's disease	Patients with diagnostic number of CAG trinucleotide repeat expansion in the Huntingtin gene (OMIM #143100)
	Hypomyelination with atrophy of the basal ganglia (TUBB4A)	Patients with mutations in *TUBB4A* (OMIM #602662)
Metabolic – Mitochondrial disorders	Kearns Sayre Syndrome	Progressive external ophthalmoplegia (PEO) and retinal dystrophy with onset before the age of 20, and in addition at least one of the following features: cardiac conduction defect, cerebellar dysfunction or elevated protein in CSF (>1 g/l)(Sofou *et al.*, 2013)
	MEGDEL	Patients with mutations in SERAC1 (OMIM #614739)
	PDHC	Patients with elevated blood and/or CSF lactate and pyruvate levels and mutations in one of the genes known to cause PDHC deficiency (See table 2.2 below)
	SLC19A3 (Biotin-Thiamine responsive basal ganglia disease)	Patients with mutations in *SLC19A3* (OMIM #607483)

Group	Diagnostic Category	Definition for inclusion in the study#
	Complex I deficiency	Patients with deficiency of mitochondrial complex I enzyme activity on muscle and or liver biopsy or demonstrated pathogenic mutation in one of the genes known to cause Complex I deficiency (See table 2.2 below)
	Complex IV deficiency	Patients with deficiency of mitochondrial complex IV enzyme activity on muscle and or liver biopsy mutation in one of the genes known to cause Complex IV deficiency (See table 2.2 below)
	Complex V deficiency	Patients with deficiency of mitochondrial complex V enzyme activity on muscle and or liver biopsy mutation in one of the genes known to cause Complex I deficiency (See table 2.2 below)
	Mitochondrial translation disorder	Patients with mutations in one of the genes know to cause a mitochondrial translation disorder (See table 2.2 below)
Metabolic – Non mitochondrial	Cockayne syndrome type B	Patients with mutations in *ERCC8* (OMIM #133540)
	Glutaric Aciduria type 1	Patients with confirmed deficiency of glutaryl-CoA dehydrogenase in fibroblasts or leucocytes and/or mutations in *GCDH* (OMIM #231670)
	Gangliosidoses	Patients with confirmed deficiency of beta galactosidase in fibroblast/leucocytes and/or mutations in *GLB1* (GM1 gangliosidosis) (OMIM #611458) Patients with confirmed deficiency of beta-hexosaminidase A in fibroblast/leucocytes and/or mutations in *HEXA* (Tay Sachs disease) (OMIM #606869) Patients with confirmed deficiency of beta-hexosaminidase B in fibroblast/leucocytes and/or mutations in *HEXB* (Sandhoff disease) (OMIM #606873)
	Krabbe disease	Patients with confirmed deficiency of galactocerebrosidase in fibroblast/leucocytes and/or mutations in *GALC* (OMIM #606890)
	Methylmalonic acidemia	Patients with isolated methylmalonic aciduria in urine and mutations in one of the genes known to cause methylmalonic acidemia (*MUT, MMAA, MMAB, MCEE, MMADHC*)(Manoli *et al.*, 2016)

Group	Diagnostic Category	Definition for inclusion in the study#
	Propionic acidemia	Patients with confirmed deficiency of propionyl-CoA carboxylase in fibroblasts/leucocytes and/or mutations in *PCCA* or *PCCB*(Baumgartner *et al.*, 2014)
	SSADH	Patients with confirmed deficiency of succinic semialdehyde dehyrdogenase in fibroblasts/leucocytes and/or mutations in *ALDH5A1* (OMIM #610045)

Abbreviations: BG – Basal ganglia, BPAN – beta propeller protein-associated neurogeneration, CoPAN-COASY protein-associated neurodegeneration, FAHN – Fatty acid hydroxylase–associated neurodegeneration, MPAN – Mitochondrial protein-associated neurodegeneration, NBIA – Neurodegeneration with brain iron accumulation, PKAN – Pantothenate kinase associated neurodegeneration, PLAN – PLA2G6 associated neurodegeneration, MRI – Magnetic resonance imaging MEGDEL – 3-methylglutaconic aciduria with sensori-neural deafness, encephalopathy, and Leigh-like syndrome, PDHC – pyruvate dehydrogenase complex deficiency, SSADH - Succinic semialdehyde dehydrogenase deficiency.

Supplementary Table 2.1 -Genes associated with selected mitochondrial biochemical subgroups used for definitions

Biochemical deficiency	Genotypic association
Pyruvate dehydrogenase complex deficiency	*Primary - DLAT, DLD, MPC1, PC, PDHA1, PDHB, PDHX, PDK3, PDP1, PDPR* *Secondary -LIPT1, LIAS, TPK1, SLC19A3, SLC25A19*
Complex I subunits and assembly factors	*NDUFA1, NDUFA2, NDUFA6, NDUFA9, NDUFA10, NDUFA11, NDUFA12, NDUFA13 NDUFB3, NDUFB8, NDUFB9, NDUFB10, NDUFB11, NDUFS1, NDUFS2, NDUFS3, NDUFS4, NDUFS6, NDUFS7, NDUFS8, NDUFV1, NDUFV2, NDUFAF1, NDUFAF2, NDUFAF3, NDUFAF4, NDUFAF5, NDUFAF6, NDUFAF7, NDUFAF8, ACAD9, ECSIT, FOXRED1, NUBPL, TIMMDC1, TMEM126B, MT-ND1, MT-ND2, MT-ND3, MT-ND4, MT-ND4L, MT-ND5, MT-ND6*
Complex IV subunits and associated factors	*COX4I1, COX4I2, COX5A, COX6A1, COX6B1, COX7B, COX8A, NDUFA4, SURF1, SCO1, SCO2, COX10, COX15, COA3, COA5, COA6, COA7, COX14, COX20, FASTKD2, PET100, PET117, CEP89, MT-CO1, MT-CO2, MT-CO3*
Complex V subunits and associated factors	*ATP5A1, ATP5D, ATP5E, ATPAF2, TMEM70,*

	USMG5, MT-ATP6, MT-ATP8
Mitochondrial translation (tRNA)	*MT-TA, MT-TC, MT-TD, MT-TD, MT-TE, MT-TF, MT-TG, MT-TH, MT-TI, MT-TK, MT-TL1, MT-TL2, MT-TM, MT-TN, MT-TP, MT-TQ, MT-TR, MT-TS, MT-TT, MT-TV, MT-TW, MT-TY*
Mitochondrial translation (aminoacyl-tRNA synthetases)	*AARS2, CARS2, DARS, DARS2, EARS2, FARS2, GARS, HARS2, IARS, IARS2, KARS, LARS, LARS2, MARS2, NARS2, PARS2, QARS, RARS2, SARS2, TARS2, VARS2, WARS2, YARS2*
Mitochondrial DNA maintainence Maintenance of mtDNA is under the control of many nuclear genes including those involved in mtDNA replication (*POLG, PEO1*) and dNTP synthesis (*POLG, PEO1, DGUOK, TK2, TP, RRM2B, SUCLA2, SUCLG1*)	*FBXL4, POL-G, SUCLA2, SUCLG1*
Other mitochondrial	*SERAC1, HIBCH*, ECHS1*, BTD*

For a more comprehensive list see Lake et al. 2016; Rahman et al. 2018

*Can lead to combined oxidative phosphorylation +/- PDHC deficiency.

References for Supplementary table 2 and 2.1

Baumgartner MR, Hörster F, Dionisi-Vici C, Haliloglu G, Karall D, Chapman KA, et al. Proposed guidelines for the diagnosis and management of methylmalonic and propionic acidemia. Orphanet journal of rare diseases 2014; 9(1): 130.

Dale RC, Merheb V, Pillai S, Wang D, Cantrill L, Murphy TK, et al. Antibodies to surface dopamine-2 receptor in autoimmune movement and psychiatric disorders. Brain 2012; 135(Pt 11): 3453-68.

Granerod J, Cunningham R, Zuckerman M, Mutton K, Davies NW, Walsh AL, et al. Causality in acute encephalitis: defining aetiologies. Epidemiology and infection 2010; 138(6): 783-800.

Hartig M, Prokisch H, Meitinger T, Klopstock T. Mitochondrial membrane protein-associated neurodegeneration (MPAN). Int Rev Neurobiol 2013; 110: 73-84.

Krupp LB, Banwell B, Tenembaum S, International Pediatric MSSG. Consensus definitions proposed for pediatric multiple sclerosis and related disorders. Neurology 2007; 68(16 Suppl 2): S7-12.

Lake NJ, Compton AG, Rahman S, Thorburn DR. Leigh syndrome: One disorder, more than 75 monogenic causes. Ann Neurol 2016; 79(2): 190-203.

Landis JR, Koch GG. The measurement of observer agreement for categorical data. Biometrics 1977; 33(1): 159-74.

Manoli I, Sloan JL, Venditti CP. Isolated methylmalonic acidemia. 2016.

Neilson D. Susceptibility to Infection-Induced Acute Encephalopathy 3. 2014.

Pediatrics AAo. Neonatal Encephalopathy and Neurologic Outcome, Second EditionReport of the American College of Obstetricians and Gynecologists' Task Force on Neonatal Encephalopathy. Pediatrics 2014; 133(5): e1482-e8.

Rahman J, Rahman S. Mitochondrial medicine in the omics era. The Lancet. 2018 Jun 23;391(10139):2560-74.

Saitsu H, Nishimura T, Muramatsu K, Kodera H, Kumada S, Sugai K, et al. De novo mutations in the autophagy gene WDR45 cause static encephalopathy of childhood with neurodegeneration in adulthood. Nat Genet 2013; 45(4): 445-9, 9e1.

Sofou K, Steneryd K, Wiklund LM, Tulinius M, Darin N. MRI of the brain in childhood-onset mitochondrial disorders with central nervous system involvement. Mitochondrion 2013; 13(4): 364-71.

Wheless JW, Carmant L, Bebin M, Conry JA, Chiron C, Elterman RD, et al. Magnetic resonance imaging abnormalities associated with vigabatrin in patients with epilepsy. Epilepsia 2009; 50(2): 195-205.

Supplementary Table 2.2 –Genes associated with mitochondrial biochemical subgroups and methylmalonic acidaemia for patients included in this study

Biochemical grouping	Gene association	n
Complex I deficiency	*NDUFS4*	2/5
	MT-ND1	1/5
	MT-ND5	1/5
	unknown	1/5
Complex IV deficiency	*MT-CO1*	1
	MT-CO2	1
	SURF1	2
Complex V deficiency	*MT-ATP6*	5/8
	unknown	3/8
Mitochondrial translation	*MT-TL1*	1/1
Pyruvate dehydrogenase complex deficiency	*PDHA1*	2/6
	PDHX	2/6
	*ECHS1**	1/6
	unknown	1/6
Methylmalonic acidaemia	*MMAA*	2/6
	MMAB	1/6
	TCN2	1/6
	MMACHC	2/6

*****ECHS1 does not primarily cause pyruvate dehydrogenase complex deficiency. This is sometimes seen as a secondary effect, that maybe combined with other markers of oxidative phosphorylation deficiency in many patients. This patient had isolated and marked pyruvate dehydrogenase complex deficiency on tissue enzymatic analysis

Supplementary table 3. MRI Rating Proforma

Patient Code	DOB	Date of Scan/Age	1.5/3 T	Scan No.	GA	Diagnosis	Onset

DEEP GREY MATTER MRI CHANGES:

	GROSS APPEARANCE			T2/FLAIR☐			DWI☐			T2*☐		T1☐			POST GAD☐	
	Hypoplasia/ Atrophy	Cystic	Swelling	Hyper intense	Hypo intense	Symmetry(S/A)	Bo hypointense	Restricted	Symmetry(S/A)	Hypointense	Symmetry (S/A)	Hyper intense	Hypo intense	Symmetry(S/A)	Enhancing	Symmetr (S/A)
Caudate h/b/t																
Putamen ant/post																
GP (int/ext)																
SN																
STN																
Thalamus ○ Dorsolat ○ Ventromed																

Functional pathways	
	**Comments**

EXTRA STRIATAL MRI CHANGES:

	GROSS APPEARANCE			T2/FLAIR☐			DWI☐			T2*☐		T1☐			POST GAD☐	
	Hypoplasia/ Atrophy	Cystic	Swelling	Hyper intense	Hypo intense	Symmet (S/A)	Hyper intense	Hypo intense	Symmet (S/A)	Hypo intense	Symmetr (S/A)	Bo hypo	Restricted	Symmetr (S/A)	Enhancing	Symmetr (S/A)
GM ○ Frontal ○ Parietal ○ Temporal																

○ Occipital ○ Global																
WM ○ Periventricular ○ Subcortical ○ Paraventricular ○ int caps ○ Ext caps																
Midline structure ○ Callosum ○ Fornix A/P ○ Commissure A/P																
Cerebellum ○ GM ○ Dentate ○ WM ○ Vermis ○ Hemisphere ○ Global ○ SCP ○ MCP ○ ICP																
Brainstem ○ MB ○ Dorsal ○ Ventral ○ Periaqueductal ○ Red nucleus ○ Pons ○ Dorsal ○ Ventral ○ Medulla ○ Dorsal ○ Ventral																

Ventricles	

Hypothalamus **Nucleus accumbens**	
Myelin abnormalities	
Comments	

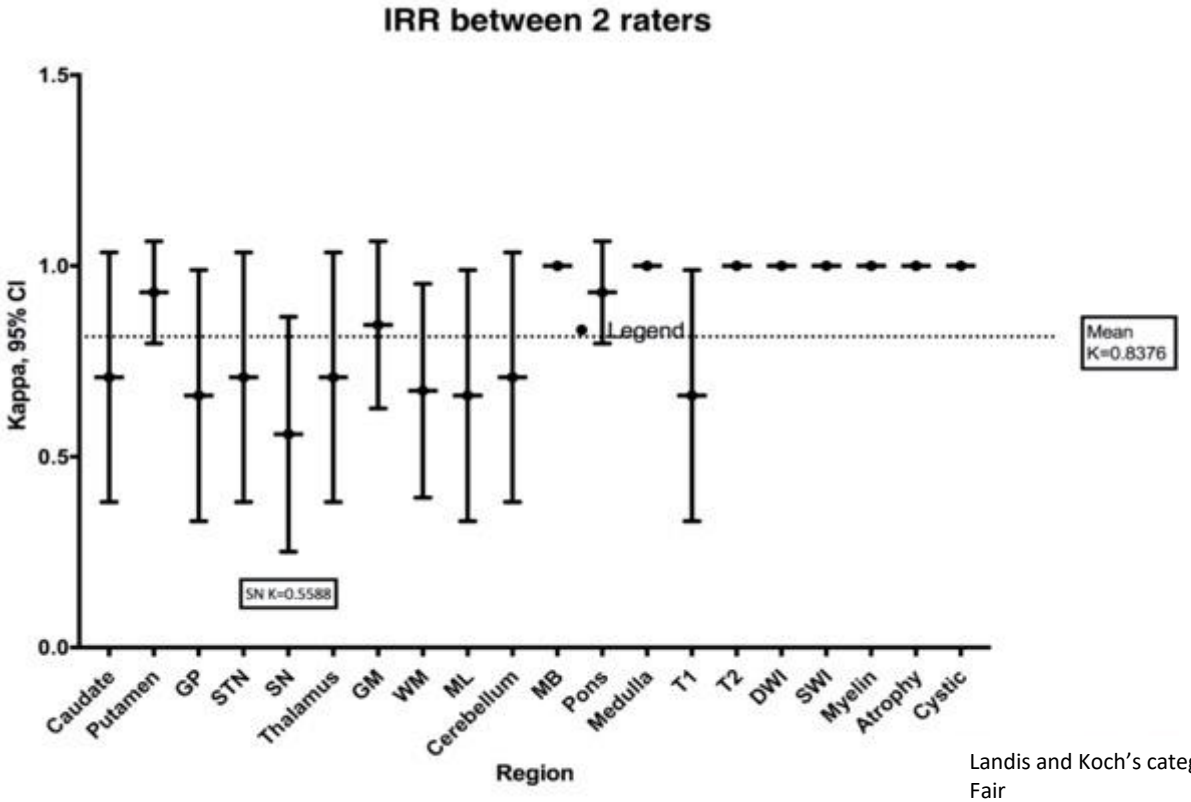

Landis and Koch's category[363]	Kappa value
Fair	0.21-0.40
Moderate	0.41-0.60
Substantial	0.61-0.80
Almost perfect	0.81-1

Supplementary figure 1a: Inter rater reliability (IRR) depicted by Fleiss' Kappa values between two blinded raters who independently analysed a random sample of 30 complete anonymised MRI datasets. Mean Kappa is depicted by the dotted line = 0.8376 (almost perfect(Landis and Koch, 1977)). The box and whiskers plots represent mean kappa for each brain region rated and the whiskers represent 95% confidence intervals. The lowest kappa value was for the substantia nigra (SN, K=0.5588, moderate)

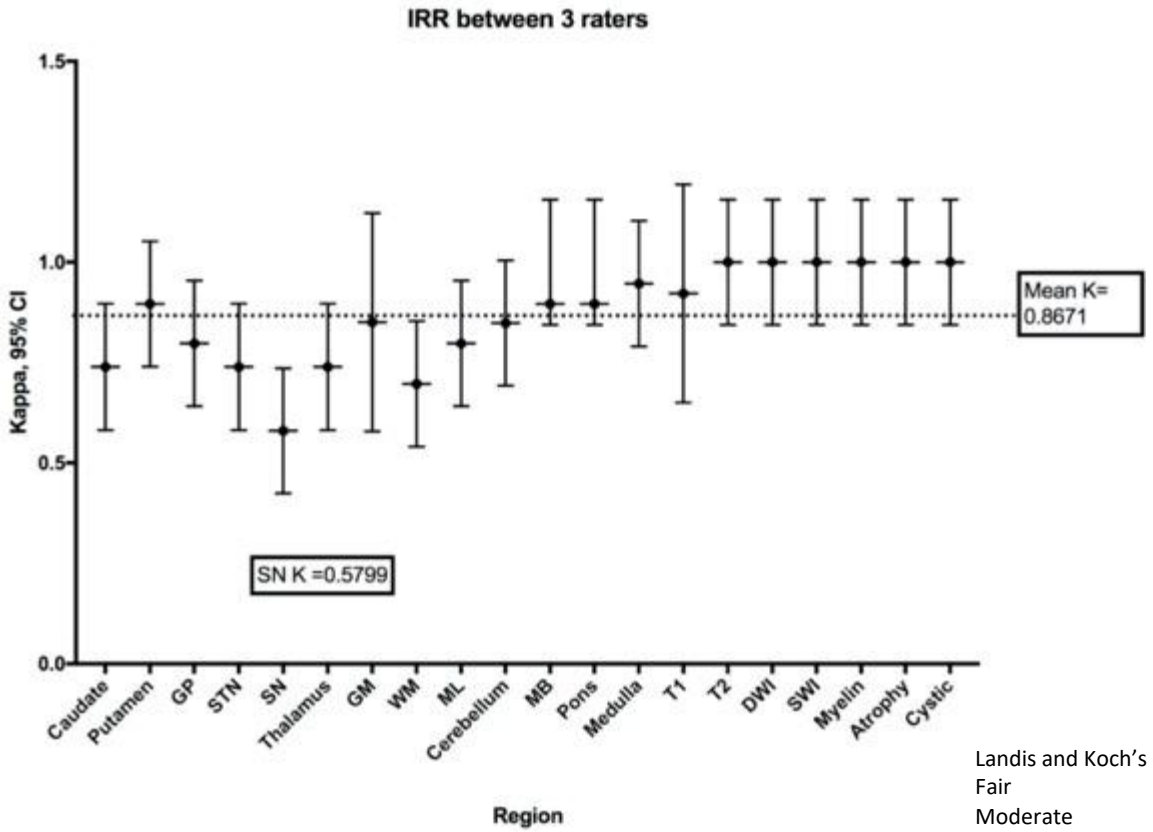

Landis and Koch's category[363]	Kappa value
Fair	0.21-0.40
Moderate	0.41-0.60
Substantial	0.61-0.80
Almost perfect	0.81-1

Supplementary figure 1b: Inter rater reliability (IRR) depicted by Fleiss' Kappa values between three raters (2 blinded raters who independently analysed a random sample of 30 complete anonymised MRI datasets) and rating done by me and Kling Chong for same MRI datasets. Mean Kappa is

depicted by the dotted line = 0.8671 (almost perfect(Landis and Koch, 1977)). The box and whiskers plots represent mean kappa for each brain region rated and the whiskers represent 95% confidence intervals. The lowest kappa value was for the substantia nigra (SN, K=0.5799, moderate)

Supplementary section 1: Cluster analysis

A spreadsheet was generated based on MRI abnormalities of any kind seen in different anatomical regions as well as MRI datasets showing abnormalities. Data for each patient was maintained in a separate row and diagnostic categories were retained against each patient's data. Columns were labelled as follows for any MRI changes noted in the respective brain regions - Caudate, Putamen, GP, StriatumOnly (where the striatal nuclei were the only basal ganglia nuclei showing any abnormality; other brain regions could be abnormal), GPonly (where the GP were the only basal ganglia nuclei showing any abnormality; other brain regions could be abnormal), SN and STN. Further columns were coded to represent any abnormalities, including atrophy or hypoplasia without signal change in the Thalamus, GM, WM, Pituitary, cc (corpus callosum), Cerebellum, MB, Pons, Medulla, Hypothalamus. Hypomyelination was coded as separate column (immature myelination and hypomyelination were combined to represent abnormal scoring in either column). The last four columns represented abnormalities noted on datasets - T1Hyper (hyperintensity on T1W imaging in any brain region), bgt1bright (hyperintensity on T1W imaging in any basal ganglia nucleus), nonBGt1bright (hyperintensity on T1W imaging in any non-basal ganglia region), Suscept (abnormal hypointensity noted on any sequence capturing susceptibility – eg. SWI, SWAN, T2*; Diffusion B0 images were used in some scans where specific susceptibility datasets were not available) and DiffRest (diffusion restriction). These made up 23 columns representing MRI features derived from the raw coding done as part of the study. As 149/201 (74%) patients had T2W hyperintensities noted in the basal ganglia and other brain regions, T2W hyperintensity was not included as one of the MRI features to generate clusters.

As described in the methods, ten different algorithms – Euclidean ward, Euclidean average, Euclidean complete, Euclidean weighted, Euclidean gaverage, Manhattan ward, Manhattan

average, Manhattan complete, Manhattan weighted and Manhattan gaverage were used to generate from 2 to 8 clusters.

Using the R package (https://www.jstatsoft.org/article/view/v061i06) the best number of clusters was determined to be 4.

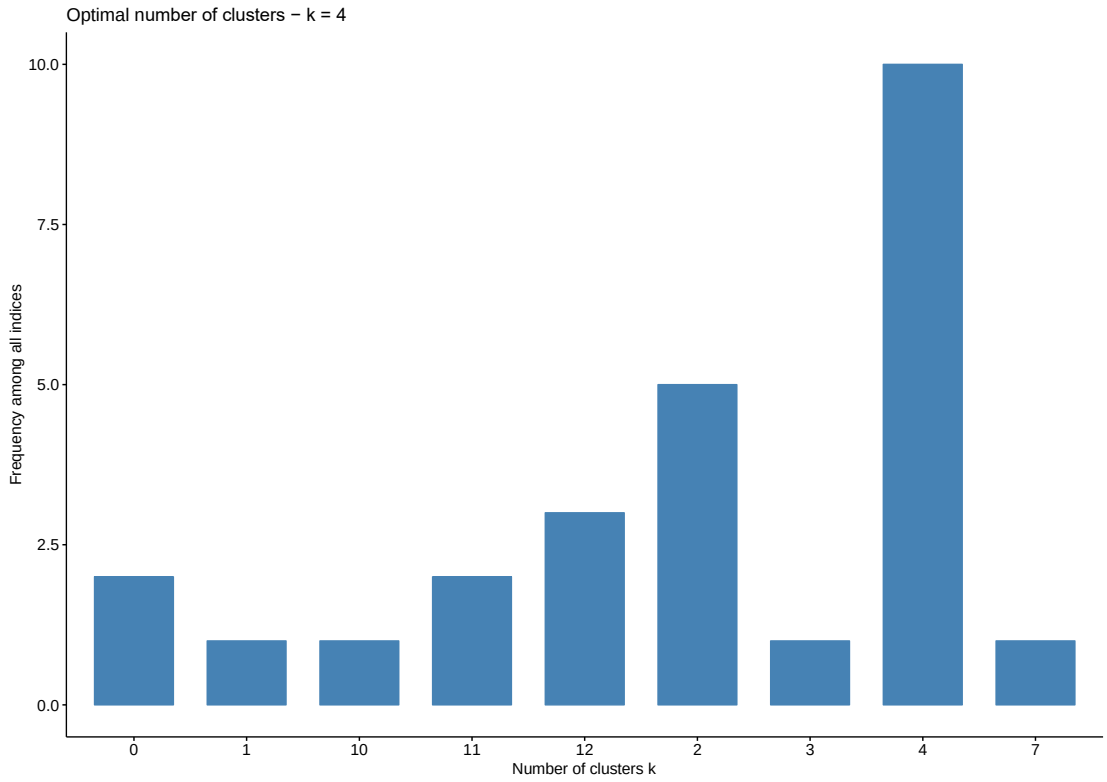

Supplementary figure 2. Bar plot showing frequency of cluster validity indices' agreement for optimal number of clusters

Supplementary section 2: Algorithm generation

The algorithm was developed around the features that generated 4 clusters using the Euclidean average methodology. MRI features were first compared using chi-square tests using SPSS v20.0.0. in the 4 cluster Euclidean average cluster plots. The main MRI features differentiating the clusters were striatal MRI abnormalities -mainly T2W hyperintensity(Cluster 1), GP T2W hyperintensity, mainly involving only the GP and not the

striatum (Cluster 2), susceptibility in the GP, sometimes with hypomyelination and thalamic T2W hypointensities (Cluster 2), GP T2W hyperintensity and diffusion restriction with brainstem, cerebellum abnormalities (Cluster 3) and diffuse T1W hyperintensities in the basal ganglia (Cluster 4). Thus**,** the entire cohort clustered into separate clusters based on either the anatomical distribution of abnormalities on MRI in different brain regions or based on the pattern of abnormalities – eg. T1W hyperintensity or Susceptibility. The cluster of patients with T1W hyperintensity clustered separately across various cluster plots and was retained as one of the branches in the first step of the algorithm. The remainder of the cohort could have other patterns of changes – T2W hyper or hypointensity, Susceptibility or diffusion restriction. In clinical practice MRI datasets are usually reviewed in continuation, for example, first all regions of the brain are reviewed on a T2W dataset, then Diffusion and so on. Hence, susceptibility changes were moved to align with T1W hyperintensity and T2W hyperintensity as the first branch points in the algorithm, even though, in cluster analysis they grouped together with T2W hyperintensity in the GP in cluster 2. Overlapping changes on different MRI datasets (Eg. T1W hyperintensity and susceptibility) were seen in some patients but did not lead to separate clustering. These branches were added to the algorithm and are discussed in the results but do not form major end points of the algorithm. The major end points of the algorithm were determined based on the cluster analysis and further features identified in literature review. Most of these major end points were labelled with a capital alphabet (A,B, C. etc) to correspond to diagnostic categories listed under the same alphabetical group in Table 2. Diagnostic categories corresponding to some of the end points are described in the discussion and the reader is guided to the relevant section heading.

Supplementary section 3: Development of a decision-making application.

Literature review

A literature review was undertaken in Medline and EMBASE to identify conditions reported with bilateral basal ganglia MRI abnormalities. This was repeated to look for description of new disorders and new reports of bilateral basal ganglia abnormalities in established disorders and updated to include publications with available full text till 31st December, 2019.

Scoring

The presence or absence of 30 discrete MRI abnormalities was categorized for each of the 34 differential diagnoses included in the study as follows – "Always present" (abnormality seen in all included patients), "mostly present" (abnormality seen in >80% included patients), "present" (abnormality seen in some but <80% of included patient), "always absent" (abnormality not seen in any included patient). Data from literature review of diagnostic categories in this study was incorporated into the categorization. If a region or dataset was reported to show abnormalities in any included diagnostic category in a previous published report but not scored as abnormal in this study, the respective categorization was changed from "always absent" to "present". T2W hyperintensities in the basal ganglia or other brain regions were not listed separately but included in categorization of different brain regions as being normal or abnormal. Subsequently, other diagnostic categories (Supplementary table 1) from literature review, not included in this study were also incorporated into the database with each region/dataset reported to show abnormalities categorized as "mostly present" or "always absent". A category of "always present" was never assigned to diagnoses obtained from the literature due to the potential associated bias. The resulting categorization was used to build a standalone application using FileMaker Pro 16 Advanced™ (FileMaker, Inc), (downloadable from http://www.kidsneuroscience.org.au/resources-epilepsy as an iOS, PC or MacOS runtime solution). Instructions on use of this application are provided in the

appendices and with the application download. A clinical summary (see below) was incorporated in the application to provide context for decision making in each category. Example images were incorporated in the application for various diagnostic categories included in the study and reference links to some key papers were added for other diagnostic categories from literature review to direct readers to typical imaging examples. This pilot decision making application is based on results from this study and literature review and requires validation and should not be used for clinical decision making.

Filemaker application

INSTRUCTIONS ON USE OF THE FILEMAKER APPLICATION –

The user selects if specific MRI findings are present, absent or not assessed for any given patient scan and this data is compared to the coded categories for each diagnosis: If a particular MRI finding is present, but is "always absent" from a particular condition, then this potential diagnosis is excluded from the final list. Similarly, if an MRI finding is absent but should be "always present", then it is also excluded from the final differential list. The presence or absence of patient MRI findings are subsequently scored as summarized in table XX and this is repeated for each of the 30 MRI criteria. The accumulated score is used to rank the refined list of differential diagnoses in order of likelihood

Supplementary table 4: Scoring matrix for MRI criteria

Example of diagnostic criteria for a specific MRI variable	Resulting score if features are present on patient MRI	Resulting score if features are absent from patient MRI
Always present	4	Diagnosis excluded
Mostly present	3	2
Present	2	3
Always absent	Diagnosis excluded	4

Clinical summary of conditions included in this study (Table 6) and those included after literature review in the decision making application (References which are the latest update for clinical summary of the condition and those which include good example images of MRI abnormalities involving the basal ganglia in these conditions – Table 7 – are included after each disorder and all references reviewed to update the scoring are included in the table below)

Supplementary table 5: Clinical summaries of diagnostic categories with bilateral basal ganglia abnormalities. Example images are included from the study cohort, where available. Both the summaries and images are also part of the electronic decision making application that is available for download.

Diagnostic category (MIM)	Clinical description
3-HMG-COA LYASE DEFICIENCY	Most patients are symptomatic with metabolic crises consisting of non-ketotic hypoglycemia and hyperammonemia in the first year of life. Diagnostic clues can be obtained by urine organic acid testing. Many reports highlight the presence of multifocal areas of white matter T2W hyperintensity superimposed on more diffuse white matter and thalamic T2W hyperintensity. Some MRI changes in the white matter can revert with treatment. In some patients pallidal T2W hyperintensities are reported in some patients, with milder T2W hyperintensities in the striatum in fewer patients. In patients diagnosed late/those with previous crises, some imaging changes such as occipital grey matter T2W hyperintensities or atrophy can be due to episodes of characteristic non-ketotic hypoglycemia.

	Autosomal recessive inheritance. Gene: *HMGCL*
2-METHYL-3-HYDROXYBUTYRYL-COA DEHYDROGENASE DEFICIENCY	An X-linked defect of isoleucine degradation. Infantile-onset progressive disorder with retinopathy, cardiomyopathy and neurological manifestations such as intellectual disability, seizures and dystonia and chorea. Metabolic crisis with hypoglycaemia and elevated lactic acid in some patients. Tiglylglycine and 2-methyl-3-hydroxybutyrate are elevated in urine. T2W hyperintensities are reported in the putamen and grey matter along with cortical grey matter atrophy. Occipital grey matter T2W hyperintensities or atrophy can be due to episodes of characteristic non-ketotic hypoglycemia. X-linked recessive inheritance. Gene: *HADH2*
ACERULOPLASMINEMIA	Triad of neurological symptoms, retinal degeneration and diabetes mellitus. Clinical onset usually in adulthood. Neurological symptoms - ataxia, cranio-facial dyskinesias (torticollis, blepharospasm, facial grimacing and tongue dystonia), parkinsonism and dysarthria. Lab tests show extremely low or undetectable serum ceruloplasmin, elevated ferritin, low iron, and low serum copper but normal urinary copper. Susceptibility is noted in the striatum, globus pallidus, thalami, dentate nuclei. White matter T2W hyperintensity can be prominent. One of the few NBIA disorders where striatal susceptibility is commonly seen in addition to other regions of susceptibility Autosomal recessive inheritance. Gene: *CP*
ACUTE DISSEMINATED	The syndrome is defined when an altered conscious state is noted with brain and spine MRI findings of demyelination noticeably in

ENCEPHALOMYELITIS	the subcortical white matter. Basal ganglia abnormalities limited mainly to striatal T2-hyperintensities without diffusion restriction are reported in some patients (Figure 1) and these may have an asymmetric and somewhat tumefactive appearance in cases of anti-MOG antibody associated demyelination (Figure 2). 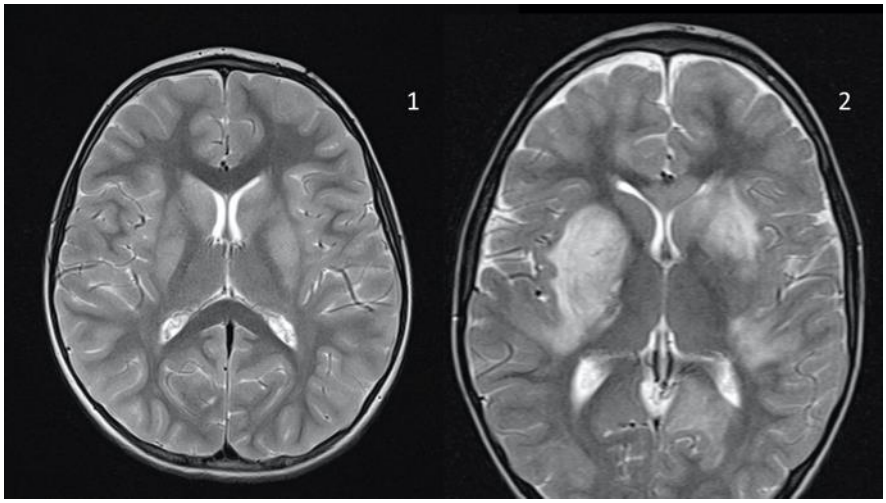
ACUTE NECROTIZING ENCEPHALOPATHY	This is an acute encephalopathy syndrome that manifests with bilateral symmetric thalamic, midbrain, and/or hindbrain abnormalties – T2 weighted hyperintensity and thalamic swelling (Figure 1). Varying diffusion restriction of involved structures may be seen in the acute stages (Figure 2). Patients present within days following acute viral illness caused by influenza A, influenza B, parainfluenza II, human herpesvirus 6 (HHV6), coxsackie virus, or an enterovirus. Some families may carry a dominantly inherited mutation in the gene that may predispose individuals to recurrences. Liver dysfunction and coagulopathy can be noted with the acute presentation. Autosomal dominant inheritance of vulnerability Gene: *RANBP2*

	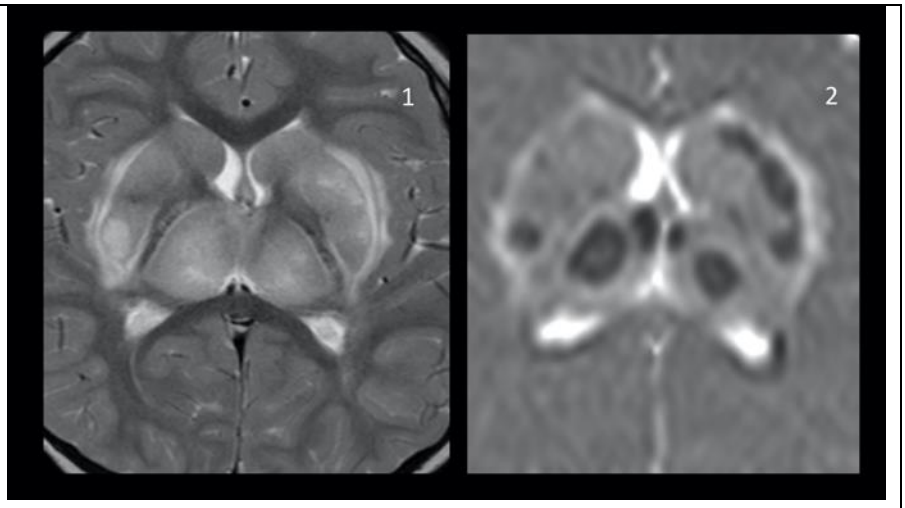
AFG3L2	Young adult-onset of cerebellar ataxia with nystagmus, progressive ophthalmoparesis and ptosis mimicking mitochondrial disease. MRI shows cerebellar atrophy prominently in the superior vermis. Homozygous mutations cause a severe phenotype, with infantile-onset epileptic encephalopathy, progressive microcephaly, increased lactate and early death. In these cases, MRI shows generalised atrophy with bilateral symmetrical T2W hyperintensities in the putamina. Progressive myoclonic epilepsy, dystonia, spasticity with neuropathy, ptosis and ataxia have been reported in homozygous mutations. Autosomal dominant inheritance. Gene: *AFG3L2*
ADAR1	Clinical presentations range from spastic paraparesis to episodic stagnation or regression of motor development. A high neopterin on cerebrospinal fluid and a typical signature on analysis of interferon-stimulated genes can help in diagnosis. On MRI symmetric and bilateral striatal T2W hyperintensities can be seen (Figure 1), sometimes with regions of partial sparing similar to mitochondrial disorders. The involved basal ganglia nuclei may demonstrate swelling in the acute stage, followed by atrophy with

	time (Figure 2). T1W hyperintensity or susceptibility in the putamen and pallidum can be noted in some cases, possibly representing regions of calcification. Susceptibility in the globus pallidus can appear symmetric and homogenous similar to other disorders with brain iron deposition. Other MRI changes described include T2W hyperintensity in the deep white matter (Figure 1) with global cortical atrophy (Figure 2). Autosomal dominant or recessive inheritance. Gene: *ADAR1* 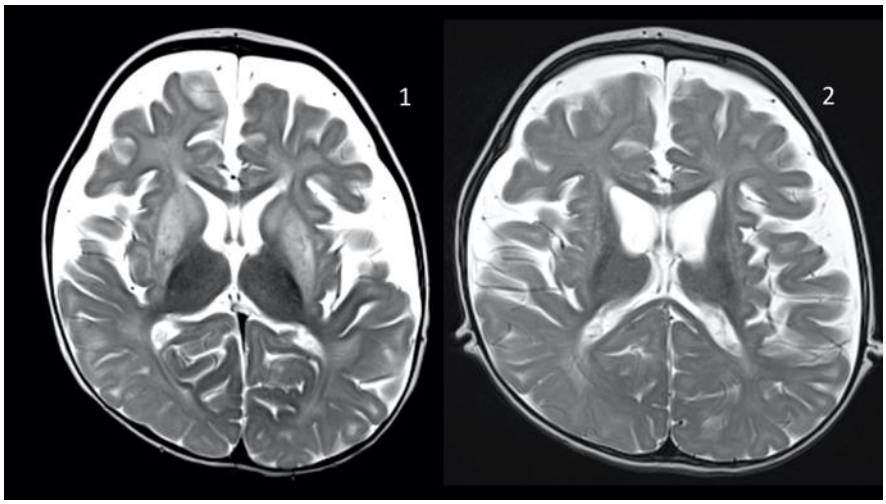
ALEXANDER DISEASE	Presentation with seizures, severe motor delay and regression, intellectual disability and megalencephaly. Usual onset in infancy though juvenile and adult-onset forms are described. Progressive white matter T2W hyperintensities are common findings on MRI. Optic chiasm hyperintensities and swelling are described in some patients. Contrast enhancement and T2W hyperintensities in the striatum and pallidum, white matter, thalamus, dentate or brainstem can be seen. Hydrocephalus with aqueductal stenosis can develop. Autosomal dominant inheritance. Gene: *GFAP*
ALPHA	Mild to severe manifestations, from infancy to childhood-onset.

MANNOSIDOSIS	Intellectual disability, myopathy, coarse facial features, macrocephaly, prominent forehead, dysostosis multiplex, hearing loss, hepatosplenomegaly and frequent infections. Ataxia is the most frequent neurological manifestation. Elevated urinary excretion of mannose-rich oligosaccharides. MRI shows empty sella turcica, cerebellar atrophy, and white matter T2W hyperitensities. Susceptibility can be seen in globus pallidus, putamen, susbtantia nigra and thalamus and hypomyelination is often noted. Autosomal recessive inheritance. Gene: *MAN2B1*
AP4 deficiency	Clinical phenotype of complex spastic paraparesis, intellectual disability, facial dysmorphism, microcephaly, optic atrophy and short stature. Cortical and white matter atrophy with thinning of the corpus callosum have been reported in most cases. Recent reports have described some individuals with susceptibility in the globus pallidus leading to the suggestion of brain iron accumulation. Autosomal recessive inheritance. Genes: *AP4E1, AP4M1, AP4S1*
ASPARTYLGLUCOSAMINURIA	At birth children with aspartylglucosaminuria are usually healthy with normal birth measurements. An early growth spurt and development of macrocephaly followed by delayed speech development, physical clumsiness and exceptional placidity or periods of hyperactivity in childhood usually raises a suspicion of aspartylglucosaminuria. Biochemical diagnosis is based on urinary oligosaccharides and assay of glycosylasparaginase activity. MRI shows T2W hypointensities in the thalamus and pallidum, corpus callosum atrophy and increased periventricular with matter T2W

	hyperintensities. Susceptibility may be noted in the striatum. Autosomal recessive inheritance. Gene: *AGA*
AUTOIMMUNE BASAL GANGLIA ENCEPHALITIS	A presentation with acquired extrapyramidal movement disorder with basal ganglia lesions in the context of new-onset encephalopathy in children and adults. Antibodies to the dopamine 2 receptor can be an associated biomarker. Dystonia-parkinsonism is the dominant movement phenotype and resolution occurs over weeks-months aided by immune therapy. Bilateral, near symmetric striatal T2--hyperintensities on MRI is the hallmark (Figure 1). Diffusion restriction and involvement of the globus pallidus or brainstem is rare. The cortical grey matter shows signal change, while white matter abnormalities are rare. Untreated cases can show progressive striatal atrophy making this a differential for "striatal necrosis" (Figure 2) 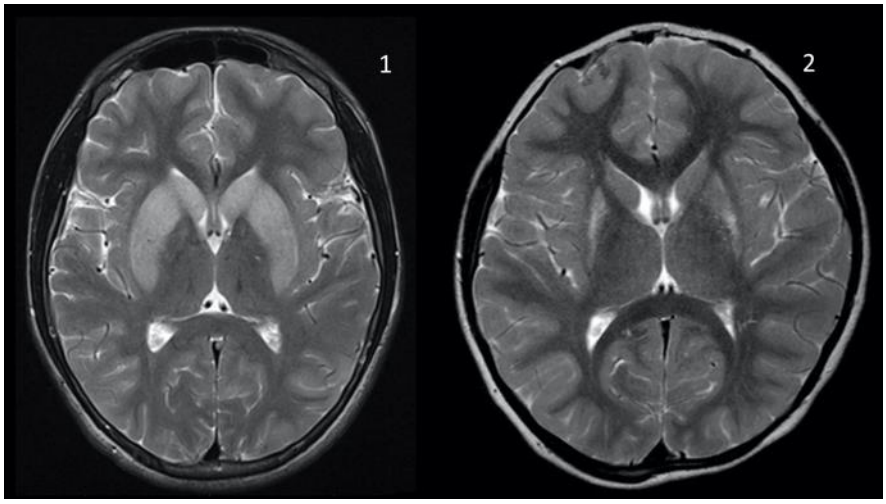
BETA KETOTHIOLASE DEFICIENCY	Impaired isoleucine catabolism and ketone body utilization that predisposes to episodic ketoacidosis. Infantile to childhood-onset of acute ketoacidosis and "metabolic stroke." Patients may develop choreoathethosis after these episodes. Urinary excretion of the

	isoleucine catabolic intermediates 2-methyl-3-hydroxybutyrate, 2-methylacetoacetate, and tiglylglycine. MRI demonstrates T2W hyperintensities of bilateral putamina or globus pallidi Autosomal recessive inheritance. Gene: *ACAT1*
BETA PROPELLER PROTEIN ASSOCIATED NEURODEGENERATION	A disorder of early childhood epilepsy with intellectual disability, Rett syndrome like features and evolving movement disorders, initially labeled as "static encephalopathy of childhood with neurodegeneration in adulthood," is also referred to as beta-propeller protein-associated neurodegeneration (BPAN). The MRI may appear normal in the first decade of life or show T1W hyperintensities around the SN (Figure 1). The pallidum (Figure 2), SN (Figure 2) and STN show susceptibility. Immature myelination and cerebellar atrophy can be seen in some cases. Calcification in the pallidum is described on CT in some cases. X-linked dominant inheritance. Gene: *WDR45* 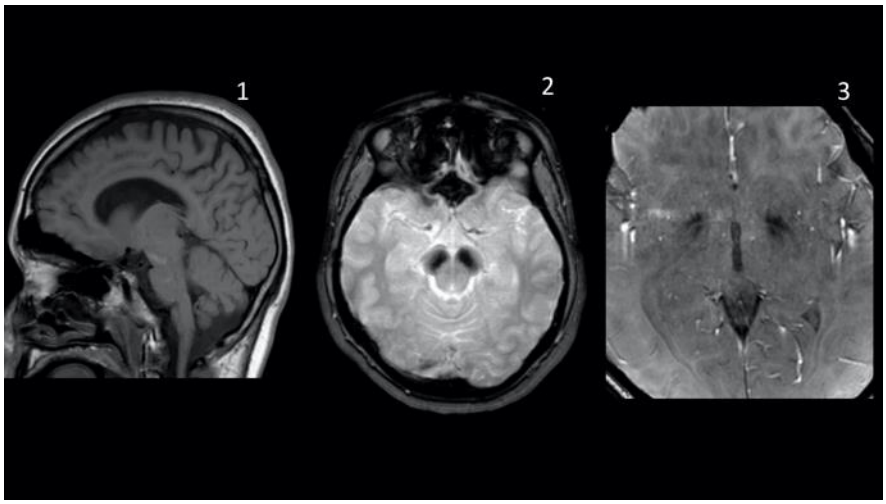
CANAVAN DISEASE	Mutations cause aspartoacylase deficiency, the enzyme that hydrolyzes N-acetylaspartic acid to acetate and aspartate. Normal milestones after birth, followed by progressive macrocephaly, head

	lag, and developmental delay. Infants often develop irritability, sleep disturbance, seizures and feeding difficulties. Patients progress to spastic quadriparesis. Mild forms of the disease are characterised with speech problems and seizures. Elevated N-acetylaspartic acid in urine and on MR spectroscopy. MRI shows symmetric diffuse T2W hyperintensities with bilateral involvement of the globus pallidus and thalamus in some cases and progressive white matter T2W hyperintensities. Striatal T2W hyperintensities are uncommon but described in some cases. Autosomal recessive inheritance. Gene: *ASPA*
CARASAL	Cathepsin A-related arteriopathy with strokes and leukoencephalopathy (CARASAL). Rare form of familial leukodystrophy. Common clinical manifestations include migraine, ischemic and haemorrhagic stroke, cognitive decline and dementia, movement disorder, dysphagia, dysarthria, vertigo and treatment resistant hypertension. MRI brain shows T2W hyperintensity of supratentorial white matter, striatum, pallidum, thalamus, midbrain, pons and medulla. Autosomal recessive inheritance. Gene: *CTSA*
CARBON MONOXIDE POISONING	Acute symptoms include headache, dizziness, vomiting, chest pain and confusion. More pronounced exposure manifests with coma, seizures or death. Patients may develop dystonia as a consequence of basal ganglia injury. T2W hyperintensity is noted in the pallidum but can involve the caudate and putamen. Patchy T1-hyperintensities and susceptibility due to haemorrhage may sometimes be seen. Diffusion restriction in the basal ganglia can be

	seen acutely.
CERBROTENDINOUS XANTHOMATOSIS	Treatable disorder of lipid metabolism. Infantile or juvenile cataracts, tendon xanthomas, pyramidal signs, neuropathy and cognitive decline. Parkinsonism is seen in adulthood, along with other classical manifestations. Elevated cholestenol in serum. MRI shows T2W white matter abnormalities in the cerebellum and middle cerebellar peduncles, with calcification of the dentate nuclei. T2W hyperintensities may be noted in the pallidum and the substantia nigra. Autosomal recessive inheritance. Gene: *CTX*
CEREBRAL CREATINE DEFICIENCY SYNDROMES 1, 2, 3	Cerebral creatine deficiency syndrome are potentially treatable conditions. In GAMT deficiency patients present in infancy with intellectual disability, abnormal behaviour and seizures. Some may have chorea, dystonia or ataxia. Presentations in adolescence have been reported. Patients with AGAT deficiency present with hypotonia and intellectual disability. Some may develop seizures. CRTR deficiency is an X-linked recessive disorder, where males present in infancy with several degrees of intellectual disability, speech disorders, and abnormal behaviour and seizures. Some may develop dystonia or ataxia. Dysmorphic features may also be seen. Age of diagnosis may range from infancy to adulthood. MRI may show pallidal T2W hyperintensities usually later in the first decade / second decade of life. Autosomal recessive inheritance. Genes: *SLC6A8, GAMT, AGAT*
CHILDHOOD-ONSET-DYSTONIA-	Childhood to adolescent-onset dystonia, with generalisation affecting bulbar and craniocervical region. Progressive anarthria is

28	frequent. Intellectual disability of different degrees. MRI may show T2W hypointensity and susceptibility in the globus pallidus. Autosomal dominant inheritance. Gene: *KMT2B*
CHOLINE TRANSPORTER-LIKE 1 DEFICIENCY	Single case series of three families with early onset of motor and speech delay. Progressive neurological worsening with tremor, visual loss, bulbar dysfunction and ataxia starting in the first decade of life. MRI changes included white matter T2W hyperintensities and cerebellar atrophy. Some individuals showed susceptibility in the pallidum with T2W hyperintensity of the internal medullary lamina reminiscent of the MRI appearance in MPAN. Autosomal recessive inheritance. Gene: *SLC44A1*
COCKAYNE SYNDROME TYPE A AND TYPE B	The phenotypic spectrum spans prenatal to later life onset and consists of marked somatic growth restriction in the early onset forms, which have a progressive course with deterioration of psychomotor function and impairment of vision and hearing. MRI changes in the basal ganglia are due to calcifications noted as T1W hyperintensities in the striatum. Calcifications may be also noted in the dentate, cortical grey matter, white matter and thalami. White matter T2W hyperintensities are prominently seen. Autosomal recessive inheritance. Gene: *ERCC8, ERCC6*
CONGENITAL DISORDER OF GLYCOSYLATION, TYPE IIn	Childhood-onset, severe multisystemic disorder, characterised by hypotonia, psychomotor delay, and seizures in some. Other features may include strabismus and recurrent infections. Blood levels of manganese and zinc are very low, whereas urine levels tended to be high. MRI shows cerebellar atrophy in the majority and bilateral

	striatal changes with a “Leigh like” presentation has been described. Autosomal recessive inheritance. Gene: *SLC39A8*
COPAN	Adolescent onset of ataxic gait, dystonia, parkinsonism, progressive spasticity, neuropathy and obsessive-compulsive behaviour. Susceptibility is noted in the pallidum but T2W hyperintensities may also be seen in the antero-medial pallidum corresponding to CT hyperdensity (possibly due to calcification) and sometimes reported in the striatum and thalamus. Autosomal recessive inheritance. Gene: *COASY*
CRAT	Infantile-onset of hypotonia, progressive cerebellar ataxia, pyramidal signs and neuropathy. Recently described disorder that mimics other causes neurodegeneration with brain iron accumulation. Autosomal recessive inheritance. Gene: *CRAT*
CYANIDE POISONING	Caused by exposure to cyanide. Early symptoms include headache, dizziness, tachycardia, dyspnoea and vomiting. This is followed by seizures, hypotension, coma and cardiac arrest. Brain MRI shows T1Whyperintensity in cortex, putamen and pallidum in the acute phase, followed by T2W hyperintensities in the chronic phase. Patchy susceptibility may sometimes be noted in the striatum in the acute phase due to haemorrhage.
DNAJC19	Infantile onset global developmental delay, hypotonia, dilated cardiomyopathy and progressive cerebellar ataxia (DCMA syndrome). Testicular dysgenesis, growth failure, and 3-methylglutaconic aciduria are also hallmarks of the disease. MRI shows cerebellar atrophy. Some cases are described with transient

	white matter T2W hyperintensities and some with bilateral T2W hyperintensities in the middle and posterolateral putamen. Autosomal recessive inheritance. Gene: *DNAJC19*
EPHEDRONE / MANGANESE TOXICITY	Intravenous mixture similar to methcathinone: potassium permanganate, ephedrine, and aspirin in drug user. Progressive parkinsonism and dystonia years after methcathinone abuse. MRI brain shows T1W hyperintensity in the globus pallidus and in the substantia nigra likely due to hypermanganesemia.
ETHYLENE GLYCOL TOXICITY	Organic solvent, found in antifreeze and household products (paints, lacquers and polishes). Intoxication is characterized by coma after ingestion and severe anion gap metabolic acidosis, osmolar gap, and calcium oxalate crystals in the urine. MRI brain shows diffuse oedema and bilateral symmetrical T2W hyperintensity in putamen, thalamus, amygdala, hippocampus, and brainstem. Delayed findings reported are putaminal necrosis. Susceptibility noted is due to patchy haemorrhage and not uniformly dark as in disorders with brain iron deposition.
FAHN	Normal early development followed by childhood onset spasticity, dystonia, ataxia and later cognitive dysfunction. Some patients may develop optic atrophy. MRI shows T2W white matter hyperintensities and susceptibility of the globus pallidus along with ponto-cerebellar atrophy, and thin corpus callosum Autosomal recessive inheritance. Gene: *FA2H*
FUCOSIDOSIS	A lysosomal storage disease caused by the deficiency of the enzyme L-fucosidase. Clinical onset is in early childhood with psychomotor

	delay. The disorder is progressive with multisystem involvement, organomegaly and dysostosis multiplex. Susceptibility is noted in the globus pallidus (Figure 2) along with immaturity of myelination on T2W/FLAIR images (Figure 2). Autosomal recessive inheritance. Gene: *FUCA1* 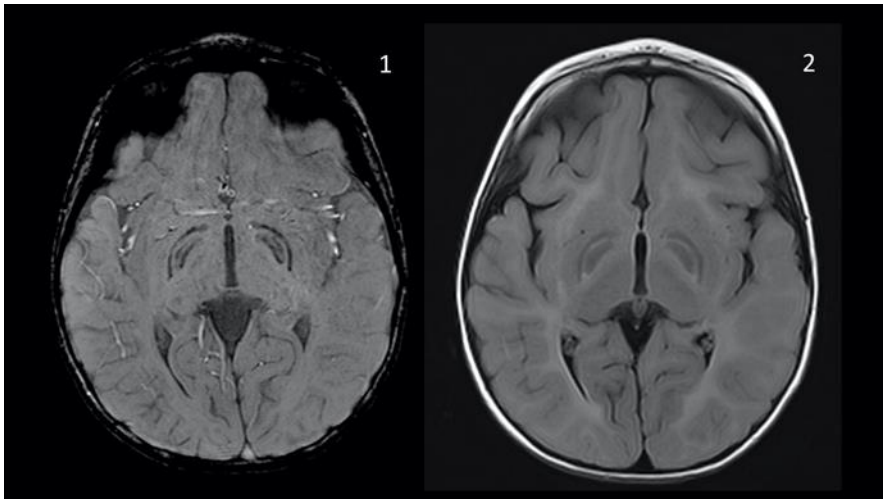
GANGLIOSIDOSES GM1 AND GM2	Gangliosidoses are a group of neurovisceral, sphingolipid storage disorders. These are divided in to GM1 (beta galactosidase deficiency) and GM2 gangliosidoses. GM2 gangliosidoses are comprised of Tay Sachs disease (beta-hexosaminidase A deficiency, HEXA gene) and Sandhoff disease (beta-hexosaminidase A and B deficiency, HEXB gene, OMIM #268800). Basal ganglia changes on neuroimaging have been described in the pallidum and striatum. The putamen may be preferentially involved in GM1 gangliosidosis. The changes consist of T2W hyperintensities (Figure) and atrophy of the striatum but T1W hyperintensity with susceptibility in the pallidum mimicking NBIA like disorders can also be noted. White matter T2W hyperintensities and immature myelination are noted in some cases. T2W hypointensities in the thalamus (Figure) with

	corresponding T1W hyperintensity are seen in both GM1 and GM2 gangliosidosis and likely indicate normal myelination of the thalami compared to surrounding structures. Autosomal recessive inheritance. Genes: *GLB1, HEXA, GM2A* 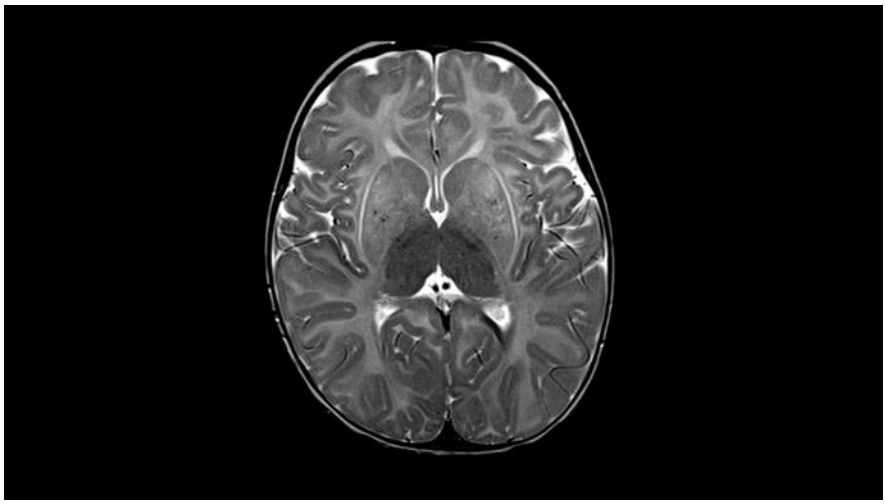
GIANT AXONAL NEUROPATHY	Childhood-onset with kinky hair, intellectual disability, progressive cerebellar ataxia and axonal motor-sensory neuropathy. Seizures and optic atrophy can be seen. Characteristic giant axons seen on nerve biopsy. MRI may show bilateral T2W hyperintensities in the pallidum, white matter and the dentate nuclei. Autosomal recessive inheritance. Gene: *GAN*
GLUTARIC ACIDURIA TYPE I	Glutaric aciduria type 1 is an autosomal recessive disorder of lysine, hydroxylysine, and tryptophan metabolism caused by deficiency of glutaryl-CoA dehydrogenase. It can present with an acute encephalopathy in early childhood or later. About 75% of affected individuals have macrocephaly. The disorder is determined by mutations in the GCDH gene, which is inherited in an autosomal recessive manner. 3-OH-glutaric acid in urine and low carnitine

	levels in plasma can be indicative of the diagnosis. The MRI changes seen in patients with GA1 are dependent on the time of recognition and treatment of the disorder and vary from striatal T2W hyperintensities (Figure 1) with swelling in the acute phase to striatal atrophy along with fronto-temporal atrophy leading to an "open operculum" appearance (Figure 2). Autosomal recessive inheritance. Gene: *GCDH* 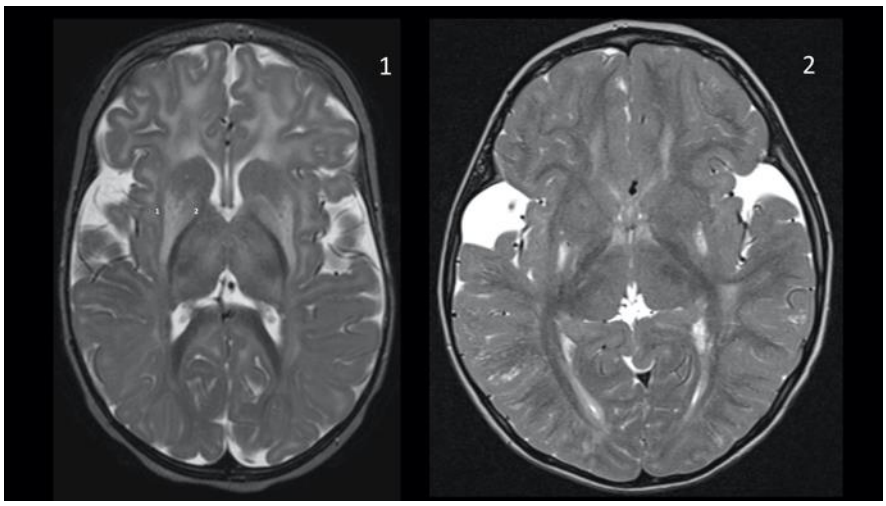
GTPBP2	Childhood-onset of motor and intellectual disability, with progressive ataxia and dystonia and distal motor neuropathy. Neuropsychiatric symptoms are also common. Only one family reported with MRI showing cerebellar vermis atrophy and susceptibility in the pallidum and substantia nigra. Autosomal recessive inheritance. Gene: *GTPBP2*
HAEMOLYTIC URAEMIC SYNDROME	Central nervous system impairment may occur in diarrhoea-associated haemolytic-uraemic syndrome. The syndrome is characterised by acute haemolytic anaemia, thrombocytopenia, and acute renal failure. Neurological impairment may include seizures, confusion, or rarely hemiparesis. MRI brain may show bilateral

	T2W hyperintensities in the putamen and thalamus similar to that seen in extrapontine myelinolysis along with diffusion restriction in the acute stage. These changes revert with metabolic stabilisation.
HYPERMANGANESEMIA WITH DYSTONIA 1	Genetic changes in SLC30A10 lead to a disorder of manganese transport manifesting with polycythemia, liver dysfunction and progressive dystonia. Onset is typically in childhood and inheritance is autosomal recessive. Very bright T1W hyperintensities are noted in the striatum and pallidum with obscuration of boundaries between the basal ganglia nuclei (Figure 1). T1W hyperintensities are also noted in the cerebellar white matter, pituitary and dentate nuclei (Figure 1 and 2). Autosomal recessive inheritance. Gene: *SLC30A10* 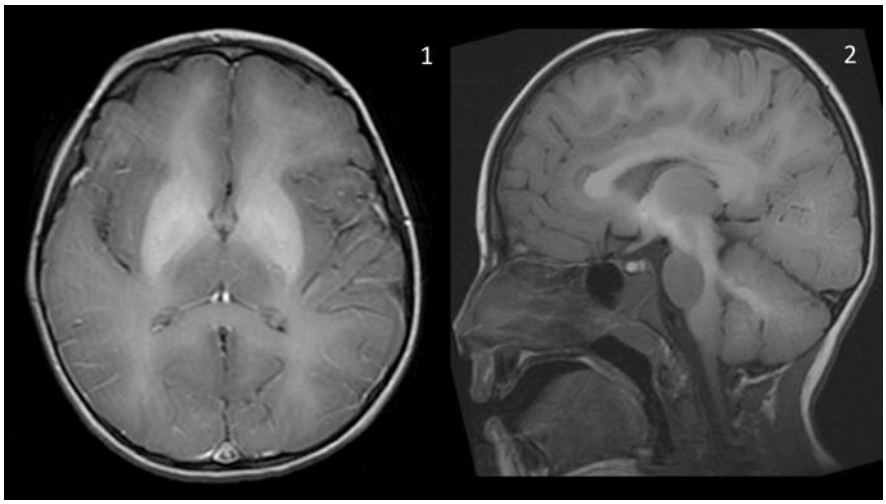
HYPERMANGANESEMIA WITH DYSTONIA 2	Genetic changes in SLC39A14 lead to a disorder of manganese transport manifesting progressive dystonia. Onset is typically in childhood and inheritance is autosomal recessive. Very bright T1W hyperintensities are noted in the globus pallidus (Figures 1), cerebellar white matter, pituitary and dentate. Striatal T1W hyperintensities appear with disease progression over years.

	Abnormal susceptibility may not be seen in most cases (Figure 2) till later stages of disease. Autosomal recessive inheritance. Gene: *SLC39A14* 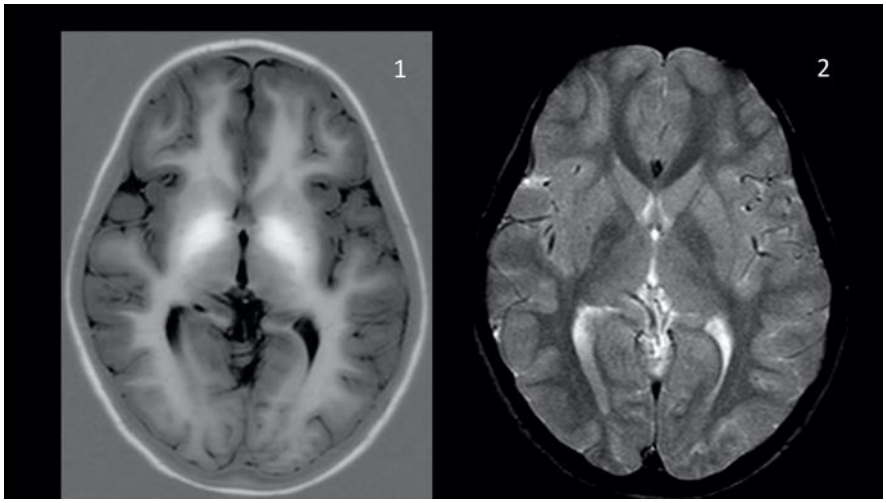
HYPOXIC ISCHAEMIC ENCEPHALOPATHY (TERM NEONATES)	Patients with a history of neonatal encephalopathy fulfilling American College of Obstetricians and Gynecologists' Task Force criteria for hypoxic ischemic encephalopathy, particularly around full term gestation are known to have MRI changes that involve the basal ganglia - a typical pattern of T2W hyperintensities in the motor cortex and surrounding white matter (Figure 1), descending through the posterior putamen and along the corticospinal tracts and ventrolateral thalami (Figure 2).

	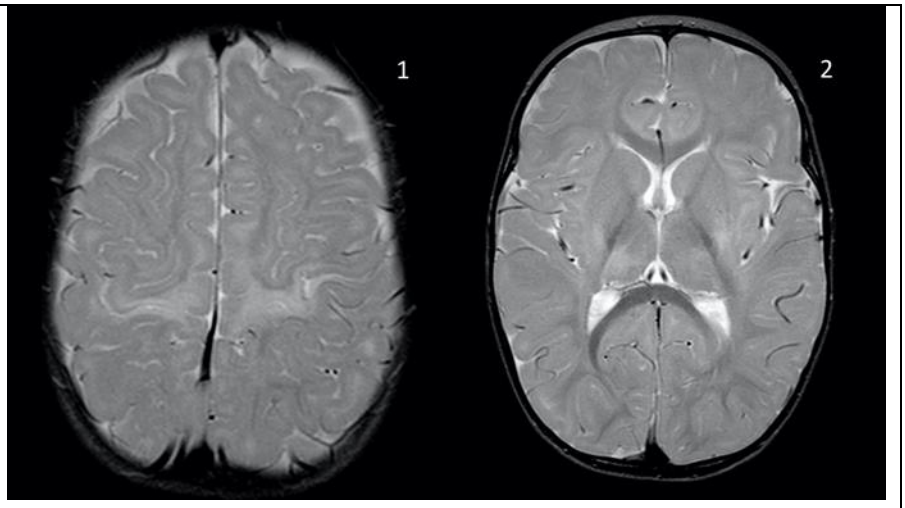
IDIOPATHIC BASAL GANGLIA CALCIFICATION (FAHR'S DISEASE)	Calcification in the brain can occur due to a genetic predisposition (primary) or secondary to other processes such as inflammation or injury. Calcium can also behave as a paramagenetic substance that can lead to T1W hyperintensity on MRI and sometimes, but not always demonstrate corresponding susceptibility. Basal ganglia calcification can therefore mimic other causes of basal ganglia susceptibility, particularly when bilateral and should be suspected when susceptibility is noted in a patchy pattern or involves the striatum in childhood . The monogenic disorders listed here are commonly associated with Fahr's disease or Idiopathic basal ganglia calcification. Familial forms can occur. There is a broader list of causes of basal ganglia calcification which is referred to in the main text with references. Autosomal dominant or recessive inheritance. Multiple genes: *SLC20A2, XPR1, PDGFRB, PDGFB, MYORG,* other monogenic associations in main text
INFECTIOUS ENCEPHALITIS	Various infectious encephalitis syndromes are known to affect the basal ganglia. Flaviviruses and Mycoplasma pneumoniae are the most commonly described infectious encephalitides with basal

	ganglia involvement. Flaviviruses include Japanese encephalitis (JE), West Nile virus (WNV) and Murray valley encephalitis. The imaging findings in JE commonly demonstrate involvement of bilateral thalami in almost all patients while basal ganglia changes are reported in ~50%. The caudate and putamen are more commonly involved in reports of WNV whereas basal ganglia involvement is less commonly noted in Murray valley virus. Haemorrhagic change may be seen in susceptibility data sets in the acute stage or during recovery in some cases of JE. Mycoplasma - The MRI changes described have mainly been limited to the striatum, with a few reports showing changes additionally in the SN or pallidum. Involvement of other structures, such as the thalamus or the brainstem have been described in few reports. Other viral encephalitis syndromes where basal ganglia involvement has been described include Herpes simplex virus, Epstein Barr virus, Cytomegalovirus, Echoviruses, Human papilloma virus, Lyssaviruses, Rabies virus and Human herpes virus 6.
ISOVALERIC ACIDEMIA	Isovaleryl-CoA dehydrogenase deficiency. Onset is during infancy, often after birth with acute neonatal encephalopathy or recurrent episodes of vomiting, metabolic acidosis, feeding difficulty, psychomotor retardation and "sweaty feet" odour. Isovalerylglycine is elevated in urine and isovaleryl (C5)-carnitine elevated in serum. MRI changes include T2W hyperintensities in the pallidum that may revert with time. Subarachnoid and intraparenchymal haemorrhages are also described in some patients. Pallidal T2W

	hyperintensities with diffusion restriction have been described in neonatal presentations. Other regions showing T2W hyperintensities are the white matter and cerebellum. Autosomal recessive inheritance. Gene: *IVD*
JUVENILE HUNTINGTON'S DISEASE	Huntington's disease (HD) is a trinucleotide repeat disorder that can manifest as a juvenile onset form that correlates with higher number of trinucleotide repeats. The clinical manifestations of predominantly akinetic and dystonic movements with psychiatric symptoms are accompanied by MRI changes, though the MRI can sometimes be normal or show only subtle abnormalities early in the disease course. The MRI changes described include T2W hyperintensities mainly in the putamen with atrophy of the caudate and putmamen that gets progressively worse with time (Figure 1). In addition, more global cortical atrophy is often seen in most cases. Susceptibility can be noted in the pallidum in some cases (Figure 2). Autosomal dominant inheritance. Expansion of CAG trinucleotide repeats in Gene: *HTT* 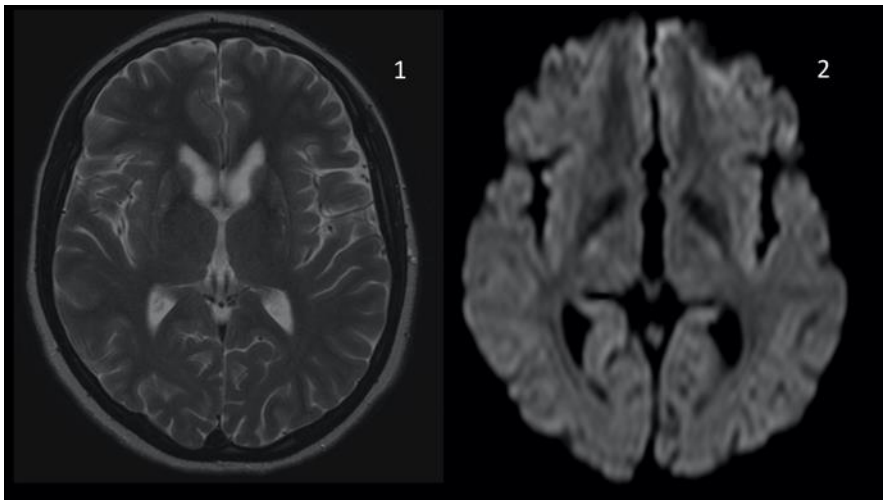

KCNQ2	Mutations in this gene have been associated with benign familial neonatal seizures or neonatal epileptic encephalopathy. In some patients, seizures are controlled in childhood. Only a few reports of T1W hyperintensities in the globus pallidus. These were noted at an early age when transient T1W hyperintensities can be noted in normal children (reference) and hence the significance of this finding should be interpreted with caution. Autosomal dominant inheritance. Gene: *KCNQ2*
KEARNS SAYRE SYNDROME	Kearns Sayre syndrome is defined by the presence of progressive external ophthalmoplegia (PEO) and retinal dystrophy with onset before the age of 20, and in addition at least one of the following features: cardiac conduction defect, cerebellar dysfunction or elevated protein in CSF (>1 g/l). It is associated with deletions in mitochondrial DNA. On MRI basal ganglia abnormalities are prominently noted in the globus pallidus with T2W hyperintensities (Figure 1) evolving to cystic changes on progression. T2W hyperintensities can also be noted in the thalami (Figure 1) and the dentate nuclei (Figure 2) 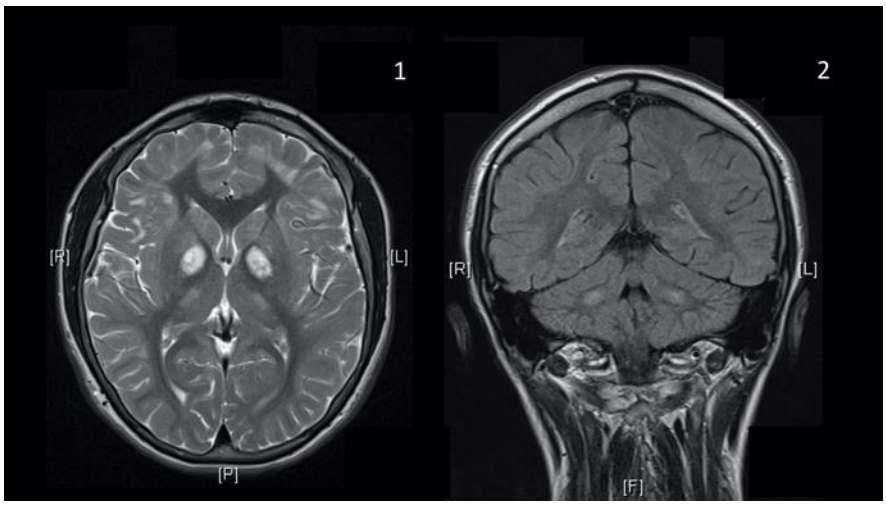

KERNICTERUS	The term kernicterus denotes pathological staining of structures in the brain, followed by neuronal necrosis. The clinical phenotype is typically a combination of dystonia, sensorineural hearing loss, vertical gaze palsy, and dental staining in an individual with a history of bilirubin encephalopathy, usually in the neonatal period. The pallidum (Figures 1 and 2) and subthalamic nuclei (Figure 2) are commonly abnormal with T2W hyperintensities while transient T1W hyperintensities in the neonatal period are difficult to convincingly determine as being abnormal. The dentate, hippocampus and thalamus may show T2W hyperintensities in some cases. 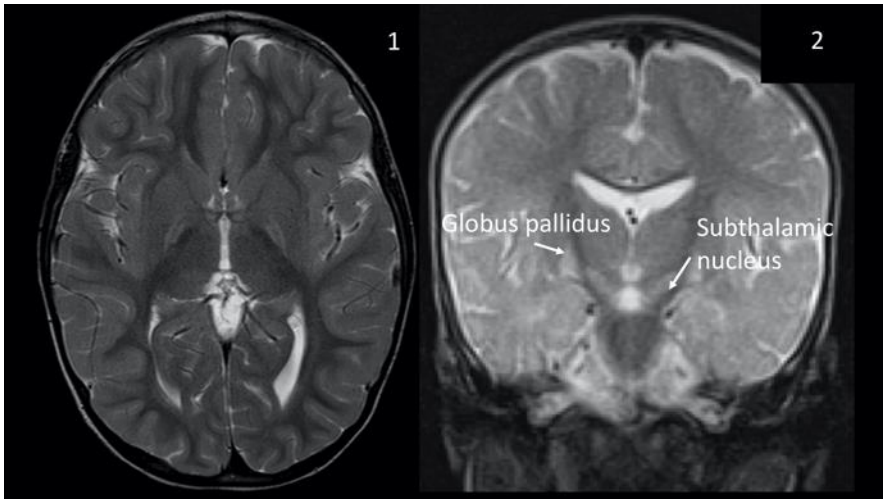
KRABBE DISEASE	A lysosomal storage disorder due to deficiency of galactocerebrosidase. Diagnosis is based on low enzyme activity in fibroblast/leucocytes and mutations in GALC. The MRI changes typically consist of T2W hyperintensities in the white matter, the corona radiata, the internal capsule, cerebellar white matter and the dentate. Pallidal and thalamic T2W hyperintensities are less commonly described. Thickening of the optic nerves/tracts (arrow

	in Figure of midline sagittal T1W image) can be a diagnostic clue. Autosomal recessive inheritance. Gene: *GALC* 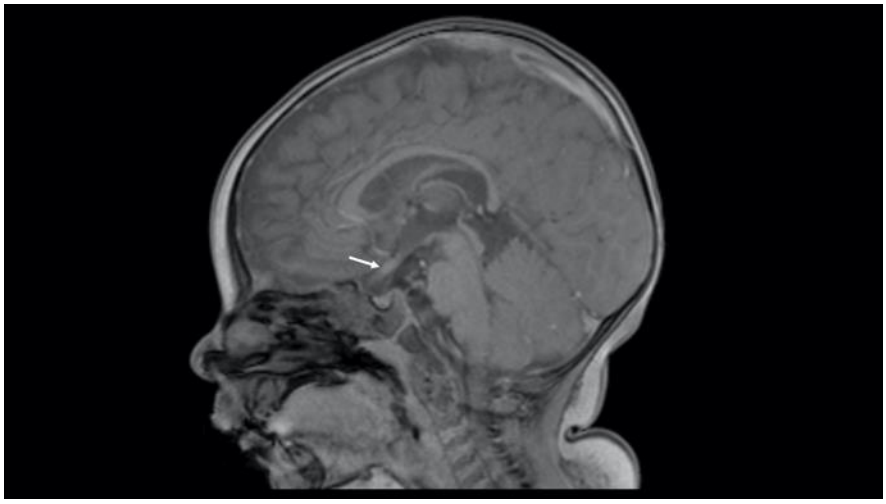
KUFOR RAKEB SYNDROME	Parkinsonism, pyramidal signs, vertical supranuclear gaze palsy, facial-finger myoclonus are hallmarks of the disease. Neuropsychiatric symptoms and cognitive decline are common. Moderate levodopa response but lost with disease progression. Generalised cortical atrophy, with or without cerebellar atrophy. Iron deposition in the striatum and pallidum leads to the appearance of susceptibility. Striatal and thalamic atrophy maybe noted with time. Autosomal recessive inheritance. Gene: *ATP13A2*
L-2-OH GLUTARIC ACIDURIA	Childhood onset intellectual disability, macrocephaly, progressive cerebellar ataxia and dystonia. L-2-hydroxyglutaric acid elevated in urine. MRI shows subcortical leukoencephalopathy, cerebellar atrophy, and T2W hyperintensities in the putamina and dentate nuclei. Autosomal recessive inheritance. Gene: *L2HGDH*
LANGERHANS CELL	Neurological involvement in Langerhans cell histiocytosis occurs due to an infiltrative or inflammatory process. MRI changes may

HISTIOCYTOSIS	include T2W hyperintensity of the cerebellar white matter and pons, cerebellar atrophy and patchy T1W hyperintensity and susceptibility in the globus, substantia nigra or the striatum. The T1W changes and susceptibility are likely due to calcification.
LEBER HEREDITARY OPTIC NEUROPATHY	Onset of painless subacute bilateral visual loss in adolescence or early adulthood. Brain MRI is typically normal though some cases may have a presentation and neuroimaging that may mimic multiple sclerosis with patchy areas of T2W hyperintensities in the white matter. Basal ganglia T2W hyperintensities are occasionally described similar to a “Leigh like” appearance involving the striatum, and sometimes the thalamus, hypothalamus, brainstem and cerebellum. Enlargement and enhancement of the optic tracts, chiasm, and optic radiations may also be seen.
MANGANESE TOXICITY	Manganese toxicity can occur due to ephedrine ingestion, industrial exposures in welding and mining, secondary to liver failure or use of total parenteral nutrition Manganese exposure causes a chronic neurological syndrome characterised by irritability, emotional lability, parkinsonism and dystonia. High stepping gait also termed “cock walk” is suggestive of the disorder. Ethylenediaminetetraacetic acid can reduce symptoms in some patients. MRI brain shows T1W hyperintensities in pallidum, substantia nigra and anterior pituitary.
MAPLE SYRUP URINE DISEASE	Characterised by elevated plasma concentrations of branched-chain amino acids (leucine, isoleucine, and valine) and allo-isoleucine. At birth neonates have a maple syrup odour in the cerumen. At day 2-

	3, irritability, poor feeding and ketonuria. At day 4-5 encephalopathy, intermittent apnoea, opisthotonus with fencing and bicycling postures. After one week of birth, coma and central respiratory failure is seen. Intermediate phenotype have partial branched-chain α-keto acid dehydrogenase enzyme deficiency that manifests as severe intermittent metabolic encephalopathy. Survivors have neurological sequels intellectual disability, mood disorders, hallucinations, dystonia, chorea, ataxia and pyramidal signs. MRI brain during the encephalopathy episodes show generalised swelling and bilateral T2W hyperintensities in putamen, pallidum, brainstem and hippocampus. Autosomal recessive inheritance. Genes: *DBT, BCKDHB, BCKDHA*
MECR	Infantile or childhood-onset progressive generalised dystonia with later appearance of optic atrophy. Relative sparing of cognitive function. MRI shows bilateral T2W hyperintensity in either caudate, putamen, or pallidum. High lactate on MRS in some cases. Autosomal recessive inheritance. Gene: *MECR*
MEGDEL	3-methylglutaconic aciduria with sensori-neural deafness, encephalopathy, and Leigh-like syndrome (MEGDEL) is a syndrome of progressive psychomotor regression and deafness with dystonia. Initial changes noted are swelling of the caudate and putamen with evolution to a typical pattern of sparing of regions of the putamen (Figure 1). Involvement of the SN and the adjacent red nucleus is described in some cases. T2W hyperintensities are noted in the affected regions. In early stages of the disease, diffusion

	restriction has been described to involve the pallidum. Striatal atrophy (Figure 2) with diffuse cerebellar and cerebral atrophy (Figure 2) are described to occur in most patients with disease progression Autosomal recessive inheritance. Gene: *SERAC1* 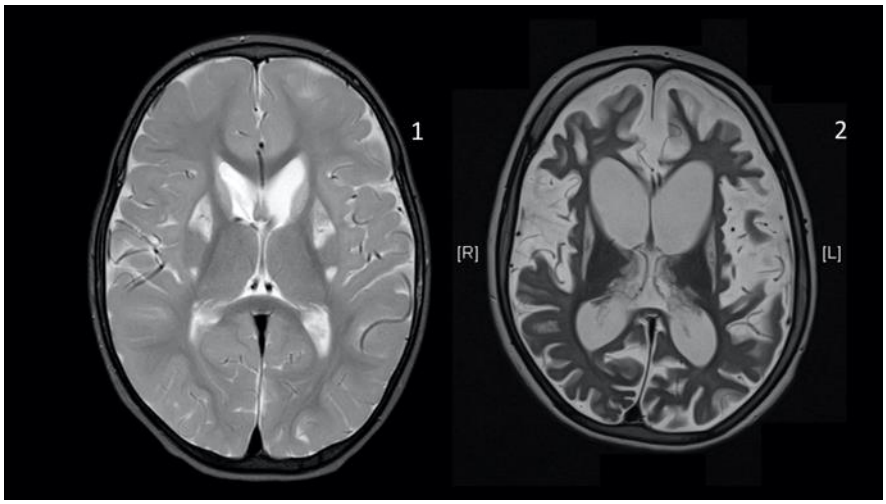
METACHROMATIC LEUKODYSTROPHY	Deficiency of arylsulfatase A. Heterogeneous clinical presentation, with infantile-onset of hypotonia, weakness followed by gait disturbance and neuropathy. Patients become cognitively impaired and develop hearing and visual loss. In childhood-adolescent onset neuropsychiatric and cognitive problem are common, with findings of pyramidal signs, ataxia and tremor. Adult presentations with dementia, psychosis and spasticity have been reported. ARSA activity in leukocytes that is less than 10% of normal. MRI shows diffuse T2W hyperintensities in the parieto-occipital region (tigroid pattern) in most individuals with late-infantile MLD, with subcortical U-fibers and cerebellar white matter spared. Basal ganglia abnormalities are rarely described and include T2W hyperintensities in the striatum but may also include T2W hypointensities in the pallidum and thalami. Autosomal recessive

	inheritance. Gene: *ARSA*
METHADONE TOXICITY	Methadone ingestion causes rapid hypotension, hypothermia, bradycardia and coma. MRI brain shows bilateral T2W hyperintensities in the putamen, brainstem, cerebellum and occipital cortex with diffusion restriction.
METHANOL TOXICITY	Nausea, vomiting, and abdominal pain after ingestion, followed by hyperventilation, high anion gap metabolic acidosis and disorder of consciousness. Papilledema, optic neuritis and retinal damage are often seen. Diffuse cerebral oedema and Putaminal T2W hyperintensities is seen. Patchy T1W hyperintensities and corresponding patchy susceptibility may be noted due to haemorrhagic lesions.
METHYLMALONIC ACIDEMIA	Methlymalonic acidemia (MMA) consists of a group of disorders that lead to accumulation and excessive excretion of methylmalonic acid as a result of defects in the conversion of methylmalonyl-coenzyme A into succinyl-coenzyme A. This most commonly occurs due to an enzyme deficiency of methylmalonyl-coenzyme A mutase. Other described forms occur due to defects in synthesis and transport of cobalamin and 5-deoxyadenosylcobalamin, which are cofactors for the enzyme. Dominant involvement of the globus pallidus with T2W hyperintensities is typical on MRI. Initially pallidal abnormalities may be subtle or involve only part of the pallidum but entire pallidal involvement and cystic changes (Figures 1 and 2) can be noted on progression in late diagnosed or

	untreated cases. Autosomal recessive inheritance. Genes: *MMUT, MMAA, MMAB, MMACHC, MMADHC, MCEE.* Also associated with *ABCD4, ACSF3, CD320, LMBRD1, MLYCD, MTR, MTRR, MUT, SUCLA2, SUCLG1, TCN2* 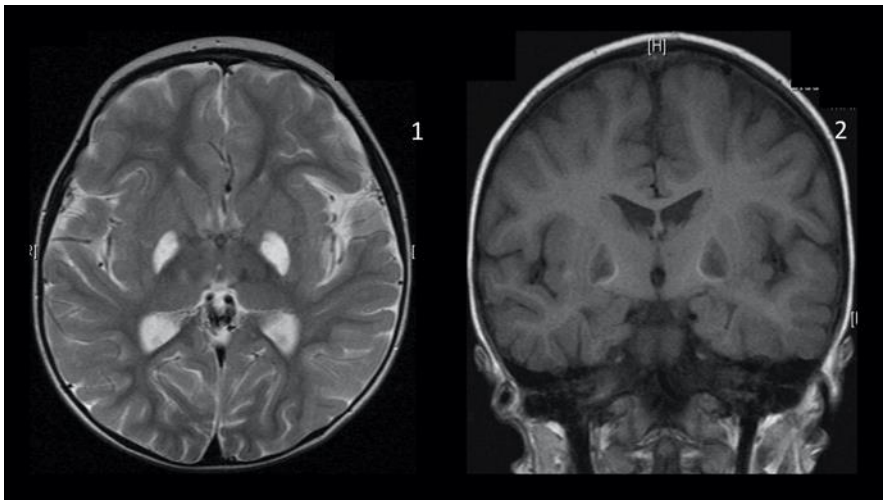
MITOCHONDRIAL COMPLEX 1 DEFICIENCY	Biochemical deficiency of Complex I of the mitochondrial electron transport chain is determined by mutations in *NDUFA1, NDUFA2, NDUFA6, NDUFA9, NDUFA10, NDUFA11, NDUFA12, NDUFA13 NDUFB3, NDUFB8, NDUFB9, NDUFB10, NDUFB11, NDUFS1, NDUFS2, NDUFS3, NDUFS4, NDUFS6, NDUFS7, NDUFS8, NDUFV1, NDUFV2, NDUFAF1, NDUFAF2, NDUFAF3, NDUFAF4, NDUFAF5, NDUFAF6, NDUFAF7, NDUFAF8, ACAD9, ECSIT, FOXRED1, NUBPL, TIMMDC1, TMEM126B, MT-ND1, MT-ND2, MT-ND3, MT-ND4, MT-ND4L, MT-ND5, MT-ND6*. Combined deficiency of Complex I can also occur with mutations in other genes. The phenotypic spectrum is variable from childhood to adult-onset of Leigh syndrome like presentations or mitochondrial encephalopathy with stroke-like episodes. Patchy T2W hyperintensities of the striatum and diffusion

	restriction are noted similar to other mitochondrial disorders. Diffusion restriction can be noted during periods of decompensation or acute crises.
MITOCHONDRIAL COMPLEX IV DEFICIENCY	Biochemical deficiency of Complex IV of the mitochondrial electron transport chain is determined by mutations in *COX4I1, COX4I2, COX5A, COX6A1, COX6B1, COX7B, COX8A, NDUFA4, SURF1, SCO1, SCO2, COX10, COX15, COA3, COA5, COA6, COA7, COX14, COX20, FASTKD2, PET100, PET117, CEP89, MT-CO1, MT-CO2, MT-CO3.* Combined deficiency of Complex IV can also occur with mutations in other genes such as those affecting mitochondrial translation. Partial or complete involvement of the putamen with T2W hyperintensities is noted. Pallidal T2W hyperintensities can also be seen accompanying putaminal change (Figure). Patchy sparing is noted in several cases in early stages of the disease with later striatal atrophy, similar to other mitochondrial disorders. Diffusion restriction can be noted during periods of decompensation or acute crises. Varying degrees of brainstem abnormalities can be seen in the acute stage, some of which can resolve with time.

	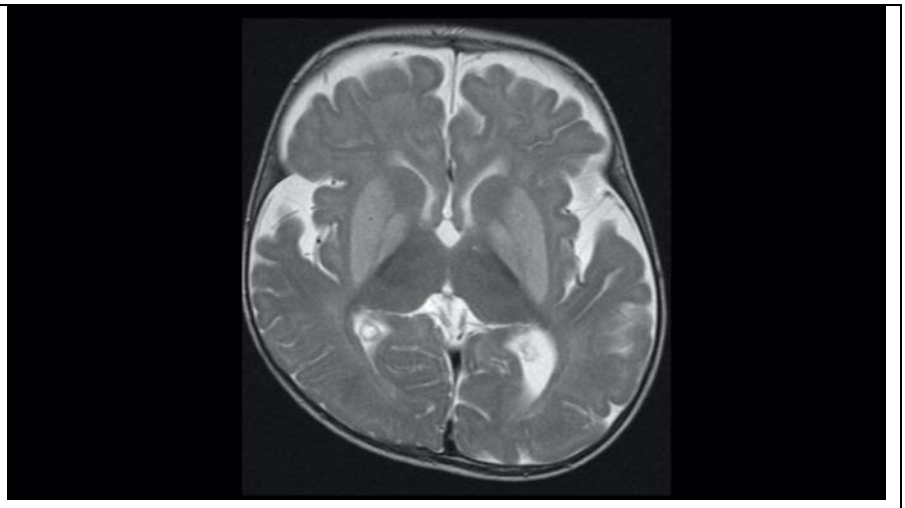
MITOCHONDRIAL COMPLEX V DEFICIENCY	Biochemical deficiency of Complex V of the mitochondrial electron transport chain is determined by mutations in *ATP5A1, ATP5D, ATP5E, ATPAF2, TMEM70, USMG5, MT-ATP6, MT-ATP8. MT-ATP6* has mainly been described with a Leigh syndrome presentation. Combined deficiency of Complex V can also occur with mutations in other genes. The phenotypic spectrum is variable from childhood to adult onset of Leigh syndrome like presentations or mitochondrial encephalopathy with stroke like episodes. Partial T2W hyperintensities of the putamen with patchy sparing is noted in several cases, similar to other mitochondrial disorders (Figure 1). Varying degrees of brainstem abnormalities can be seen in the acute stage (Figure 2), some of which can resolve with time. Diffusion restriction can be noted during periods of decompensation or acute crises.

	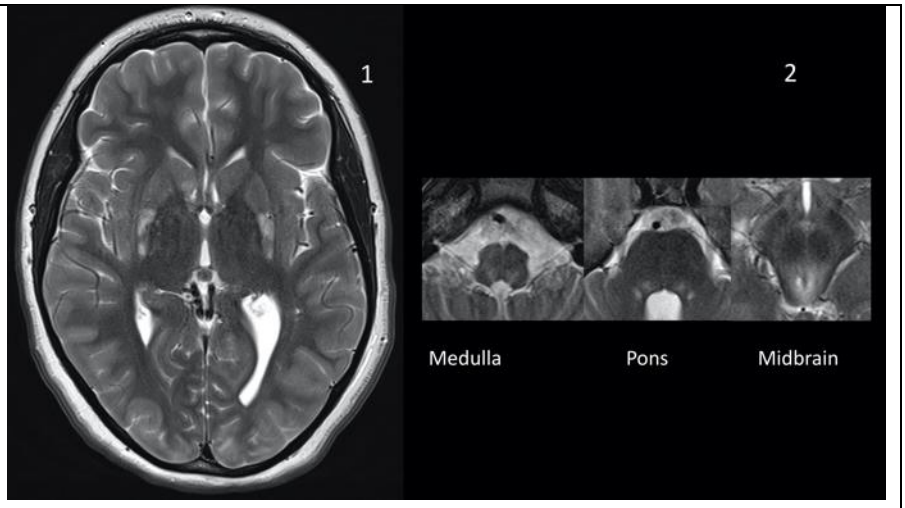
MITOCHONDRIAL MAINTAINENCE	Multisystemic disorders to specific syndromes involving muscle, brain, and gastrointestinal symptoms. Mutations in mtDNA maintenance genes(SLC25A4, TFAM, POLG1, POLG2, TWNK, DNA2, RNASEH1, MGME1, TP, TK2, DGUOK, RRM2B, SUCLA2, SUCLG1, MPV17, OPA1, MFN2, AFG3L2, SPG7). MRI pleiotrophy in these disorders is not well-described as genetic associations are still being described. The MRI rating for this group of disorders should therefore be interpreted with caution in the current version of this tool.
MITOCHONDRIAL MEMBRANE PROTEIN ASSOCIATED NEURODEGENERATION	Childhood or adolescence onset with progressive dystonia-parkinsonism, pyramidal signs, neuropsychiatric symptoms, optic atrophy and later axonal motor neuronopathy. Susceptibility is described in the pallidum and SN in most described cases. The medial medullary lamina in the pallidum is usually spared (Figure 1) and is sometimes reported to show T2W hyperintense "streaking". Cerebellar atrophy can be noted in some cases (Figure 2, which also shows thin optic tracts). Autosomal recessive inheritance. Gene: *C19orf12*

	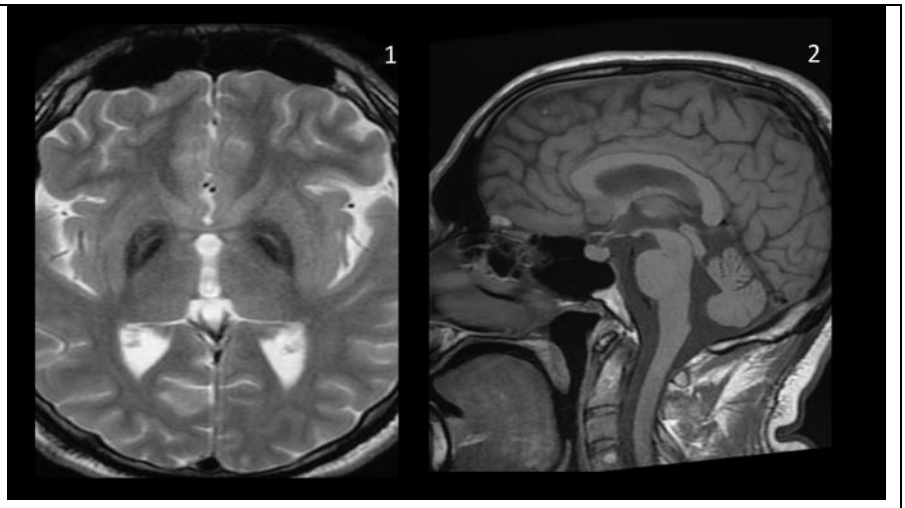
MITOCHONDRIAL THIAMINE TRANSPORTER	SLC25A19 gene mutations cause Amish congenital lethal microcephaly and bilateral striatal necrosis with axonal polyneuropathy. The onset is during infancy or childhood acute or recurrent encephalopathy with flaccid paralysis, dystonia, and neuropathy. High excretion of alpha-ketoglutaric acid in urine. MRI shows symmetrical T2W hyperintensities in caudate and putamen. Clinical improvement after thiamine supplementation. Autosomal recessive inheritance. Gene: *SLC25A19*
MITOCHONDRIAL TRANSLATION	Although most of the proteins present in mitochondria are encoded by the nDNA, a few are encoded by the mtDNA and are synthesized by the separate mitochondrial translation system. Many different genetic changes in genes such as MT-TL1, EARS2 and other Amino acyl tRNA synthetases 2 (aaRS2) genes. These disorders can have variable ages of onset. The clinical phenotypes are very heterogeneous and some individuals can present with a Leigh like syndrome. Some mutations such as those in NARS2 can have associated deafness. MRI pleiotropy in these disorders is not well-described as genetic associations are still being described. The MRI

	rating for this group of disorders should therefore be interpreted with caution in the current version of this tool.
MUCOLIPIDOSIS TYPE IV	Most reported cases in the Ashkenazi Jewish population. Mucolipidosis type IV typically results in intellectual disability, corneal opacities, and delayed motor milestones during infancy, with a relatively static course. Visual impairment results mainly from corneal clouding and retinal degeneration. The reduction of gastric hydrochloric acid (achlorhydria) is believed due to the dysfunction of parietal cells of the gastric mucosa. This consequently increases gastrin as a compensatory mechanism. MRI shows thin corpus callosum and cerebral and cerebellar atrophy with microcephaly. Susceptibility on MRI is described to involve the pallidum and sometimes the striatum. Hypomyelination is also reported in some cases. Autosomal recessive inheritance. Gene: *MCOLN1*
MYELINOLYSIS	Myelinolysis has been described in association with rapid alterations in sodium levels and various other conditions like lupus, Wilson's disease, diabetes mellitus, haematological malignancies and with other electrolyte imbalances. ~10% cases have extrapontine involvement. The striatum is generally involved with acute swelling and T2W hyperintensities. A rim of brighter T2W hyperintensity may be noted around the putamen (Figure 1). The thalamus (Figure 2) and the dorsal pons (Figure 3) are commonly involved with sparing of the ventral pons. Diffusion restriction may be noted in the acute stages. Signal changes on MRI are described

	to resolve over time but the interval to complete resolution is variable and can be weeks-months. 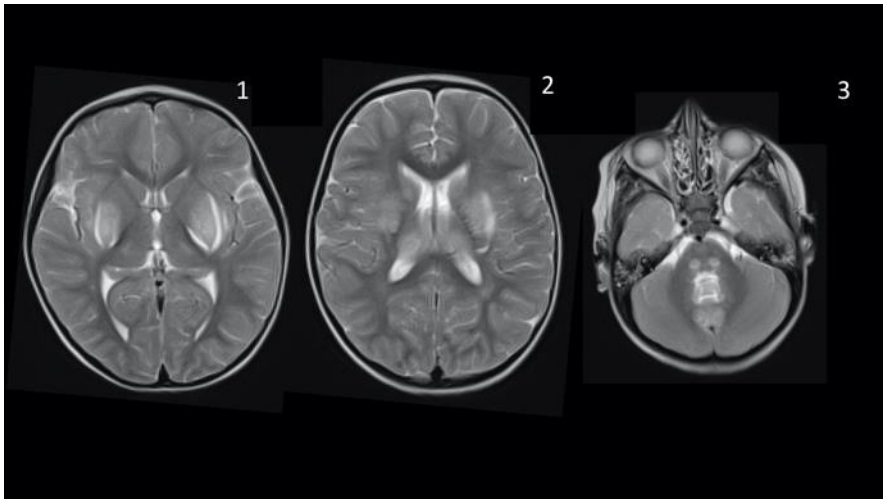
NEUROFERRITINOPATHY	Clinical onset in adulthood with psychiatric symptoms, chorea, dystonia and spasticity. Cerebellar symptoms, palatal tremor and akinesia are also reported. Low serum ferritin is an indicator. T2W hyperintensities and cystic changes in the striatum and pallidum with disease progression with surrounding rim of susceptibility. Thalamic and dentate T2W hyperintensities and cystic change are also described. Cortical lining of susceptibility change has been described in some cases. Autosomal dominant inheritance. Gene: *FTL*
NUP62	Infantile onset choreoathetoid movements, dystonia, horizontal pendular nystagmus, optic atrophy, developmental regression and spastic quadriparesis. MRI shows progressive symmetrical T2W hyperintensities in the putamen, followed by atrophy in both putamen and caudate. Autosomal recessive inheritance. Gene: *NUP62*

PANTOTHENATE KINASE ASSOCIATED NEURODEGENERATION	Pantothenate kinase-associated neurodegeneration (PKAN) is the prototypic NBIA disorder. Susceptibility on MRI is noted in the pallidum and sometimes in the SN. In some cases imaged early in the disease course, the pallidum may only show an eccentric region of T2W hyperintensity without susceptibility (Figure 1). The "eye-of-the-tiger" sign is used to describe the appearance of the pallidum on T2W and susceptibility sensitive data sets of a central area of hyperintensity with surrounding hypointense pallidum (Figure 2). Although commonly reported in cases of PKAN, the 'eye-of-the-tiger' is not a universal finding and may depend on the disease stage at which imaging is undertaken, and possibly on the genotype. Many individuals develop retinal degeneration with time. Cerebellar atrophy can be noted in some cases. Calcification within the pallidum has been descibed in some cases noted on CT scan. Autosomal recessive inheritance. Gene: *PANK2* 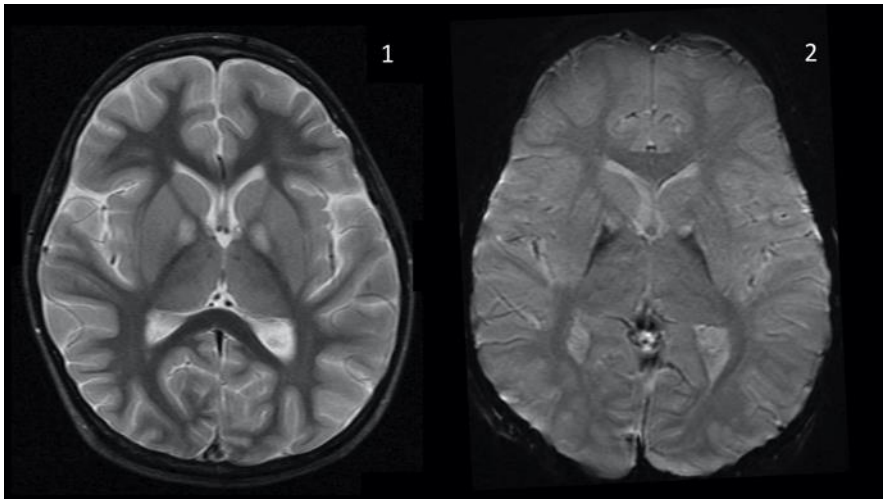
PDE8B	Familial adult-onset progressive parkinsonism. MRI shows striatal T2W hyperintensities followed by progressive degeneration. T2W hyperintensities are also noted in the thalami and rarely intermixed

	regions of T1W hyperintensity are also noted. Only two families reported. Autosomal dominant inheritance. Gene: *PDE8B*
PDE10A	Biallelic mutations. Infantile-onset chorea and dystonia, usually with normal cognition and developmental milestones. Some cases of infantile chorea with latter adult-onset parkinsonism have been reported. Chorea may respond to levodopa in some cases. Diurnal fluctuations of chorea have been also reported. Brain MRI may be normal or may show symmetrical bilateral T2W hyperintensities, including the caudate nucleus and putamen with progressive striatal atrophy. Autosomal recessive inheritance. Gene: *PDE10A*
PLA2G6 ASSOCIATED NEURODEGENERATION	PLA2G6-associated neurodegeneration (PLAN) is one of the NBIA disorders with a spectrum of clinical presentations from infantile onset neuroaxonal dystrophy to presentations at later ages with dystonia-parkinsonism. MRI may appear normal in early stages of the disease or only show T2W hyperintensities in the anteromedial globus pallidus. Susceptibility is noted in the globus pallidus in 40-50% of cases overall (Figure 2) and can also be noted in the substantia nigra. T2W hyperintensities are noted in the optic tracts and sometimes noted in the striatum. Cerebellar (Figure 3) and optic atrophy are other commonly described features. Autosomal recessive inheritance. Gene: *PLA2G6*

	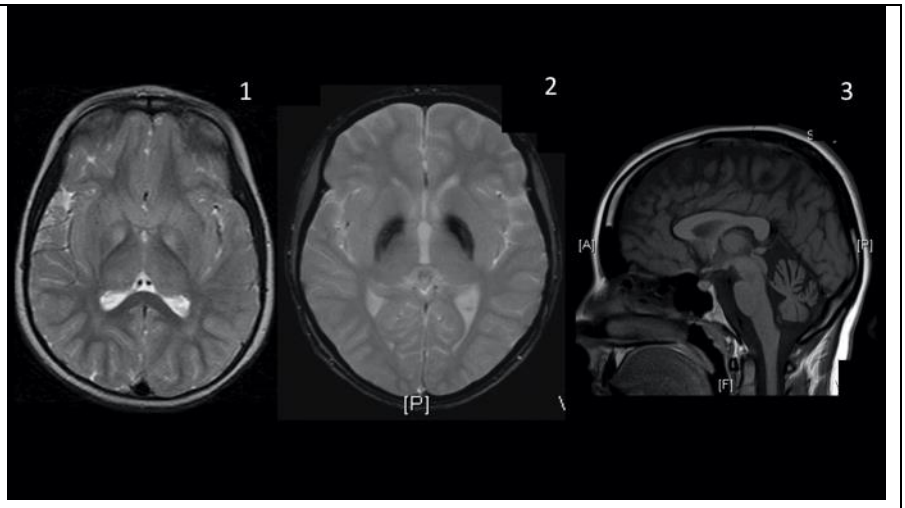
POLR3A	Childhood presentation with cerebellar ataxia, extraphyramidal signs and varying combination of extra-neurological features. It is classified as Hypomyelinating leukodystrophy 7 and the clinical syndrome can make up the 4H syndrome of hypomyelination, hypogonadotropic hypogonadism, and hypodontia. MRI classically shows diffuse hypomyelination along with cerebellar atrophy and thinning of the corpus callosum though variant cases with striatal atrophy and T2W hyperintensities are noted to have less diffuse hypomyelination or no white matter change and may have signal changes in the mid brain, superior cerebellar peduncles and dentate nuclei.
PRKRA	Childhood-onset generalized dystonia and dystonia-parkinsonism non-responsive to levodopa. Bulbar and cranial-cervical dystonia are often prominent. MRI is normal in the majority of cases and striatal T2W hyperintensities with striatal atrophy have been reported in a single case. Autosomal recessive inheritance. Gene: *PRKRA*

PROPIONIC ACIDEMIA	Propionic acidemia is a disorder of amino acid metabolism due to deficiency of propionyl-CoA carboxylase. It can manifest in early or later childhood and can sometimes have an acute encephalopathic presentation with extrapyramidal movement disorder. MRI findings include T2W hyperintensities in the putamen (Figure 1) and sometimes seen in a central linear pattern in the thalami (Figure 1) or the dentate nuclei (Figure 2). Cortical grey matter and corpus callosum atrophy, as well as striatal atrophy, can be seen with disease progression. Autosomal recessive inheritance. Gene: *PCCA,PCCB* 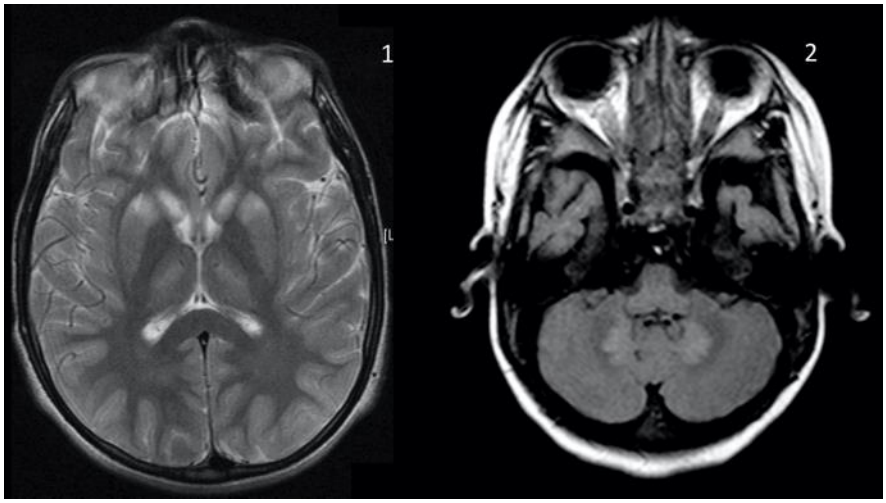
PYRUVATE DEHYDROGENASE COMPLEX DEFICIENCY	The pyruvate dehydrogenase complex (PDHC) of enzymes is responsible for converting pyruvate to acetyl-coenzyme A, which is a rate-limiting step of aerobic glycolysis. The biochemical dysfunction of PDHC and associated lactic acidosis can occur with genetic changes in one of these nuclear encoded mitochondrial genes - *Primary - DLAT, DLD, MPC1, PC, PDHA1, PDHB, PDHX, PDK3, PDP1, PDPR Secondary -LIPT1, LIAS, TPK1, SLC19A3, SLC25A19*. Can be combined with other biochemical changes

	HIBCH, ECHS1, Other genetic associations of functional pyruvate dehydrogenase deficiency are related to mutations in genes that determine the availability of cofactors of PDHC - LIPT1- and LIAS (lipoic acid) and TPK1, SLC19A3 and SLC25A19 (thiamine pyrophosphate) or genetic defects which lead to inhibition of PDHC such as mutations in ECHS1. Clinical presentation can be heterogeneous and some patients can present with episodic encephalopathy and stepwise regression or a leigh syndrome-like phenotype. Predominant globus pallidus T2W hyperintensities, sometimes with associated posterior putaminal involvement is typical when the basal ganglia show abnormality in cases with PDHC deficiency. Diffusion restriction is noted during the acute phases of the disease (Figure 2) 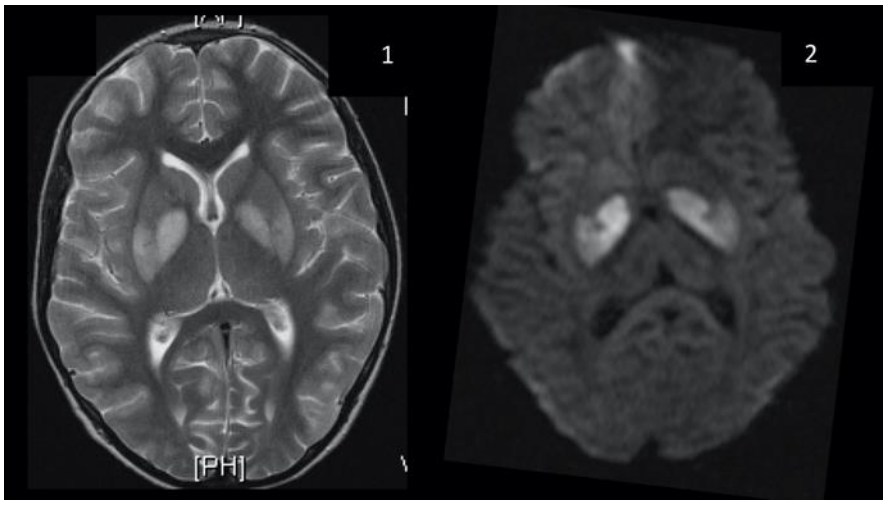
RAB39B	Intellectual disability with juvenile or adult-onset parkinsonism with or without pyramidal signs. Moderate response to levodopa. Affected family members may have intellectual disabilities with autism spectrum disorder, epileptic seizures, and macrocephaly. CT scan may show punctuated pallidal calcifications and MRI may

	show susceptibility and T2W hypointensities in the globus pallidus, putamen, red nuclei and thalami. X-linked recessive inheritance. Gene: *RAB39B*
REPS1	Infantile-onset of trunk hypotonia followed by progressive cerebellar ataxia, pyramidal syndrome. MRI may show T2W hypointensity and susceptibility in the pallidum and peduncles along with cortical and cerebellar atrophy. Autosomal recessive inheritance. Gene: *REPS1*
SCP2	Sterol carrier protein X (SCPx) deficiency leads to the accumulation of branch chain fatty acids. Only two patients reported. Adolescent/Adult-onset cerebellar ataxia, dystonic tremor, nystagmus, hyposmia and deafness. MRI shows T2W hypointensity and susceptibility in the globus pallidus and susbtantia nigra or may show T2W hyperintensities in thalamus, white matter and brainstem. Autosomal recessive inheritance. Gene: *SCP2*
SQSTM1	Childhood-onset ataxia, dysarthria, dystonia, vertical gaze palsy, cognitive decline, dyskinesia. Brain MRI can be normal or in some cases may show mild cerebellar atrophy as well as striatal and pallidal susceptibility likely due to calcification and iron deposition. Autosomal recessive inheritance. Gene: *SQSTM1*
SUCCINIC SEMIALDEHYDE DEHYDROGENASE DEFICIENCY	Succinic semialdehyde dehydrogenase deficiency (SSADH) is a disorder of GABA recycling, detected by 4-hydroxybutyric acid in the urine. Mutations in ALDH5A1 are confirmatory. Symptoms can start in late infancy or early childhood with progressive movement disorders. The pallidum (Figures 1 and 2) and STN commonly show

	T2W hyperintensities with corresponding T1W hypointensities while striatal involvement is rare. Diffusion restriction can be seen acutely. Progressive atrophy can affect the pallidum or the cerebellum. Other regions involved include the thalamus, dentate, white matter and brainstem. Immature myelination has also been reported in some cases. Autosomal recessive inheritance. Gene: *ALDH5A1* 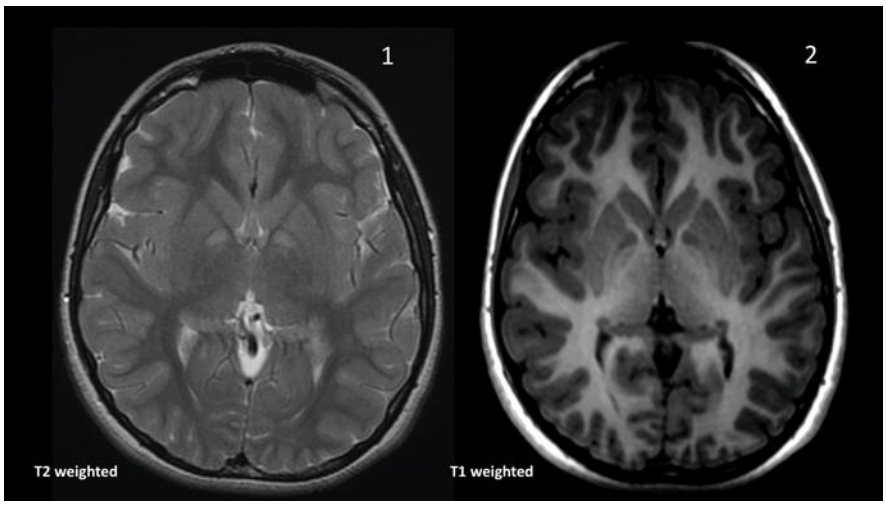
SULFITE OXIDASE AND MOLYBDENUM COFACTOR DEFICIENCY	Disorders of sulfur-containing amino acid metabolism. Neonatal or infant onset of hypotonia and epilepsy. The spectrum includes facial dysmorphism, severe psychomotor retardation, failure to thrive, microcephaly, hyperplexia, lens dislocation and renal stones. CT scan may show calcification in the basal ganglia and thalamus. The characteristic MRI brain findings include progressive subcortical encephalomalacia, T2W hyperintensities in the putamen or pallidum, cerebral atrophy and thinning of the corpus callosum Autosomal recessive inheritance. Genes: *MOCS1, MOCS2, GEPH, SUOX*

THIAMINE RESPONSIVE BASAL GANGLIA DISEASE	Thiamine metabolism dysfunction syndrome-2 (THMD2) or biotin-responsive basal ganglia disease, is a disorder that can manifest with a Leigh like syndrome. It occurs due to mutations in the SLC19A3 gene leading to a cofactor deficiency for the PDHC. The striatum is commonly involved showing swelling and T2W hyperintensity in the acute stage (Figure 1) and the pallidum is rarely abnormal. Changes are also commonly noted in the cortical grey matter and multifocal T2W hyperintensities that may be diffusion restricting can be a clue (Figure 2). Other regions showing abnormalities are the thalamus and midbrain. Diffusion restriction can be noted acutely and the MRI signal changes are often patchy. Treated cases can show resolution of the MRI changes. Late diagnosed or untreated cases can show progressive changes with striatal atrophy and cystic change (Figure 3). Autosomal recessive inheritance. Gene: *SLC19A3*
TUBB4A	Mutations in TUBB4A gene were identified to be associated with the progressive 'Hypomyelination with -atrophy of the basal ganglia and cerebellum (H-ABC syndrome) radiological syndrome described by Van der knaap et al. in 2001. Inheritance is autosomal recessive. The clinical presentation usually starts in early childhood with progressive motor difficulty and dystonia. Choreiform movements and signs of cerebellar dysfunction can be noted. Cognition and speech may be preserved though dysarthria may become apparent with time. Prominent MRI features are cerebellar atrophy (Figure 1) along with hypomyelination (Figure 2). Atrophy

	of the striatum may not be seen in all cases. Susceptibility can be noted in the pallidum (Figure 2) and T2W hypointensities noted in the thalami reflect thalamic myelination that stands out in contrast to undermyelinated surrounding structures. Autosomal dominant inheritance. Gene: *TUBB4A* 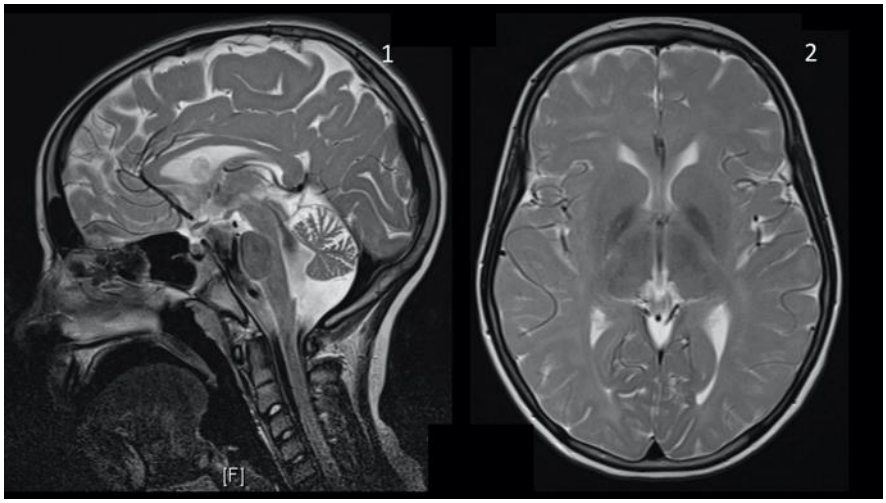
UFM1	Infantile hypotonia and severe global neurodevelopmental delay and seizures. MRI brain show generalised hypomyelination and atrophy of the putamen. The caudate nucleus is atrophic and the caudate head may show T2W hyperintensities. Atrophy of the cortical grey matter, cerebellum and corpus callosum may also be noted and many patients may fulfil clinical criteria for 'Hypomyelination with -atrophy of the basal ganglia and cerebellum (H-ABC syndrome) Autosomal recessive inheritance. Gene: *UFM1*
VAC14	Juvenile onset generalised dystonia or dystonia-parkinsonism, frequent pyramidal signs and rapid progression. No levodopa response. In some patients, bilateral symmetrical T2W hyperintensities in the putamen are seen on MRI. T2W hypointensities and susceptibility in the pallidum and substantia

	nigra suggestive of iron accumulation along with retinitis pigmentosa has been reported in some cases. Autosomal recessive inheritance. Gene: *VAC14*
VIGABATRIN TOXICITY	Vigabatrin can precipitate neuroradiological changes that may sometimes present acutely with an encephalopathy and extrapyramidal movements or may become apparent over a longer time period without a clear encephalopathic correlate. The changes can appear acutely or insidiously over months. These changes may resolve with follow up scans on stopping Vigabatrin, and even while continuing Vigabatrin in some cases. The pattern of abnormalities with T2W hyperintensities in the pallidum (Figure 1), hypothalamus (Figure 2), brainstem and dentate nuclei (Figure 3) is very suggestive of the diagnosis in the correct clinical context. 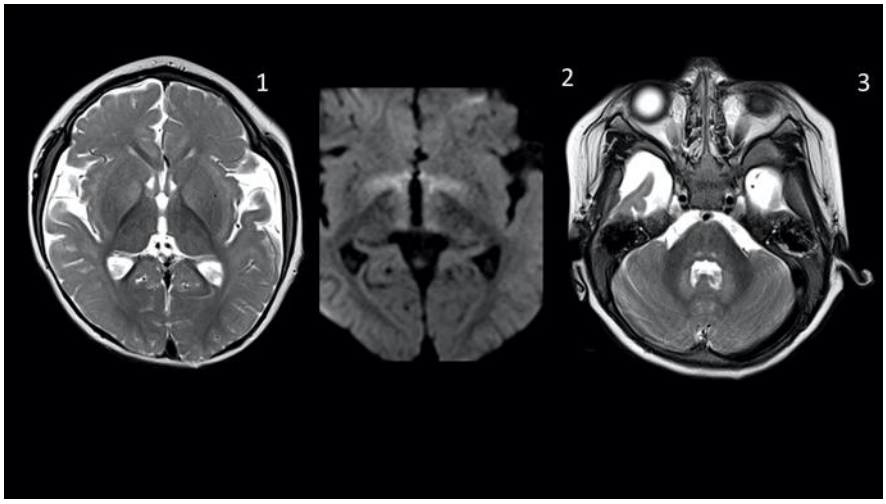
VPS13A	Chorea and dystonia, usually young adult onset with few childhood onset cases described. Erythrocytic acanthocytosis. MRI commonly shows T2W hyperintensity in the striatum along with progressive striatal atrophy. MRI changes reported in few cases include T2W hyperintensities in the white matter, thalamus, pons, cerebral

	peduncles and corpus callosum. Susceptibility in the striatum and pallidum is also reported in few cases. Autosomal recessive inheritance. Gene: *VPS13A*
VPS13D	Childhood to adult-onset ataxia, with frequent pyramidal and extrapyramidal signs such as chorea and dystonia. The disorder progresses to spastic ataxia or generalized dystonia. Saccadic eye intrusions, neuropathy and myoclonus in some families. MRI may show bilateral and symmetrical T2W putaminal and caudate hyperintensities.T2W hyperintensities may also be seen in the globus pallidus, thalamus, white matter, subthalamic nuclei and brainstem. Cerebellar atrophy is mild. Autosomal recessive inheritance. Gene: *VPS13D*
WILSON'S DISEASE	Wilson's disease is a disorder of copper metabolism that leads to accumulation of copper in the liver and later, in the brain. It is associated with mutations in the ATP7B gene. The putamen is the most common basal ganglia nucleus involved with T2W hyperintensities and sometimes a surrounding rim of brighter T2W hyperintensity. Other regions involved include the thalamus, pons, midbrain, cerebellum and white matter. T2W hyperintensities of the ventral midbrain, with relative sparing of the red nuclei can lead to an appearance of the so called "giant panda" face in some cases. T1W hyperintensity and susceptibility are not seen in all cases but can be sometimes noted prominently in the striatum and may denote concomitant iron deposition as noted on autopsy analysis in some cases. Autosomal recessive inheritance. Gene: *ATP7B*

WOODHOUSE SAKATI SYNDROME	Clinical onset commonly in childhood with dysmorphic facial appearance, endocrine dysfunction (diabetes mellitus, hypogonadotropic hypogonadism), alopecia, sensorineural hearing loss, keratoconus and flattened T waves on electrocardiogram. Dystonia is progressive. White matter changes are more common while basal ganglia susceptibility is described in some reports. MRI shows frontal and parietal white matter T2W hyperintensities, susceptibility in the striatum, pallidum, substantia nigra and red nucleus. The pituitary gland shows susceptibility and atrophy. Autosomal recessive inheritance. Gene: *DCAF17*

Supplementary table 6. Publications from literature review used to develop the decision-making tool

Diagnostic category (*Gene symbol if applicable*)	**References for selected publications describing basal ganglia abnormalities**
3-HMG-COA LYASE DEFICIENCY (*HMGCL*)	van der Knaap MS, Bakker HD, Valk J. MR imaging and proton spectroscopy in 3-hydroxy-3-methylglutaryl coenzyme A lyase deficiency. AJNR Am J Neuroradiol 1998; 19(2): 378-82. Yalcinkaya C, Dincer A, Gunduz E, Ficicioglu C, Kocer N, Aydin A. MRI and MRS in HMG-CoA lyase deficiency. Pediatr Neurol 1999; 20(5): 375-80. Zafeiriou DI, Vargiami E, Mayapetek E, Augoustidou-Savvopoulou P, Mitchell GA. 3-Hydroxy-3-methylglutaryl coenzyme a lyase deficiency with reversible white matter changes after treatment. Pediatr Neurol 2007; 37(1): 47-50.
2-Methyl-3-Hydroxybutyryl-CoA Dehydrogenase Deficiency	Cazorla MR, Verdu A, Perez-Cerda C, Ribes A. Neuroimage findings in 2-methyl-3-hydroxybutyryl-CoA dehydrogenase deficiency. Pediatr Neurol 2007; 36(4): 264-7. Sass JO, Forstner R, Sperl W. 2-Methyl-3-hydroxybutyryl-CoA dehydrogenase deficiency: impaired catabolism of isoleucine presenting as neurodegenerative disease. Brain Dev 2004; 26(1): 12-4. Su L, Li X, Lin R, Sheng H, Feng Z, Liu L. Clinical and

	molecular analysis of 6 Chinese patients with isoleucine metabolism defects: identification of 3 novel mutations in the HSD17B10 and ACAT1 gene. Metab Brain Dis 2017; 32(6): 2063-71.
ACERULOPLASMINEMIA	Daimon M, Moriai S, Susa S, Yamatani K, Hosoya T, Kato T. Hypocaeruloplasminaemia with heteroallelic caeruloplasmin gene mutation: MRI of the brain. Neuroradiology 1999; 41(3): 185-7. Grisoli M, Piperno A, Chiapparini L, Mariani R, Savoiardo M. MR imaging of cerebral cortical involvement in aceruloplasminemia. AJNR Am J Neuroradiol 2005; 26(3): 657-61.
ACUTE DISSEMINATED ENCEPHALOMYELITIS	Alper G, Heyman R, Wang L. Multiple sclerosis and acute disseminated encephalomyelitis diagnosed in children after long-term follow-up: comparison of presenting features. Dev Med Child Neurol 2009; 51(6): 480-6. Anlar B, Basaran C, Kose G, Guven A, Haspolat S, Yakut A, *et al.* Acute disseminated encephalomyelitis in children: outcome and prognosis. Neuropediatrics 2003; 34(4): 194-9. Atzori M, Battistella PA, Perini P, Calabrese M, Fontanin M, Laverda AM, *et al.* Clinical and diagnostic aspects of multiple sclerosis and acute monophasic encephalomyelitis in pediatric patients: a single centre prospective study. Mult Scler 2009; 15(3): 363-70. Baum PA, Barkovich AJ, Koch TK, Berg BO. Deep gray matter involvement in children with acute disseminated encephalomyelitis. AJNR Am J Neuroradiol 1994; 15(7): 1275-83. Callen DJ, Shroff MM, Branson HM, Li DK, Lotze T, Stephens D, *et al.* Role of MRI in the differentiation of ADEM from MS in children. Neurology 2009; 72(11): 968-73. Dale RC, Church AJ, Cardoso F, Goddard E, Cox TC, Chong WK, *et al.* Poststreptococcal acute disseminated encephalomyelitis with basal ganglia involvement and auto-reactive antibasal ganglia antibodies. Ann Neurol 2001; 50(5): 588-95. Dale RC, de Sousa C, Chong WK, Cox TC, Harding B, Neville BG. Acute disseminated encephalomyelitis, multiphasic disseminated encephalomyelitis and multiple sclerosis in children. Brain : a journal of neurology 2000; 123 Pt 12: 2407-22. Gupte G, Stonehouse M, Wassmer E, Coad NA, Whitehouse WP. Acute disseminated encephalomyelitis: a review of 18 cases in childhood. Journal of paediatrics and child health 2003; 39(5): 336-42. Hung KL, Liao HT, Tsai ML. The spectrum of postinfectious encephalomyelitis. Brain Dev 2001; 23(1): 42-5. Hynson JL, Kornberg AJ, Coleman LT, Shield L, Harvey AS, Kean MJ. Clinical and neuroradiologic features of acute disseminated encephalomyelitis in children. Neurology 2001;

	56(10): 1308-12. Khong PL, Ho HK, Cheng PW, Wong VC, Goh W, Chan FL. Childhood acute disseminated encephalomyelitis: the role of brain and spinal cord MRI. Pediatr Radiol 2002; 32(1): 59-66. Leake JA, Albani S, Kao AS, Senac MO, Billman GF, Nespeca MP, *et al.* Acute disseminated encephalomyelitis in childhood: epidemiologic, clinical and laboratory features. Pediatr Infect Dis J 2004; 23(8): 756-64. Madan S, Aneja S, Tripathi RP, Batra A, Seth A, Taluja V. Acute disseminated encephalomyelitis--a case series. Indian Pediatr 2005; 42(4): 367-71. Mikaeloff Y, Caridade G, Husson B, Suissa S, Tardieu M, Neuropediatric KSGotFNS. Acute disseminated encephalomyelitis cohort study: prognostic factors for relapse. European journal of paediatric neurology : EJPN : official journal of the European Paediatric Neurology Society 2007; 11(2): 90-5. Murthy SN, Faden HS, Cohen ME, Bakshi R. Acute disseminated encephalomyelitis in children. Pediatrics 2002; 110(2 Pt 1): e21. Richer LP, Sinclair DB, Bhargava R. Neuroimaging features of acute disseminated encephalomyelitis in childhood. Pediatr Neurol 2005; 32(1): 30-6. Singhi PD, Ray M, Singhi S, Kumar Khandelwal N. Acute disseminated encephalomyelitis in North Indian children: clinical profile and follow-up. J Child Neurol 2006; 21(10): 851-7. Visudtibhan A, Tuntiyathorn L, Vaewpanich J, Sukjit P, Khongkatithum C, Thampratankul L, *et al.* Acute disseminated encephalomyelitis: a 10-year cohort study in Thai children. European journal of paediatric neurology : EJPN : official journal of the European Paediatric Neurology Society 2010; 14(6): 513-8.
ACUTE NECROTIZING ENCEPHALOPATHY	Denier C, Balu L, Husson B, Nasser G, Burglen L, Rodriguez D, *et al.* Familial acute necrotizing encephalopathy due to mutation in the RANBP2 gene. Journal of the neurological sciences 2014; 345(1-2): 236-8. Mizuguchi M. Acute necrotizing encephalopathy of childhood: a novel form of acute encephalopathy prevalent in Japan and Taiwan. Brain Dev 1997; 19(2): 81-92. Mizuguchi M, Yamanouchi H, Ichiyama T, Shiomi M. Acute encephalopathy associated with influenza and other viral infections. Acta Neurol Scand 2007; 115(4 Suppl): 45-56. Neilson DE. The interplay of infection and genetics in acute necrotizing encephalopathy. Current opinion in pediatrics 2010; 22(6): 751-7. Ravid S, Topper L, Eviatar L. Acute necrotizing encephalopathy presenting as a basal ganglia syndrome. J Child Neurol 2001; 16(6): 461-2. Singh RR, Sedani S, Lim M, Wassmer E, Absoud M. RANBP2 mutation and acute necrotizing encephalopathy: 2 cases and a literature review of the expanding clinico-radiological phenotype.

	European journal of paediatric neurology : EJPN : official journal of the European Paediatric Neurology Society 2015; 19(2): 106-13.
AFG3L2	Eskandrani A, AlHashem A, Ali ES, AlShahwan S, Tlili K, Hundallah K, *et al.* Recessive AFG3L2 Mutation Causes Progressive Microcephaly, Early Onset Seizures, Spasticity, and Basal Ganglia Involvement. Pediatr Neurol 2017; 71: 24-8. Tunc S, Dulovic-Mahlow M, Baumann H, Baaske MK, Jahn M, Junker J, *et al.* Spinocerebellar Ataxia Type 28-Phenotypic and Molecular Characterization of a Family with Heterozygous and Compound-Heterozygous Mutations in AFG3L2. Cerebellum 2019; 18(4): 817-22.
ADAR1	La Piana R, Uggetti C, Olivieri I, Tonduti D, Balottin U, Fazzi E, *et al.* Bilateral striatal necrosis in two subjects with Aicardi-Goutieres syndrome due to mutations in ADAR1 (AGS6). Am J Med Genet A 2014; 164A(3): 815-9. Livingston JH, Lin JP, Dale RC, Gill D, Brogan P, Munnich A, *et al.* A type I interferon signature identifies bilateral striatal necrosis due to mutations in ADAR1. J Med Genet 2014; 51(2): 76-82.
ALEXANDER DISEASE (*GFAP*)	Barkovich AJ. Pediatric neuroimaging: Lippincott Williams & Wilkins; 2005. van der Knaap MS, Naidu S, Breiter SN, Blaser S, Stroink H, Springer S, *et al.* Alexander disease: diagnosis with MR imaging. AJNR Am J Neuroradiol 2001; 22(3): 541-52.
ALPHA MANNOSIDOSIS (*MAN2B1*)	Zoons E, de Koning TJ, Abeling NG, Tijssen MA. Neurodegeneration with Brain Iron Accumulation on MRI: An Adult Case of alpha-Mannosidosis. JIMD Rep 2012; 4: 99-102.
AP4 deficiency *(AP4E1, AP4M1, AP4S1)*	Moreno-De-Luca A, Helmers SL, Mao H, Burns TG, Melton AM, Schmidt KR, *et al.* Adaptor protein complex-4 (AP-4) deficiency causes a novel autosomal recessive cerebral palsy syndrome with microcephaly and intellectual disability. J Med Genet 2011; 48(2): 141-4. Roubertie A, Hieu N, Roux CJ, Leboucq N, Manes G, Charif M, *et al.* AP4 deficiency: A novel form of neurodegeneration with brain iron accumulation? Neurol Genet 2018; 4(1): e217. Vill K, Muller-Felber W, Alhaddad B, Strom TM, Teusch V, Weigand H, *et al.* A homozygous splice variant in AP4S1 mimicking neurodegeneration with brain iron accumulation. Mov Disord 2017; 32(5): 797-9.
ASPARTYLGLUCOSAMINURIA (*AGA*)	Arvio M, Mononen I. Aspartylglycosaminuria: a review. Orphanet Journal of Rare Diseases 2016; 11(1): 162. Autti T, Lonnqvist T, Joensuu R. Bilateral pulvinar signal intensity decrease on T2-weighted images in patients with aspartylglucosaminuria. Acta Radiol 2008; 49(6): 687-92. Tokola AM, Aberg LE, Autti TH. Brain MRI findings in aspartylglucosaminuria. J Neuroradiol 2015; 42(6): 345-57.
AUTOIMMUNE BASAL GANGLIA ENCEPHALITIS	Dale RC, Merheb V, Pillai S, Wang D, Cantrill L, Murphy TK, *et al.* Antibodies to surface dopamine-2 receptor in autoimmune movement and psychiatric disorders. Brain : a journal of

	neurology 2012; 135(Pt 11): 3453-68.
BETA KETOTHIOLASE DEFICIENCY (*ACAT1*)	Buhas D, Bernard G, Fukao T, Decarie JC, Chouinard S, Mitchell GA. A treatable new cause of chorea: beta-ketothiolase deficiency. Mov Disord 2013; 28(8): 1054-6. O'Neill ML, Kuo F, Saigal G. MRI of pallidal involvement in Beta-ketothiolase deficiency. J Neuroimaging 2014; 24(4): 414-7. Tortori-Donati P, Rossi A. Pediatric Neuroradiology: Brain. Head, Neck and Spine: Springer Science & Business Media; 2005. Wojcik MH, Wierenga KJ, Rodan LH, Sahai I, Ferdinandusse S, Genetti CA, *et al.* Beta-Ketothiolase Deficiency Presenting with Metabolic Stroke After a Normal Newborn Screen in Two Individuals. JIMD Rep 2018; 39: 45-54.
BETA PROPELLER PROTEIN ASSOCIATED NEURODEGENERATION (*WDR45*)	Haack TB, Hogarth P, Gregory A, Prokisch H, Hayflick SJ. BPAN: the only X-linked dominant NBIA disorder. Int Rev Neurobiol 2013; 110: 85-90. Haack TB, Hogarth P, Kruer MC, Gregory A, Wieland T, Schwarzmayr T, *et al.* Exome sequencing reveals de novo WDR45 mutations causing a phenotypically distinct, X-linked dominant form of NBIA. Am J Hum Genet 2012; 91(6): 1144-9. Kimura Y, Sato N, Sugai K, Maruyama S, Ota M, Kamiya K, *et al.* MRI, MR spectroscopy, and diffusion tensor imaging findings in patient with static encephalopathy of childhood with neurodegeneration in adulthood (SENDA). Brain Dev 2013; 35(5): 458-61. Kruer MC, Boddaert N, Schneider SA, Houlden H, Bhatia KP, Gregory A, *et al.* Neuroimaging features of neurodegeneration with brain iron accumulation. AJNR Am J Neuroradiol 2012; 33(3): 407-14. Nakashima M, Takano K, Tsuyusaki Y, Yoshitomi S, Shimono M, Aoki Y, *et al.* WDR45 mutations in three male patients with West syndrome. J Hum Genet 2016; 61(7): 653-61. Nishioka K, Oyama G, Yoshino H, Li Y, Matsushima T, Takeuchi C, *et al.* High frequency of beta-propeller protein-associated neurodegeneration (BPAN) among patients with intellectual disability and young-onset parkinsonism. Neurobiol Aging 2015; 36(5): 2004 e9- e15. Schneider SA, Dusek P, Hardy J, Westenberger A, Jankovic J, Bhatia KP. Genetics and Pathophysiology of Neurodegeneration with Brain Iron Accumulation (NBIA). Curr Neuropharmacol 2013; 11(1): 59-79. Van Goethem G, Livingston JH, Warren D, Oojageer AJ, Rice GI, Crow YJ. Basal ganglia calcification in a patient with beta-propeller protein-associated neurodegeneration. Pediatr Neurol 2014; 51(6): 843-5. Yoganathan S, Arunachal G, Sudhakar SV, Rajaraman V, Thomas M, Danda S. Beta Propellar Protein-Associated

	Neurodegeneration: A Rare Cause of Infantile Autistic Regression and Intracranial Calcification. Neuropediatrics 2016; 47(2): 123-7.
CANAVAN DISEASE (*ASPA*)	Surendran S, Bamforth FJ, Chan A, Tyring SK, Goodman SI, Matalon R. Mild elevation of N-acetylaspartic acid and macrocephaly: diagnostic problem. J Child Neurol. 2003;18:809–12. Yalcinkaya C, Benbir G, Salomons GS, Karaarslan E, Rolland MO, Jakobs C, van der Knaap MS. Atypical MRI findings in Canavan disease: a patient with a mild course. Neuropediatrics. 2005;36:336–9 van der Knaap MS, Valk J. Canavan Disease. Magnetic Resonance of Myelination and Myelin Disorders 2005: 326-33.
CARASAL (*CTSA*)	Bugiani M, Kevelam SH, Bakels HS, Waisfisz Q, Ceuterick-de Groote C, Niessen HW, *et al.* Cathepsin A-related arteriopathy with strokes and leukoencephalopathy (CARASAL). Neurology 2016; 87(17): 1777-86.
CARBON MONOXIDE POISONING	Hopkins RO, Fearing MA, Weaver LK, Foley JF. Basal ganglia lesions following carbon monoxide poisoning. Brain Inj 2006; 20(3): 273-81. O'Donnell P, Buxton PJ, Pitkin A, Jarvis LJ. The magnetic resonance imaging appearances of the brain in acute carbon monoxide poisoning. Clin Radiol 2000; 55(4): 273-80.
CERBROTENDINOUS XANTHOMATOSIS (*CTX*)	Barkhof F, Verrips A, Wesseling P, van Der Knaap MS, van Engelen BG, Gabreels FJ, *et al.* Cerebrotendinous xanthomatosis: the spectrum of imaging findings and the correlation with neuropathologic findings. Radiology 2000; 217(3): 869-76. Pudhiavan A, Agrawal A, Chaudhari S, Shukla A. Cerebrotendinous xanthomatosis--the spectrum of imaging findings. J Radiol Case Rep 2013; 7(4): 1-9.
CEREBRAL CREATINE DEFICIENCY SYNDROMES 1, 2, 3 (*SLC6A8, GAMT, AGAT*)	Osaka H, Takagi A, Tsuyusaki Y, Wada T, Iai M, Yamashita S, *et al.* Contiguous deletion of SLC6A8 and BAP31 in a patient with severe dystonia and sensorineural deafness. Mol Genet Metab 2012; 106(1): 43-7. Viau KS, Ernst SL, Pasquali M, Botto LD, Hedlund G, Longo N. Evidence-based treatment of guanidinoacetate methyltransferase (GAMT) deficiency. Mol Genet Metab 2013; 110(3): 255-62.
CHILDHOOD-ONSET-DYSTONIA-28 (*KMT2B*)	Meyer E, Carss KJ, Rankin J, Nichols JM, Grozeva D, Joseph AP, et al. Mutations in the histone methyltransferase gene KMT2B cause complex early-onset dystonia. Nat Genet 2017; 49(2): 223-37.
CHOLINE TRANSPORTER-LIKE 1 DEFICIENCY *(SLC44A1)*	Fagerberg CR, Taylor A, Distelmaier F, Schroder HD, Kibaek M, Wieczorek D, et al. Choline transporter-like 1 deficiency causes a new type of childhood-onset neurodegeneration. Brain 2019; 143(1): 94-111.
COCKAYNE SYNDROME TYPE A AND TYPE B (*ERCC8, ERCC6*)	Demaerel P, Kendall BE, Kingsley D. Cranial CT and MRI in diseases with DNA repair defects. Neuroradiology 1992; 34(2): 117-21. Koob M, Laugel V, Durand M, Fothergill H, Dalloz C,

	Sauvanaud F, *et al.* Neuroimaging in Cockayne syndrome. AJNR Am J Neuroradiol 2010; 31(9): 1623-30. Koob M, Rousseau F, Laugel V, Meyer N, Armspach JP, Girard N, *et al.* Cockayne syndrome: a diffusion tensor imaging and volumetric study. Br J Radiol 2016; 89(1067): 20151033. Simon B, Oommen SP, Shah K, Mani SE, Gibikote S. Cockayne syndrome: characteristic neuroimaging features. Acta neurologica Belgica 2015; 115(3): 427-8. Wagner MW, Poretti A, Wang T, Crawford TO, Huisman TA, Bosemani T. Susceptibility-weighted imaging for calcification in Cockayne syndrome. J Pediatr 2014; 165(2): 416- e1.
CONGENITAL DISORDER OF GLYCOSYLATION, TYPE IIn (*SLC39A8*)	Riley LG, Cowley MJ, Gayevskiy V, Roscioli T, Thorburn DR, Prelog K, *et al.* A SLC39A8 variant causes manganese deficiency, and glycosylation and mitochondrial disorders. J Inherit Metab Dis 2016. Park, J. H., Hogrebe, M., Gruneberg, M., DuChesne, I., von der Heiden, A. L., Reunert, J., Schlingmann, K. P., Boycott, K. M., Beaulieu, C. L., Mhanni, A. A., Innes, A. M., Hortnagel, K., and 12 others. SLC39A8 deficiency: a disorder of manganese transport and glycosylation. Am. J. Hum. Genet. 97: 894-903, 2015.
COPAN (*COASY*)	Dusi S, Valletta L, Haack TB, Tsuchiya Y, Venco P, Pasqualato S, *et al.* Exome sequence reveals mutations in CoA synthase as a cause of neurodegeneration with brain iron accumulation. Am J Hum Genet 2014; 94(1): 11-22. Evers C, Seitz A, Assmann B, Opladen T, Karch S, Hinderhofer K, *et al.* Diagnosis of CoPAN by whole exome sequencing: Waking up a sleeping tiger's eye. Am J Med Genet A 2017; 173(7): 1878-86. Yoganathan S, Sudhakar SV, Thomas M, Dutta AK, Danda S. "Eye of tiger sign" mimic in an adolescent boy with mitochondrial membrane protein associated neurodegeneration (MPAN). Brain Dev 2016; 38(5): 516-9.
CRAT	Drecourt A, Babdor J, Dussiot M, Petit F, Goudin N, Garfa-Traore M, et al. Impaired Transferrin Receptor Palmitoylation and Recycling in Neurodegeneration with Brain Iron Accumulation. Am J Hum Genet 2018; 102(2): 266-77.
CYANIDE POISONING	Beltz EE, Mullins ME. Radiological reasoning: hyperintensity of the basal ganglia and cortex on FLAIR and diffusion-weighted imaging. AJR Am J Roentgenol 2010; 195(3 Suppl): S1-8 (Quiz S9-11). Rachinger J, Fellner FA, Stieglbauer K, Trenkler J. MR changes after acute cyanide intoxication. AJNR Am J Neuroradiol 2002; 23(8): 1398-401.
DNAJC19	Al Teneiji A, Siriwardena K, George K, Mital S, Mercimek-Mahmutoglu S. Progressive Cerebellar Atrophy and a Novel Homozygous Pathogenic DNAJC19 Variant as a Cause of Dilated Cardiomyopathy Ataxia Syndrome. Pediatr Neurol 2016; 62: 58-61. Ucar SK, Mayr JA, Feichtinger RG, Canda E, Coker M,

	Wortmann SB. Previously Unreported Biallelic Mutation in DNAJC19: Are Sensorineural Hearing Loss and Basal Ganglia Lesions Additional Features of Dilated Cardiomyopathy and Ataxia (DCMA) Syndrome? JIMD Rep 2017; 35: 39-45.
EPHEDRONE / MANGANESE TOXICITY	Varlibas F, Delipoyraz I, Yuksel G, Filiz G, Tireli H, Gecim NO. Neurotoxicity following chronic intravenous use of "Russian cocktail". Clin Toxicol (Phila) 2009; 47(2): 157-60.
ETHYLENE GLYCOL TOXICITY	Malhotra A, Mongelluzzo G, Wu X, Durand D, Kalra VB, LeSar B, *et al.* Ethylene glycol toxicity : MRI brain findings. Clin Neuroradiol 2017; 27(1): 109-13. Moore MM, Kanekar SG, Dhamija R. Ethylene Glycol Toxicity: Chemistry, Pathogenesis, and Imaging. Radiol Case Rep 2008; 3(1): 122.
FAHN (*FA2H*)	Edvardson S, Hama H, Shaag A, Gomori JM, Berger I, Soffer D, *et al.* Mutations in the fatty acid 2-hydroxylase gene are associated with leukodystrophy with spastic paraparesis and dystonia. Am J Hum Genet 2008; 83(5): 643-8. Kruer MC, Paisan-Ruiz C, Boddaert N, Yoon MY, Hama H, Gregory A, *et al.* Defective FA2H leads to a novel form of neurodegeneration with brain iron accumulation (NBIA). Ann Neurol 2010; 68(5): 611-8. Salomao RP, Pedroso JL, Gama MT, Dutra LA, Maciel RH, Godeiro-Junior C, *et al.* A diagnostic approach for neurodegeneration with brain iron accumulation: clinical features, genetics and brain imaging. Arquivos de neuro-psiquiatria 2016; 74(7): 587-96.
FUCOSIDOSIS (*FUCA1*)	Galluzzi P, Rufa A, Balestri P, Cerase A, Federico A. MR brain imaging of fucosidosis type I. AJNR Am J Neuroradiol 2001; 22(4): 777-80. Kau T, Karlo C, Gungor T, Prietsch V, Kellenberger CJ, Scheer I, *et al.* Increased cerebellar volume in the early stage of fucosidosis: a case control study. Neuroradiology 2011; 53(7): 509-16. Oner AY, Cansu A, Akpek S, Serdaroglu A. Fucosidosis: MRI and MRS findings. Pediatr Radiol 2007; 37(10): 1050-2. Provenzale JM, Barboriak DP, Sims K. Neuroradiologic findings in fucosidosis, a rare lysosomal storage disease. AJNR Am J Neuroradiol 1995; 16(4 Suppl): 809-13. Steenweg ME, Vanderver A, Blaser S, Bizzi A, de Koning TJ, Mancini GM, *et al.* Magnetic resonance imaging pattern recognition in hypomyelinating disorders. Brain : a journal of neurology 2010; 133(10): 2971-82. Zubarioglu T, Kiykim E, Zeybek CA, Cansever MS, Benbir G, Aydin A, *et al.* Clinical and neuroradiological approach to fucosidosis in a child with atypical presentation. Annals of Indian Academy of Neurology 2015; 18(4): 471.

GANGLIOSIDOSES GM1 AND GM2 (*GLB1*, *HEXA*, *GM2A*)	De Grandis E, Di Rocco M, Pessagno A, Veneselli E, Rossi A. MR imaging findings in 2 cases of late infantile GM1 gangliosidosis. AJNR Am J Neuroradiol 2009; 30(7): 1325-7. Fukumizu M, Yoshikawa H, Takashima S, Sakuragawa N, Kurokawa T. Tay-Sachs disease: progression of changes on neuroimaging in four cases. Neuroradiology 1992; 34(6): 483-6. Gururaj A, Sztriha L, Hertecant J, Johansen JG, Georgiou T, Campos Y, *et al.* Magnetic resonance imaging findings and novel mutations in GM1 gangliosidosis. J Child Neurol 2005; 20(1): 57-60. Inui K, Namba R, Ihara Y, Nobukuni K, Taniike M, Midorikawa M, *et al.* A case of chronic GM1 gangliosidosis presenting as dystonia: clinical and biochemical studies. Journal of neurology 1990; 237(8): 491-3. Koelfen W, Freund M, Jaschke W, Koenig S, Schultze C. GM-2 gangliosidosis (Sandhoff's disease): two year follow-up by MRI. Neuroradiology 1994; 36(2): 152-4. Uyama E, Terasaki T, Watanabe S, Naito M, Owada M, Araki S, *et al.* Type 3 GM1 gangliosidosis: characteristic MRI findings correlated with dystonia. Acta Neurol Scand 1992; 86(6): 609-15. Yoshikawa H, Yamada K, Sakuragawa N. MRI in the early stage of Tay-Sachs disease. Neuroradiology 1992; 34(5): 394-5.
GIANT AXONAL NEUROPATHY (*GAN*)	Hentati F, Hentati E, Amouri R. Giant axonal neuropathy. Handb Clin Neurol 2013; 115: 933-8.
GLUTARIC ACIDURIA TYPE I (*GCDH*)	Aicardi J, Goutieres F, Saudubray JM, Ogier H. CT scans of infants with glutaric aciduria. Dev Med Child Neurol 1985; 27(3): 403-4. Amir N, Elpeleg ON, Shalev RS, Christensen E. Glutaric aciduria type I: enzymatic and neuroradiologic investigations of two kindreds. J Pediatr 1989; 114(6): 983-9. Drigo P, Piovan S, Battistella PA, Della Puppa A, Burlina AB. Macrocephaly, subarachnoid fluid collection, and glutaric aciduria type I. J Child Neurol 1996; 11(5): 414-7. Hedlund GL, Longo N, Pasquali M. Glutaric acidemia type 1. Am J Med Genet C Semin Med Genet 2006; 142C(2): 86-94. Nunes J, Loureiro S, Carvalho S, Pais RP, Alfaiate C, Faria A, *et al.* Brain MRI findings as an important diagnostic clue in glutaric aciduria type 1. Neuroradiol J 2013; 26(2): 155-61. Twomey EL, Naughten ER, Donoghue VB, Ryan S. Neuroimaging findings in glutaric aciduria type 1. Pediatr Radiol 2003; 33(12): 823-30. Woelfle J, Kreft B, Emons D, Haverkamp F. Subdural hemorrhage as an initial sign of glutaric aciduria type 1: a diagnostic pitfall. Pediatr Radiol 1996; 26(11): 779-81. Yager JY, McClarty BM, Seshia SS. CT-scan findings in an infant with glutaric aciduria type I. Dev Med Child Neurol 1988; 30(6): 808-11.
GTPBP2	Drecourt A, Babdor J, Dussiot M, Petit F, Goudin N, Garfa-Traore M, et al. Impaired Transferrin Receptor Palmitoylation and Recycling in Neurodegeneration with Brain Iron

	Accumulation. Am J Hum Genet 2018; 102(2): 266-77. Jaberi E, Rohani M, Shahidi GA, Nafissi S, Arefian E, Soleimani M, et al. Identification of mutation in GTPBP2 in patients of a family with neurodegeneration accompanied by iron deposition in the brain. Neurobiol Aging 2016; 38: 216 e11- e18.
HAEMOLYTIC URAEMIC SYNDROME	DiMario FJ, Jr., Bronte-Stewart H, Sherbotie J, Turner ME. Lacunar infarction of the basal ganglia as a complication of hemolytic-uremic syndrome. MRI and clinical correlations. Clin Pediatr (Phila) 1987; 26(11): 586-90. Jeong YK, Kim IO, Kim WS, Hwang YS, Choi Y, Yeon KM. Hemolytic uremic syndrome: MR findings of CNS complications. Pediatr Radiol 1994; 24(8): 585-6. Sherwood JW, Wagle WA. Hemolytic uremic syndrome: MR findings of CNS complications. AJNR Am J Neuroradiol 1991; 12(4): 703-4.
HYPERMANGANESEMIA WITH DYSTONIA 1 (*SLC30A10*)	Quadri M, Kamate M, Sharma S, Olgiati S, Graafland J, Breedveld GJ, *et al.* Manganese transport disorder: novel SLC30A10 mutations and early phenotypes. Movement disorders : official journal of the Movement Disorder Society 2015; 30(7): 996-1001. Stamelou M, Tuschl K, Chong WK, Burroughs AK, Mills PB, Bhatia KP, *et al.* Dystonia with brain manganese accumulation resulting from SLC30A10 mutations: a new treatable disorder. Movement disorders : official journal of the Movement Disorder Society 2012; 27(10): 1317-22. Tuschl K, Clayton PT, Gospe SM, Jr., Gulab S, Ibrahim S, Singhi P, *et al.* Syndrome of hepatic cirrhosis, dystonia, polycythemia, and hypermanganesemia caused by mutations in SLC30A10, a manganese transporter in man. Am J Hum Genet 2012; 90(3): 457-66.
HYPERMANGANESEMIA WITH DYSTONIA 2 (SLC39A14)	Tuschl K, Meyer E, Valdivia LE, Zhao N, Dadswell C, Abdul-Sada A, *et al.* Mutations in SLC39A14 disrupt manganese homeostasis and cause childhood-onset parkinsonism-dystonia. Nat Commun 2016; 7: 11601.
HYPOXIC ISCHAEMIC ENCEPHALOPATHY (TERM NEONATES)	Griffiths PD, Radon MR, Crossman AR, Zurakowski D, Connolly DJ. Anatomic localization of dyskinesia in children with "profound" perinatal hypoxic-ischemic injury. AJNR Am J Neuroradiol 2010; 31(3): 436-41. Huang BY, Castillo M. Hypoxic-ischemic brain injury: imaging findings from birth to adulthood. Radiographics 2008; 28(2): 417-39; quiz 617. Maller AI, Hankins LL, Yeakley JW, Butler IJ. Rolandic type cerebral palsy in children as a pattern of hypoxic-ischemic injury in the full-term neonate. J Child Neurol 1998; 13(7): 313-21. Rademakers RP, van der Knaap MS, Verbeeten B, Jr., Barth PG, Valk J. Central cortico-subcortical involvement: a distinct pattern of brain damage caused by perinatal and postnatal asphyxia in term infants. J Comput Assist Tomogr 1995; 19(2): 256-63.
IDIOPATHIC BASAL GANGLIA CALCIFICATION	Batla A, Bhatia KP. A new gene for Fahr's syndrome-PDGF-B. Movement disorders : official journal of the Movement Disorder

(FAHR'S DISEASE) (*SLC20A2, XPR1, PDGFRB, PDGFB, MYORG*)	Society 2014; 29(3): 307. Batla A, Tai XY, Schottlaender L, Erro R, Balint B, Bhatia KP. Deconstructing Fahr's disease/syndrome of brain calcification in the era of new genes. Parkinsonism & related disorders 2016. Giovannini D, Touhami J, Charnet P, Sitbon M, Battini JL. Inorganic phosphate export by the retrovirus receptor XPR1 in metazoans. Cell Rep 2013; 3(6): 1866-73. Livingston JH, Stivaros S, van der Knaap MS, Crow YJ. Recognizable phenotypes associated with intracranial calcification. Dev Med Child Neurol 2013; 55(1): 46-57. Nicolas G, Pottier C, Maltete D, Coutant S, Rovelet-Lecrux A, Legallic S, *et al.* Mutation of the PDGFRB gene as a cause of idiopathic basal ganglia calcification. Neurology 2013; 80(2): 181-7. Tadic V, Westenberger A, Domingo A, Alvarez-Fischer D, Klein C, Kasten M. Primary familial brain calcification with known gene mutations: a systematic review and challenges of phenotypic characterization. JAMA neurology 2015; 72(4): 460-7. Wang C, Li Y, Shi L, Ren J, Patti M, Wang T, *et al.* Mutations in SLC20A2 link familial idiopathic basal ganglia calcification with phosphate homeostasis. Nat Genet 2012; 44(3): 254-6.
INFECTIOUS ENCEPHALITIS	Abe T, Kojima K, Shoji H, Tanaka N, Fujimoto K, Uchida M, *et al.* Japanese encephalitis. J Magn Reson Imaging 1998; 8(4): 755-61. Al-Mateen M, Gibbs M, Dietrich R, Mitchell WG, Menkes JH. Encephalitis lethargica-like illness in a girl with mycoplasma infection. Neurology 1988; 38(7): 1155-8. Brandel JP, Vidailhet M, Noseda G, Harpey JP, Agid Y. Mycoplasma pneumoniae postinfectious encephalomyelitis with bilateral striatal necrosis. Movement disorders : official journal of the Movement Disorder Society 1996; 11(3): 333-6. Einsiedel L, Kat E, Ravindran J, Slavotinek J, Gordon DL. MR findings in Murray Valley encephalitis. AJNR Am J Neuroradiol 2003; 24(7): 1379-82. Francis JR, Nourse C, Vaska VL, Calvert S, Northill JA, McCall B, *et al.* Australian Bat Lyssavirus in a child: the first reported case. Pediatrics 2014; 133(4): e1063-7. Freund A, Zass R, Kurlemann G, Schuierer G, Ullrich K. Bilateral oedema of the basal ganglia in an echovirus type 21 infection: complete clinical and radiological normalization. Dev Med Child Neurol 1998; 40(6): 421-4. Fusco C, Bonini E, Soncini G, Frattini D, Giovannini S, Della Giustina E. Transient basal ganglia and thalamic involvement following Mycoplasma pneumoniae infection associated with antiganglioside antibodies. J Child Neurol 2010; 25(8): 1029-33. Handique SK, Das RR, Barman K, Medhi N, Saharia B, Saikia P, *et al.* Temporal lobe involvement in Japanese encephalitis: problems in differential diagnosis. AJNR Am J Neuroradiol

2006; 27(5): 1027-31.
Hausler M, Ramaekers VT, Doenges M, Schweizer K, Ritter K, Schaade L. Neurological complications of acute and persistent Epstein-Barr virus infection in paediatric patients. J Med Virol 2002; 68(2): 253-63.
Jain H, Deshpande A, Favaz AM, Rajagopal KV. MRI in rabies encephalitis. BMJ Case Rep 2013; 2013.
Kalita J, Misra UK. Comparison of CT scan and MRI findings in the diagnosis of Japanese encephalitis. Journal of the neurological sciences 2000a; 174(1): 3-8.
Kalita J, Misra UK. The substantia nigra is also involved in Japanese encephalitis. AJNR Am J Neuroradiol 2000b; 21(10): 1978-80.
Kalita J, Misra UK, Pandey S, Dhole TN. A comparison of clinical and radiological findings in adults and children with Japanese encephalitis. Archives of neurology 2003; 60(12): 1760-4.
Kim JS, Choi IS, Lee MC. Reversible parkinsonism and dystonia following probable mycoplasma pneumoniae infection. Movement disorders : official journal of the Movement Disorder Society 1995; 10(4): 510-2.
Kubo T, Sato K, Kobayashi D, Motegi A, Kobayashi O, Takeshita S, *et al.* A case of HHV-6 associated acute necrotizing encephalopathy with increase of CD56bright NKcells. Scand J Infect Dis 2006; 38(11-12): 1122-5.
Kullnat MW, Morse RP. Choreoathetosis after herpes simplex encephalitis with basal ganglia involvement on MRI. Pediatrics 2008; 121(4): e1003-7.
Kumar S, Misra UK, Kalita J, Salwani V, Gupta RK, Gujral R. MRI in Japanese encephalitis. Neuroradiology 1997; 39(3): 180-4.
Larsen PD, Crisp D. Acute bilateral striatal necrosis associated with Mycoplasma pneumoniae infection. Pediatr Infect Dis J 1996; 15(12): 1124-6.
Misra UK, Kalita J. Overview: Japanese encephalitis. Prog Neurobiol 2010; 91(2): 108-20.
Misra UK, Kalita J, Phadke RV, Wadwekar V, Boruah DK, Srivastava A, *et al.* Usefulness of various MRI sequences in the diagnosis of viral encephalitis. Acta Trop 2010; 116(3): 206-11.
Ozbek O, Koc O, Paksoy Y, Aydin K, Nayman A. Epstein-Barr virus encephalitis: findings of MRI, MRS, diffusion and perfusion. Turk J Pediatr 2011; 53(6): 680-3.
Petropoulou KA, Gordon SM, Prayson RA, Ruggierri PM. West Nile virus meningoencephalitis: MR imaging findings. AJNR Am J Neuroradiol 2005; 26(8): 1986-95.
Phowthongkum P, Phantumchinda K, Jutivorakool K, Suankratay C. Basal ganglia and brainstem encephalitis, optic neuritis, and radiculomyelitis in Epstein-Barr virus infection. J Infect 2007; 54(3): e141-4.
Prakash M, Kumar S, Gupta RK. Diffusion-weighted MR

	imaging in Japanese encephalitis. J Comput Assist Tomogr 2004; 28(6): 756-61. Quattrocchi CC, Longo D, Delfino LN, Errante Y, Aiello C, Fariello G, *et al.* MR differential diagnosis of acute deep grey matter pathology in paediatric patients. Pediatr Radiol 2013; 43(6): 743-61. Rosas H, Wippold FJ, 2nd. West Nile virus: case report with MR imaging findings. AJNR Am J Neuroradiol 2003; 24(7): 1376-8. Saitoh S, Wada T, Narita M, Kohsaka S, Mizukami S, Togashi T, *et al.* Mycoplasma pneumoniae infection may cause striatal lesions leading to acute neurologic dysfunction. Neurology 1993; 43(10): 2150-1. Sakoulas G. Brainstem and striatal encephalitis complicating Mycoplasma pneumoniae pneumonia: possible benefit of intravenous immunoglobulin. Pediatr Infect Dis J 2001; 20(5): 543-5. Shaw DW, Cohen WA. Viral infections of the CNS in children: imaging features. AJR Am J Roentgenol 1993; 160(1): 125-33. Shoji H, Hiraki Y, Kuwasaki N, Toyomasu T, Kaji M, Okudera T. Japanese encephalitis in the Kurume region of Japan: CT and MRI findings. Journal of neurology 1989; 236(5): 255-9. Teoh HL, Mohammad SS, Britton PN, Kandula T, Lorentzos MS, Booy R, *et al.* Clinical Characteristics and Functional Motor Outcomes of Enterovirus 71 Neurological Disease in Children. JAMA neurology 2016; 73(3): 300-7. Termine C, Uggetti C, Veggiotti P, Balottin U, Rossi G, Egitto MG, *et al.* Long-term follow-up of an adolescent who had bilateral striatal necrosis secondary to Mycoplasma pneumoniae infection. Brain Dev 2005; 27(1): 62-5. van Buiren M, Uhl M. Images in clinical medicine. Bilateral striatal necrosis associated with Mycoplasma pneumoniae infection. The New England journal of medicine 2003; 348(8): 720. Verma R. MRI features of Japanese encephalitis. BMJ Case Rep 2012; 2012. Yuan ZF, Chen B, Mao SS, Shen J, Yu YL, Gao F, *et al.* Reversible bilateral striatal lesions following Mycoplasma pneumoniae infection associated with elevated levels of interleukins 6 and 8. Brain Dev 2016; 38(1): 149-53. Zambrino CA, Zorzi G, Lanzi G, Uggetti C, Egitto MG. Bilateral striatal necrosis associated with Mycoplasma pneumoniae infection in an adolescent: clinical and neuroradiologic follow up. Movement disorders : official journal of the Movement Disorder Society 2000; 15(5): 1023-6.
ISOVALERIC ACIDEMIA (*IVD*)	Nizon M, Ottolenghi C, Valayannopoulos V, Arnoux J-B, Barbier V, Habarou F, *et al.* Long-term neurological outcome of a cohort of 80 patients with classical organic acidurias. Orphanet journal of rare diseases 2013; 8(1): 148. Sogut A, Acun C, Aydin K, Tomac N, Demirel F, Aktuglu C.

	Isovaleric acidaemia: cranial CT and MRI findings. Pediatr Radiol 2004; 34(2): 160-2. Wani NA, Qureshi UA, Jehangir M, Ahmad K, Hussain Z. Atypical MR lenticular signal change in infantile isovaleric acidemia. Indian J Radiol Imaging 2016; 26(1): 131-4.
JUVENILE HUNTINGTON'S DISEASE	Cetica PD, Solari AJ, Merani MS, De Rosas JC, Burgos MH. Evolutionary sperm morphology and morphometry in armadillos. J Submicrosc Cytol Pathol 1998; 30(2): 309-14. Ho VB, Chuang HS, Rovira MJ, Koo B. Juvenile Huntington disease: CT and MR features. AJNR Am J Neuroradiol 1995; 16(7): 1405-12. Mirowitz SA, Sartor K, Prensky AJ, Gado M, Hodges FJ, 3rd. Neurodegenerative diseases of childhood: MR and CT evaluation. J Comput Assist Tomogr 1991; 15(2): 210-22. Schapiro M, Cecil KM, Doescher J, Kiefer AM, Jones BV. MR imaging and spectroscopy in juvenile Huntington disease. Pediatr Radiol 2004; 34(8): 640-3.
KCNQ2	Weckhuysen S, Mandelstam S, Suls A, Audenaert D, Deconinck T, Claes LR, et al. KCNQ2 encephalopathy: emerging phenotype of a neonatal epileptic encephalopathy. Ann Neurol 2012; 71(1): 15-25.
KEARNS SAYRE SYNDROME	Barragan-Campos HM, Vallee JN, Lo D, Barrera-Ramirez CF, Argote-Greene M, Sanchez-Guerrero J, *et al.* Brain magnetic resonance imaging findings in patients with mitochondrial cytopathies. Archives of neurology 2005; 62(5): 737-42. Chu BC, Terae S, Takahashi C, Kikuchi Y, Miyasaka K, Abe S, *et al.* MRI of the brain in the Kearns-Sayre syndrome: report of four cases and a review. Neuroradiology 1999; 41(10): 759-64. Crisi G, Ferrari G, Merelli E, Cocconcelli P. MRI in a case of Kearns-Sayre syndrome confirmed by molecular analysis. Neuroradiology 1994; 36(1): 37-8. Demange P, Gia HP, Kalifa G, Sellier N. MR of Kearns-Sayre syndrome. AJNR Am J Neuroradiol 1989; 10(5 Suppl): S91. Elsas T, Rinck PA, Isaksen C, Nilsen G, Schjetne OB. Cerebral nuclear magnetic resonance (MRI) in Kearns syndrome. Acta Ophthalmol (Copenh) 1988; 66(4): 469-73. Kapeller P, Fazekas F, Offenbacher H, Stollberger R, Schmidt R, Bergloff J, *et al.* Magnetic resonance imaging and spectroscopy of progressive cerebral involvement in Kearns Sayre Syndrome. Journal of the neurological sciences 1996; 135(2): 126-30. Sacher M, Fatterpekar GM, Edelstein S, Sansaricq C, Naidich TP. MRI findings in an atypical case of Kearns-Sayre syndrome: a case report. Neuroradiology 2005; 47(4): 241-4. Seigel RS, Seeger JF, Gabrielsen TO, Allen RJ. Computed tomography in oculocraniosomatic disease (Kearns-Sayre syndrome). Radiology 1979; 130(1): 159-64.
KERNICTERUS	Ahdab-Barmada M, Moossy J. The neuropathology of kernicterus in the premature neonate: diagnostic problems. J Neuropathol Exp Neurol 1984; 43(1): 45-56. Barkovich AJ. MR of the normal neonatal brain: assessment of

	deep structures. AJNR Am J Neuroradiol 1998; 19(8): 1397-403. Cece H, Abuhandan M, Cakmak A, Yildiz S, Calik M, Karakas E, *et al.* Diffusion-weighted imaging of patients with neonatal bilirubin encephalopathy. Jpn J Radiol 2013; 31(3): 179-85. Harris MC, Bernbaum JC, Polin JR, Zimmerman R, Polin RA. Developmental follow-up of breastfed term and near-term infants with marked hyperbilirubinemia. Pediatrics 2001; 107(5): 1075-80. Katar S. Glucose-6-phosphate dehydrogenase deficiency and kernicterus of South-East anatolia. Journal of pediatric hematology/oncology 2007; 29(5): 284-6. Katar S, Akay HO, Taskesen M, Devecioglu C. Clinical and cranial magnetic resonance imaging (MRI) findings of 21 patients with serious hyperbilirubinemia. J Child Neurol 2008; 23(4): 415-7. Martich-Kriss V, Kollias SS, Ball WS, Jr. MR findings in kernicterus. AJNR Am J Neuroradiol 1995; 16(4 Suppl): 819-21. Newman TB, Maisels MJ. Magnetic resonance imaging and kernicterus. Pediatrics 2002; 109(3): 555. Penn AA, Enzmann DR, Hahn JS, Stevenson DK. Kernicterus in a full term infant. Pediatrics 1994; 93(6 Pt 1): 1003-6. Shapiro SM. Definition of the clinical spectrum of kernicterus and bilirubin-induced neurologic dysfunction (BIND). J Perinatol 2005; 25(1): 54-9. Shapiro SM. Chronic bilirubin encephalopathy: diagnosis and outcome. Semin Fetal Neonatal Med 2010; 15(3): 157-63. Sugama S, Soeda A, Eto Y. Magnetic resonance imaging in three children with kernicterus. Pediatr Neurol 2001; 25(4): 328-31. van Toorn R, Brink P, Smith J, Ackermann C, Solomons R. Bilirubin-Induced Neurological Dysfunction: A Clinico-Radiological-Neurophysiological Correlation in 30 Consecutive Children. J Child Neurol 2016; 31(14): 1579-83. Wisnowski JL, Panigrahy A, Painter MJ, Watchko JF. Magnetic resonance imaging of bilirubin encephalopathy: current limitations and future promise. Semin Perinatol 2014; 38(7): 422-8. Yilmaz Y, Alper G, Kilicoglu G, Celik L, Karadeniz L, Yilmaz-Degirmenci S. Magnetic resonance imaging findings in patients with severe neonatal indirect hyperbilirubinemia. J Child Neurol 2001; 16(6): 452-5. Yilmaz Y, Ekinci G. Thalamic involvement in a patient with kernicterus. Eur Radiol 2002; 12(7): 1837-9. Yokochi K. Magnetic resonance imaging in children with kernicterus. Acta paediatrica 1995; 84(8): 937-9.
KRABBE DISEASE (*GALC*)	Abdelhalim AN, Alberico RA, Barczykowski AL, Duffner PK. Patterns of magnetic resonance imaging abnormalities in symptomatic patients with Krabbe disease correspond to phenotype. Pediatr Neurol 2014; 50(2): 127-34. Baram TZ, Goldman AM, Percy AK. Krabbe disease: specific

	MRI and CT findings. Neurology 1986; 36(1): 111-5. Loes DJ, Peters C, Krivit W. Globoid cell leukodystrophy: distinguishing early-onset from late-onset disease using a brain MR imaging scoring method. AJNR Am J Neuroradiol 1999; 20(2): 316-23. Nagar VA, Ursekar MA, Krishnan P, Jankharia BG. Krabbe disease: unusual MRI findings. Pediatr Radiol 2006; 36(1): 61-4. Sasaki M, Sakuragawa N, Takashima S, Hanaoka S, Arima M. MRI and CT findings in Krabbe disease. Pediatr Neurol 1991; 7(4): 283-8.
KUFOR RAKEB SYNDROME (*ATP13A2*)	Chien HF, Bonifati V, Barbosa ER. ATP13A2-related neurodegeneration (PARK9) without evidence of brain iron accumulation. Movement disorders : official journal of the Movement Disorder Society 2011; 26(7): 1364-5. Salomao RP, Pedroso JL, Gama MT, Dutra LA, Maciel RH, Godeiro-Junior C, *et al.* A diagnostic approach for neurodegeneration with brain iron accumulation: clinical features, genetics and brain imaging. Arquivos de neuro-psiquiatria 2016; 74(7): 587-96. Schneider SA, Paisan-Ruiz C, Quinn NP, Lees AJ, Houlden H, Hardy J, *et al.* ATP13A2 mutations (PARK9) cause neurodegeneration with brain iron accumulation. Movement disorders : official journal of the Movement Disorder Society 2010; 25(8): 979-84.
L-2-OH GLUTARIC ACIDURIA (*L2HGDH*)	Barth, P. G., Hoffmann, G. F., Jaeken, J., Lehnert, W., Hanefeld, F., van Gennip, A. H., Duran, M., Valk, J., Schutgens, R. B. H., Trefz, F. K., Reimann, G., Hartung, H.-P. L-2-hydroxyglutaric acidemia: a novel inherited neurometabolic disease. Ann. Neurol. 32: 66-71, 1992. Cachia D, Stine C. Child Neurology: cognitive delay in a 7-year-old girl. Neurology 2013; 81(20): e148-50.
LANGERHANS CELL HISTIOCYTOSIS	de Haan S, van der Velden W, Meijer FJA. Striatal Involvement in Neurodegenerative Langerhans Cell Histiocytosis. Mov Disord Clin Pract 2019; 6(8): 719-21. Ertan G, Huisman T. Susceptibility-weighted imaging in neurodegeneration in Langerhans cell histiocytosis. J Pediatr 2010; 156(6): 1032. Grois N, Fahrner B, Arceci RJ, Henter JI, McClain K, Lassmann H, *et al.* Central nervous system disease in Langerhans cell histiocytosis. J Pediatr 2010; 156(6): 873-81 e1.
LEBER HEREDITARY OPTIC NEUROPATHY	Mercuri MA, White H, Oliveira C. Vision Loss and Symmetric Basal Ganglia Lesions in Leber Hereditary Optic Neuropathy. J Neuroophthalmol 2017; 37(4): 411-3. Miyaue N, Yamanishi Y, Tada S, Ando R, Yabe H, Nagai M, *et al.* Repetitive brainstem lesions in mitochondrial DNA 11778G>A mutation of Leber hereditary optic neuropathy. eNeurologicalSci 2019; 14: 74-6.
MANGANESE TOXICITY	Hegde AN, Mohan S, Lath N, Lim CC. Differential diagnosis for bilateral abnormalities of the basal ganglia and thalamus. Radiographics 2011; 31(1): 5-30.

	Ono J, Harada K, Kodaka R, Sakurai K, Tajiri H, Takagi Y, *et al.* Manganese deposition in the brain during long-term total parenteral nutrition. JPEN J Parenter Enteral Nutr 1995; 19(4): 310-2. Quaghebeur G, Taylor WJ, Kingsley DP, Fell JM, Reynolds AP, Milla PJ. MRI in children receiving total parenteral nutrition. Neuroradiology 1996; 38(7): 680-3. Zuccoli G, Yannes MP, Nardone R, Bailey A, Goldstein A. Bilateral symmetrical basal ganglia and thalamic lesions in children: an update (2015). Neuroradiology 2015; 57(10): 973-89.
MAPLE SYRUP URINE DISEASE (*DBT*, *BCKDHB*, *BCKDHA*)	Gropman AL. Patterns of brain injury in inborn errors of metabolism. Semin Pediatr Neurol 2012; 19(4): 203-10. Zuccoli G, Yannes MP, Nardone R, Bailey A, Goldstein A. Bilateral symmetrical basal ganglia and thalamic lesions in children: an update (2015). Neuroradiology 2015; 57(10): 973-89.
MECR	Gorukmez O, Gorukmez O, Havali C. Novel MECR Mutation in Childhood-Onset Dystonia, Optic Atrophy, and Basal Ganglia Signal Abnormalities. Neuropediatrics 2019; 50(5): 336-7. Heimer G, Keratar JM, Riley LG, Balasubramaniam S, Eyal E, Pietikainen LP, et al. MECR Mutations Cause Childhood-Onset Dystonia and Optic Atrophy, a Mitochondrial Fatty Acid Synthesis Disorder. Am J Hum Genet 2016; 99(6): 1229-44.
MEGDEL (SERAC1)	Wortmann S, Rodenburg RJ, Huizing M, Loupatty FJ, de Koning T, Kluijtmans LA, *et al.* Association of 3-methylglutaconic aciduria with sensori-neural deafness, encephalopathy, and Leigh-like syndrome (MEGDEL association) in four patients with a disorder of the oxidative phosphorylation. Mol Genet Metab 2006; 88(1): 47-52. Wortmann SB, van Hasselt PM, Baric I, Burlina A, Darin N, Horster F, *et al.* Eyes on MEGDEL: Distinctive Basal Ganglia Involvement in Dystonia Deafness Syndrome. Neuropediatrics 2015. Wortmann SB, Vaz FM, Gardeitchik T, Vissers LE, Renkema GH, Schuurs-Hoeijmakers JH, *et al.* Mutations in the phospholipid remodeling gene SERAC1 impair mitochondrial function and intracellular cholesterol trafficking and cause dystonia and deafness. Nat Genet 2012; 44(7): 797-802.
METACHROMATIC LEUKODYSTROPHY (*ARSA*)	Becker LE. Lysosomes, peroxisomes and mitochondria: function and disorder. AJNR Am J Neuroradiol 1992; 13(2): 609-20. Eichler F, Grodd W, Grant E, Sessa M, Biffi A, Bley A, *et al.* Metachromatic leukodystrophy: a scoring system for brain MR imaging observations. AJNR Am J Neuroradiol 2009; 30(10): 1893-7. Mirowitz SA, Sartor K, Prensky AJ, Gado M, Hodges FJ, 3rd. Neurodegenerative diseases of childhood: MR and CT evaluation. J Comput Assist Tomogr 1991; 15(2): 210-22. Ho VB, Fitz CR, Chuang SH, Geyer CA. Bilateral basal ganglia lesions: pediatric differential considerations. Radiographics 1993;

	13(2): 269-92.
METHADONE TOXICITY	Zuccoli G, Yannes MP, Nardone R, Bailey A, Goldstein A. Bilateral symmetrical basal ganglia and thalamic lesions in children: an update (2015). Neuroradiology 2015; 57(10): 973-89.
METHANOL TOXICITY	Anderson JC, Costantino MM, Stratford T. Basal ganglia: anatomy, pathology, and imaging characteristics. Curr Probl Diagn Radiol 2004; 33(1): 28-41.
METHYLMALONIC ACIDEMIA (*MULTIPLE GENES*)	Baker EH, Sloan JL, Hauser NS, Gropman AL, Adams DR, Toro C, *et al.* MRI characteristics of globus pallidus infarcts in isolated methylmalonic acidemia. AJNR Am J Neuroradiol 2015; 36(1): 194-201. Brismar J, Ozand PT. CT and MR of the brain in disorders of the propionate and methylmalonate metabolism. AJNR Am J Neuroradiol 1994; 15(8): 1459-73. Burlina AP, Manara R, Calderone M, Catuogno S, Burlina AB. Diffusion-weighted imaging in the assessment of neurological damage in patients with methylmalonic aciduria. J Inherit Metab Dis 2003; 26(5): 417-22. Enns GM, Barkovich AJ, Rosenblatt DS, Fredrick DR, Weisiger K, Ohnstad C, *et al.* Progressive neurological deterioration and MRI changes in cblC methylmalonic acidaemia treated with hydroxocobalamin. J Inherit Metab Dis 1999; 22(5): 599-607. Harting I, Seitz A, Geb S, Zwickler T, Porto L, Lindner M, *et al.* Looking beyond the basal ganglia: the spectrum of MRI changes in methylmalonic acidaemia. J Inherit Metab Dis 2008; 31(3): 368-78. Isikay S, Temel L, Keskin M. Imaging findings associated with methylmalonic aciduria. Pediatr Neurol 2014; 50(4): 435-6. Kanaumi T, Takashima S, Hirose S, Kodama T, Iwasaki H. Neuropathology of methylmalonic acidemia in a child. Pediatr Neurol 2006; 34(2): 156-9. Michel SJ, Given CA, 2nd, Robertson WC, Jr. Imaging of the brain, including diffusion-weighted imaging in methylmalonic acidemia. Pediatr Radiol 2004; 34(7): 580-2. Radmanesh A, Zaman T, Ghanaati H, Molaei S, Robertson RL, Zamani AA. Methylmalonic acidemia: brain imaging findings in 52 children and a review of the literature. Pediatr Radiol 2008; 38(10): 1054-61. Roodhooft AM, Baumgartner ER, Martin JJ, Blom W, Van Acker KJ. Symmetrical necrosis of the basal ganglia in methylmalonic acidaemia. European journal of pediatrics 1990; 149(8): 582-4. Takeuchi M, Harada M, Matsuzaki K, Hisaoka S, Nishitani H, Mori K. Magnetic resonance imaging and spectroscopy in a patient with treated methylmalonic acidemia. J Comput Assist Tomogr 2003; 27(4): 547-51.

MITOCHONDRIAL COMPLEX 1 DEFICIENCY *(MULTIPLE GENES)* MITOCHONDRIAL COMPLEX IV DEFICIENCY *(MULTIPLE GENES)* MITOCHONDRIAL COMPLEX V DEFICIENCY *(MULTIPLE GENES)* MITOCHONDRIAL MAINTAINENCE *(MULTIPLE GENES)*	Bricout M, Grevent D, Lebre AS, Rio M, Desguerre I, De Lonlay P, *et al.* Brain imaging in mitochondrial respiratory chain deficiency: combination of brain MRI features as a useful tool for genotype/phenotype correlations. J Med Genet 2014; 51(7): 429-35. Carrozzo R, Dionisi-Vici C, Steuerwald U, Lucioli S, Deodato F, Di Giandomenico S, *et al.* SUCLA2 mutations are associated with mild methylmalonic aciduria, Leigh-like encephalomyopathy, dystonia and deafness. Brain : a journal of neurology 2007; 130(Pt 3): 862-74. Finsterer J. Leigh and Leigh-like syndrome in children and adults. Pediatr Neurol 2008; 39(4): 223-35. Medina L, Chi TL, DeVivo DC, Hilal SK. MR findings in patients with subacute necrotizing encephalomyelopathy (Leigh syndrome): correlation with biochemical defect. AJR Am J Roentgenol 1990; 154(6): 1269-74. Saneto RP, Friedman SD, Shaw DW. Neuroimaging of mitochondrial disease. Mitochondrion 2008; 8(5-6): 396-413. Sofou K, Steneryd K, Wiklund LM, Tulinius M, Darin N. MRI of the brain in childhood-onset mitochondrial disorders with central nervous system involvement. Mitochondrion 2013; 13(4): 364-71. Valanne L, Ketonen L, Majander A, Suomalainen A, Pihko H. Neuroradiologic findings in children with mitochondrial disorders. AJNR Am J Neuroradiol 1998; 19(2): 369-77.
MITOCHONDRIAL MEMBRANE PROTEIN ASSOCIATED NEURODEGENERATION (*C19orf12*)	Al Macki N, Al Rashdi I. A Novel Deletion Mutation of Exon 2 of the C19orf12 Gene in an Omani Family with Mitochondrial Membrane Protein-Associated Neurodegeneration (MPAN). Oman Med J 2017; 32(1): 66-8. Hartig M, Prokisch H, Meitinger T, Klopstock T. Mitochondrial membrane protein-associated neurodegeneration (MPAN). Int Rev Neurobiol 2013; 110: 73-84. Hartig MB, Iuso A, Haack T, Kmiec T, Jurkiewicz E, Heim K, *et al.* Absence of an orphan mitochondrial protein, c19orf12, causes a distinct clinical subtype of neurodegeneration with brain iron accumulation. Am J Hum Genet 2011; 89(4): 543-50. Hogarth P, Gregory A, Kruer MC, Sanford L, Wagoner W, Natowicz MR, *et al.* New NBIA subtype: genetic, clinical, pathologic, and radiographic features of MPAN. Neurology 2013; 80(3): 268-75. Schulte EC, Claussen MC, Jochim A, Haack T, Hartig M, Hempel M, *et al.* Mitochondrial membrane protein associated neurodegenration: a novel variant of neurodegeneration with brain iron accumulation. Movement disorders : official journal of the Movement Disorder Society 2013; 28(2): 224-7. Skowronska M, Kmiec T, Kurkowska-Jastrzebska I, Czlonkowska A. Eye of the tiger sign in a 23 year patient with mitochondrial membrane protein associated neurodegeneration. Journal of the neurological sciences 2015; 352(1-2): 110-1. Yilmaz S, Gokben S, Ceylaner S. Mitochondrial Membrane

	Protein-Associated Neurodegeneration. Pediatr Neurol 2015; 53(4): 373-4. Yoganathan S, Sudhakar SV, Thomas M, Dutta AK, Danda S. "Eye of tiger sign" mimic in an adolescent boy with mitochondrial membrane protein associated neurodegeneration (MPAN). Brain Dev 2016; 38(5): 516-9.
MITOCHONDRIAL THIAMINE TRANSPORTER (*SLC25A19*)	Ortigoza-Escobar JD, Alfadhel M, Molero-Luis M, Darin N, Spiegel R, de Coo IF, *et al.* Thiamine deficiency in childhood with attention to genetic causes: Survival and outcome predictors. Ann Neurol 2017; 82(3): 317-30.
MITOCHONDRIAL TRANSLATION (*MULTIPLE GENES*)	D'Souza AR, Minczuk M. Mitochondrial transcription and translation: overview. Essays Biochem 2018; 62(3): 309-20. Smits P, Smeitink J, van den Heuvel L. Mitochondrial translation and beyond: processes implicated in combined oxidative phosphorylation deficiencies. J Biomed Biotechnol 2010; 2010: 737385.
MUCOLIPIDOSIS TYPE IV (*MCOLN1*)	Frei KP, Patronas NJ, Crutchfield KE, Altarescu G, Schiffmann R. Mucolipidosis type IV: characteristic MRI findings. Neurology. 1998;51(2):565-9. Altarescu G, Sun M, Moore DF, Smith JA, Wiggs EA, Solomon BI, et al. The neurogenetics of mucolipidosis type IV. Neurology. 2002;59(3):306-13. Wakabayashi K, Gustafson AM, Sidransky E, Goldin E. Mucolipidosis type IV: an update. Mol Genet Metab. 2011;104(3):206-13.
MYELINOLYSIS	Adams RD, Victor M, Mancall EL. Central pontine myelinolysis: a hitherto undescribed disease occurring in alcoholic and malnourished patients. AMA Arch Neurol Psychiatry 1959; 81(2): 154-72. Bekiesinska-Figatowska M, Bulski T, Rozyczka I, Furmanek M, Walecki J. MR imaging of seven presumed cases of central pontine and extrapontine myelinolysis. Acta Neurobiol Exp (Wars) 2001; 61(2): 141-4. Brown WD, Caruso JM. Extrapontine myelinolysis with involvement of the hippocampus in three children with severe hypernatremia. J Child Neurol 1999; 14(7): 428-33. Forster A, Nolte I, Wenz H, Al-Zghloul M, Kerl HU, Brockmann C, *et al.* Value of diffusion-weighted imaging in central pontine and extrapontine myelinolysis. Neuroradiology 2013; 55(1): 49-56. Gocht A, Colmant HJ. Central pontine and extrapontine myelinolysis: a report of 58 cases. Clin Neuropathol 1987; 6(6): 262-70. Lampl C, Yazdi K. Central pontine myelinolysis. European neurology 2002; 47(1): 3-10. Miller GM, Baker HL, Jr., Okazaki H, Whisnant JP. Central pontine myelinolysis and its imitators: MR findings. Radiology 1988; 168(3): 795-802. Ranger AM, Chaudhary N, Avery M, Fraser D. Central pontine

	and extrapontine myelinolysis in children: a review of 76 patients. J Child Neurol 2012; 27(8): 1027-37. Ruzek KA, Campeau NG, Miller GM. Early diagnosis of central pontine myelinolysis with diffusion-weighted imaging. AJNR Am J Neuroradiol 2004; 25(2): 210-3. Wright DG, Laureno R, Victor M. Pontine and extrapontine myelinolysis. Brain : a journal of neurology 1979; 102(2): 361-85.
NEUROFERRITINOPATHY (*FTL*)	Batla A, Adams ME, Erro R, Ganos C, Balint B, Mencacci NE, *et al.* Cortical pencil lining in neuroferritinopathy: a diagnostic clue. Neurology 2015; 84(17): 1816-8. Salomao RP, Pedroso JL, Gama MT, Dutra LA, Maciel RH, Godeiro-Junior C, *et al.* A diagnostic approach for neurodegeneration with brain iron accumulation: clinical features, genetics and brain imaging. Arquivos de neuro-psiquiatria 2016; 74(7): 587-96. Kumar N, Rizek P, Jog M. Neuroferritinopathy: Pathophysiology, Presentation, Differential Diagnoses and Management. Tremor Other Hyperkinet Mov (N Y) 2016; 6: 355.
NUP62	Basel-Vanagaite L, Muncher L, Straussberg R, Pasmanik-Chor M, Yahav M, Rainshtein L, et al. Mutated nup62 causes autosomal recessive infantile bilateral striatal necrosis. Ann Neurol 2006; 60(2): 214-22. Straussberg R, Shorer Z, Weitz R, Basel L, Kornreich L, Corie CI, et al. Familial infantile bilateral striatal necrosis: clinical features and response to biotin treatment. Neurology 2002; 59(7): 983-9.
PANTOTHENATE KINASE ASSOCIATED NEURODEGENERATION (*PANK2*)	Fasano A, Shahidi G, Lang AE, Rohani M. Basal ganglia calcification in a case of PKAN. Parkinsonism & related disorders 2016. Fermin-Delgado R, Roa-Sanchez P, Speckter H, Perez-Then E, Rivera-Mejia D, Foerster B, *et al.* Involvement of globus pallidus and midbrain nuclei in pantothenate kinase-associated neurodegeneration: measurement of T2 and T2* time. Clin Neuroradiol 2013; 23(1): 11-5. Kurian MA, Hayflick SJ. Pantothenate kinase-associated neurodegeneration (PKAN) and PLA2G6-associated neurodegeneration (PLAN): review of two major neurodegeneration with brain iron accumulation (NBIA) phenotypes. International review of neurobiology 2013; 110: 49-71. McNeill A, Birchall D, Hayflick SJ, Gregory A, Schenk JF, Zimmerman EA, *et al.* T2* and FSE MRI distinguishes four subtypes of neurodegeneration with brain iron accumulation. Neurology 2008; 70(18): 1614-9. Wu YW, Hess CP, Singhal NS, Groden C, Toro C. Idiopathic basal ganglia calcifications: an atypical presentation of PKAN. Pediatr Neurol 2013; 49(5): 351-4.
PDE8B	Appenzeller S, Schirmacher A, Halfter H, Baumer S, Pendziwiat M, Timmerman V, *et al.* Autosomal-dominant striatal

	degeneration is caused by a mutation in the phosphodiesterase 8B gene. Am J Hum Genet 2010; 86(1): 83-7. Ni J, Yi X, Liu Z, Sun W, Yuan Y, Yang J, *et al.* Clinical findings of autosomal-dominant striatal degeneration and PDE8B mutation screening in parkinsonism and related disorders. Parkinsonism Relat Disord 2019; 69: 94-8.
PDE10A	Diggle CP, Sukoff Rizzo SJ, Popiolek M, Hinttala R, Schulke JP, Kurian MA, *et al.* Biallelic Mutations in PDE10A Lead to Loss of Striatal PDE10A and a Hyperkinetic Movement Disorder with Onset in Infancy. Am J Hum Genet 2016; 98(4): 735-43. Esposito S, Carecchio M, Tonduti D, Saletti V, Panteghini C, Chiapparini L, *et al.* A PDE10A de novo mutation causes childhood-onset chorea with diurnal fluctuations. Mov Disord 2017; 32(11): 1646-7. Knopp C, Hausler M, Muller B, Damen R, Stoppe A, Mull M, *et al.* PDE10A mutation in two sisters with a hyperkinetic movement disorder - Response to levodopa. Parkinsonism Relat Disord 2019; 63: 240-2. Mencacci NE, Kamsteeg EJ, Nakashima K, R'Bibo L, Lynch DS, Balint B, *et al.* De Novo Mutations in PDE10A Cause Childhood-Onset Chorea with Bilateral Striatal Lesions. Am J Hum Genet 2016; 98(4): 763-71.
PLA2G6 ASSOCIATED NEURODEGENERATION (*PLA2G6*)	Al-Maawali A, Yoon G, Feigenbaum AS, Halliday WC, Clarke JT, Branson HM, *et al.* Validation of the finding of hypertrophy of the clava in infantile neuroaxonal dystrophy/PLA2G6 by biometric analysis. Neuroradiology 2016; 58(10): 1035-42. Carrilho I, Santos M, Guimaraes A, Teixeira J, Chorao R, Martins M, *et al.* Infantile neuroaxonal dystrophy: what's most important for the diagnosis? European journal of paediatric neurology : EJPN : official journal of the European Paediatric Neurology Society 2008; 12(6): 491-500. Farina L, Nardocci N, Bruzzone MG, D'Incerti L, Zorzi G, Verga L, *et al.* Infantile neuroaxonal dystrophy: neuroradiological studies in 11 patients. Neuroradiology 1999; 41(5): 376-80. Gregory A, Kurian MA, Maher ER, Hogarth P, Hayflick SJ. PLA2G6-associated neurodegeneration. 2015.
POLR3A	Azmanov DN, Siira SJ, Chamova T, Kaprelyan A, Guergueltcheva V, Shearwood AM, Liu G, Morar B, Rackham O, Bynevelt M, Grudkova M. Transcriptome-wide effects of a POLR3A gene mutation in patients with an unusual phenotype of striatal involvement. Human molecular genetics. 2016 Oct 1;25(19):4302-14.
PRKRA	Lemmon ME, Lavenstein B, Applegate CD, Hamosh A, Tekes A, Singer HS. A novel presentation of DYT 16: acute onset in infancy and association with MRI abnormalities. Mov Disord 2013; 28(14): 1937-8.
PROPIONIC ACIDEMIA (*PCCA*, *PCCB*)	Bergman AJ, Van der Knaap MS, Smeitink JA, Duran M, Dorland L, Valk J, *et al.* Magnetic resonance imaging and spectroscopy of the brain in propionic acidemia: clinical and

	biochemical considerations. Pediatr Res 1996; 40(3): 404-9. Delgado C, Macias C, de la Sierra Garcia-Valdecasas M, Perez M, del Portal LR, Jimenez LM. Subacute presentation of propionic acidemia. J Child Neurol 2007; 22(12): 1405-7. Hamilton RL, Haas RH, Nyhan WL, Powell HC, Grafe MR. Neuropathology of propionic acidemia: a report of two patients with basal ganglia lesions. J Child Neurol 1995; 10(1): 25-30. Johnson JA, Le KL, Palacios E. Propionic acidemia: case report and review of neurologic sequelae. Pediatr Neurol 2009; 40(4): 317-20. Kandel A, Amatya SK, Yeh EA. Reversible diffusion weighted imaging changes in propionic acidemia. J Child Neurol 2013; 28(1): 128-31.
PYRUVATE DEHYDROGENASE COMPLEX DEFICIENCY (*MULTIPLE GENES*)	Barnerias C, Saudubray JM, Touati G, De Lonlay P, Dulac O, Ponsot G, *et al.* Pyruvate dehydrogenase complex deficiency: four neurological phenotypes with differing pathogenesis. Dev Med Child Neurol 2010; 52(2): e1-9. Castiglioni C, Verrigni D, Okuma C, Diaz A, Alvarez K, Rizza T, *et al.* Pyruvate dehydrogenase deficiency presenting as isolated paroxysmal exercise induced dystonia successfully reversed with thiamine supplementation. Case report and mini-review. European journal of paediatric neurology : EJPN : official journal of the European Paediatric Neurology Society 2015; 19(5): 497-503. De Meirleir L, Lissens W, Denis R, Wayenberg JL, Michotte A, Brucher JM, *et al.* Pyruvate dehydrogenase deficiency: clinical and biochemical diagnosis. Pediatr Neurol 1993; 9(3): 216-20. Giribaldi G, Doria-Lamba L, Biancheri R, Severino M, Rossi A, Santorelli FM, *et al.* Intermittent-relapsing pyruvate dehydrogenase complex deficiency: a case with clinical, biochemical, and neuroradiological reversibility. Dev Med Child Neurol 2012; 54(5): 472-6.
RAB39B	Giannandrea M, Bianchi V, Mignogna ML, Sirri A, Carrabino S, D'Elia E, et al. Mutations in the small GTPase gene RAB39B are responsible for X-linked mental retardation associated with autism, epilepsy, and macrocephaly. Am J Hum Genet 2010; 86(2): 185-95. Shi CH, Zhang SY, Yang ZH, Yang J, Shang DD, Mao CY, et al. A novel RAB39B gene mutation in X-linked juvenile parkinsonism with basal ganglia calcification. Mov Disord 2016; 31(12): 1905-9. Wilson GR, Sim JC, McLean C, Giannandrea M, Galea CA, Riseley JR, et al. Mutations in RAB39B cause X-linked intellectual disability and early-onset Parkinson disease with alpha-synuclein pathology. Am J Hum Genet 2014; 95(6): 729-35.
REPS1	Drecourt A, Babdor J, Dussiot M, Petit F, Goudin N, Garfa-Traore M, et al. Impaired Transferrin Receptor Palmitoylation and Recycling in Neurodegeneration with Brain Iron Accumulation. Am J Hum Genet 2018; 102(2): 266-77.

	Levi S, Tiranti V. Neurodegeneration with Brain Iron Accumulation Disorders: Valuable Models Aimed at Understanding the Pathogenesis of Iron Deposition. Pharmaceuticals (Basel) 2019; 12(1).
SCP2	Horvath R, Lewis-Smith D, Douroudis K, Duff J, Keogh M, Pyle A, et al. SCP2 mutations and neurodegeneration with brain iron accumulation. Neurology 2015; 85(21): 1909-11. Levi S, Tiranti V. Neurodegeneration with Brain Iron Accumulation Disorders: Valuable Models Aimed at Understanding the Pathogenesis of Iron Deposition. Pharmaceuticals (Basel) 2019; 12(1). Ferdinandusse S, Kostopoulos P, Denis S, Rusch H, Overmars H, Dillmann U, *et al.* Mutations in the gene encoding peroxisomal sterol carrier protein X (SCPx) cause leukencephalopathy with dystonia and motor neuropathy. Am J Hum Genet 2006; 78(6): 1046-52.
SQSTM1	Muto V, Flex E, Kupchinsky Z, Primiano G, Galehdari H, Dehghani M, *et al.* Biallelic SQSTM1 mutations in early-onset, variably progressive neurodegeneration. Neurology 2018; 91(4): e319-e30.
SUCCINIC SEMIALDEHYDE DEHYDROGENASE DEFICIENCY (*ALDH5A1*)	Acosta MT, Munasinghe J, Pearl PL, Gupta M, Finegersh A, Gibson KM, *et al.* Cerebellar atrophy in human and murine succinic semialdehyde dehydrogenase deficiency. J Child Neurol 2010; 25(12): 1457-61. Bosemani T, Anghelescu C, Boltshauser E, Hoon AH, Jr., Pearl PL, Craiu D, *et al.* Subthalamic nucleus involvement in children: a neuroimaging pattern-recognition approach. European journal of paediatric neurology : EJPN : official journal of the European Paediatric Neurology Society 2014; 18(3): 249-56. Lin CY, Weng WC, Lee WT. A novel mutation of ALDH5A1 gene associated with succinic semialdehyde dehydrogenase deficiency. J Child Neurol 2015; 30(4): 486-9. Pearl PL, Gibson KM, Acosta MT, Vezina LG, Theodore WH, Rogawski MA, *et al.* Clinical spectrum of succinic semialdehyde dehydrogenase deficiency. Neurology 2003a; 60(9): 1413-7. Pearl PL, Gibson KM, Quezado Z, Dustin I, Taylor J, Trzcinski S, *et al.* Decreased GABA-A binding on FMZ-PET in succinic semialdehyde dehydrogenase deficiency. Neurology 2009; 73(6): 423-9. Pearl PL, Novotny EJ, Acosta MT, Jakobs C, Gibson KM. Succinic semialdehyde dehydrogenase deficiency in children and adults. Ann Neurol 2003b; 54 Suppl 6: S73-80. Yalcinkaya C, Gibson KM, Gunduz E, Kocer N, Ficicioglu C, Kucukercan I. MRI findings in succinic semialdehyde dehydrogenase deficiency. Neuropediatrics 2000; 31(1): 45-6. Yamakawa Y, Nakazawa T, Ishida A, Saito N, Komatsu M, Matsubara T, *et al.* A boy with a severe phenotype of succinic semialdehyde dehydrogenase deficiency. Brain Dev 2012; 34(2): 107-12. Ziyeh S, Berlis A, Korinthenberg R, Spreer J, Schumacher M.

	Selective involvement of the globus pallidus and dentate nucleus in succinic semialdehyde dehydrogenase deficiency. Pediatr Radiol 2002; 32(8): 598-600.
SULFITE OXIDASE AND MOLYBDENUM COFACTOR DEFICIENCY (*MOCS1, MOCS2, GEPH, SUOX*)	Tonduti D, Chiapparini L, Moroni I, Ardissone A, Zorzi G, Zibordi F, *et al.* Neurological Disorders Associated with Striatal Lesions: Classification and Diagnostic Approach. Curr Neurol Neurosci Rep 2016; 16(6): 54.
THIAMINE RESPONSIVE BASAL GANGLIA DISEASE (*SLC19A3*)	Alfadhel M, Almuntashri M, Jadah RH, Bashiri FA, Al Rifai MT, Al Shalaan H, *et al.* Biotin-responsive basal ganglia disease should be renamed biotin-thiamine-responsive basal ganglia disease: a retrospective review of the clinical, radiological and molecular findings of 18 new cases. Orphanet J Rare Dis 2013; 8: 83. Gerards M, Kamps R, van Oevelen J, Boesten I, Jongen E, de Koning B, *et al.* Exome sequencing reveals a novel Moroccan founder mutation in SLC19A3 as a new cause of early-childhood fatal Leigh syndrome. Brain : a journal of neurology 2013; 136(Pt 3): 882-90. Kono S, Miyajima H, Yoshida K, Togawa A, Shirakawa K, Suzuki H. Mutations in a thiamine-transporter gene and Wernicke's-like encephalopathy. The New England journal of medicine 2009; 360(17): 1792-4. Ozand PT, Gascon GG, Al Essa M, Joshi S, Al Jishi E, Bakheet S, *et al.* Biotin-responsive basal ganglia disease: a novel entity. Brain : a journal of neurology 1998; 121 (Pt 7): 1267-79. Tabarki B, Al-Hashem A, Alfadhel M. Biotin-Thiamine-Responsive Basal Ganglia Disease. In: Pagon RA, Adam MP, Ardinger HH, Wallace SE, Amemiya A, Bean LJH, *et al.*, editors. GeneReviews(R). Seattle (WA); 1993. Tabarki B, Al-Shafi S, Al-Shahwan S, Azmat Z, Al-Hashem A, Al-Adwani N, *et al.* Biotin-responsive basal ganglia disease revisited: clinical, radiologic, and genetic findings. Neurology 2013; 80(3): 261-7. Yamada K, Miura K, Hara K, Suzuki M, Nakanishi K, Kumagai T, *et al.* A wide spectrum of clinical and brain MRI findings in patients with SLC19A3 mutations. BMC Med Genet 2010; 11: 171.
TUBB4A	Ferreira C, Poretti A, Cohen J, Hamosh A, Naidu S. Novel TUBB4A mutations and expansion of the neuroimaging phenotype of hypomyelination with atrophy of the basal ganglia and cerebellum (H-ABC). Am J Med Genet A 2014; 164A(7): 1802-7. Hamilton EM, Polder E, Vanderver A, Naidu S, Schiffmann R, Fisher K, et al. Hypomyelination with atrophy of the basal ganglia and cerebellum: further delineation of the phenotype and genotype-phenotype correlation. Brain : a journal of neurology 2014; 137(Pt 7): 1921-30. Simons C, Wolf NI, McNeil N, Caldovic L, Devaney JM, Takanohashi A, et al. A de novo mutation in the beta-tubulin gene TUBB4A results in the leukoencephalopathy

	hypomyelination with atrophy of the basal ganglia and cerebellum. Am J Hum Genet 2013; 92(5): 767-73.
UFM1	Colin E, Daniel J, Ziegler A, Wakim J, Scrivo A, Haack TB, *et al.* Biallelic Variants in UBA5 Reveal that Disruption of the UFM1 Cascade Can Result in Early-Onset Encephalopathy. Am J Hum Genet 2016; 99(3): 695-703. Hamilton EMC, Bertini E, Kalaydjieva L, Morar B, Dojcakova D, Liu J, *et al.* UFM1 founder mutation in the Roma population causes recessive variant of H-ABC. Neurology 2017; 89(17): 1821-8. Muona M, Ishimura R, Laari A, Ichimura Y, Linnankivi T, Keski-Filppula R, *et al.* Biallelic Variants in UBA5 Link Dysfunctional UFM1 Ubiquitin-like Modifier Pathway to Severe Infantile-Onset Encephalopathy. Am J Hum Genet 2016; 99(3): 683-94. Nahorski MS, Maddirevula S, Ishimura R, Alsahli S, Brady AF, Begemann A, *et al.* Biallelic UFM1 and UFC1 mutations expand the essential role of ufmylation in brain development. Brain 2018; 141(7): 1934-45.
VAC14	de Gusmao CM, Stone S, Waugh JL, Yang E, Lenk GM, Rodan LH. VAC14 Gene-Related Parkinsonism-Dystonia With Response to Deep Brain Stimulation. Mov Disord Clin Pract 2019; 6(6): 494-7. Lenk GM, Szymanska K, Debska-Vielhaber G, Rydzanicz M, Walczak A, Bekiesinska-Figatowska M, et al. Biallelic Mutations of VAC14 in Pediatric-Onset Neurological Disease. Am J Hum Genet 2016; 99(1): 188-94. Lyon GJ, Marchi E, Ekstein J, Meiner V, Hirsch Y, Scher S, et al. VAC14 syndrome in two siblings with retinitis pigmentosa and neurodegeneration with brain iron accumulation. Cold Spring Harb Mol Case Stud 2019; 5(6).
VIGABATRIN TOXICITY	Cocito L, Maffini M, Loeb C. MRI findings in epileptic patients on vigabatrin for more than 5 years. Seizure 1992; 1(3): 163-5. Cohen JA, Fisher RS, Brigell MG, Peyster RG, Sze G. The potential for vigabatrin-induced intramyelinic edema in humans. Epilepsia 2000; 41(2): 148-57. Dill P, Datta AN, Weber P, Schneider J. Are vigabatrin induced T2 hyperintensities in cranial MRI associated with acute encephalopathy and extrapyramidal symptoms? European journal of paediatric neurology : EJPN : official journal of the European Paediatric Neurology Society 2013; 17(3): 311-5. Dracopoulos A, Widjaja E, Raybaud C, Westall CA, Snead OC, 3rd. Vigabatrin-associated reversible MRI signal changes in patients with infantile spasms. Epilepsia 2010; 51(7): 1297-304. Fong CY, Osborne JP, Edwards SW, Hemingway C, Hancock E, Johnson AL, *et al.* An investigation into the relationship between vigabatrin, movement disorders, and brain magnetic resonance imaging abnormalities in children with infantile spasms. Dev Med Child Neurol 2013; 55(9): 862-7.

	Hammond EJ, Ballinger WE, Jr., Lu L, Wilder BJ, Uthman BM, Reid SA. Absence of cortical white matter changes in three patients undergoing long-term vigabatrin therapy. Epilepsy Res 1992; 12(3): 261-5. Milh M, Villeneuve N, Chapon F, Pineau S, Lamoureux S, Livet MO, *et al.* Transient brain magnetic resonance imaging hyperintensity in basal ganglia and brain stem of epileptic infants treated with vigabatrin. J Child Neurol 2009; 24(3): 305-15. Pearl PL, Vezina LG, Saneto RP, McCarter R, Molloy-Wells E, Heffron A, *et al.* Cerebral MRI abnormalities associated with vigabatrin therapy. Epilepsia 2009; 50(2): 184-94. Schonstedt V, Stecher X, Venegas V, Silva C. Vigabatrin-induced MRI changes associated with extrapyramidal symptoms in a child with infantile spasms. Neuroradiol J 2015; 28(5): 515-8. Wheless JW, Carmant L, Bebin M, Conry JA, Chiron C, Elterman RD, *et al.* Magnetic resonance imaging abnormalities associated with vigabatrin in patients with epilepsy. Epilepsia 2009; 50(2): 195-205.
VPS13A	Lee JH, Lee SM, Baik SK. Demonstration of striatopallidal iron deposition in chorea-acanthocytosis by susceptibility-weighted imaging. J Neurol 2011; 258(2): 321-2. Nicholl DJ, Sutton I, Dotti MT, Supple SG, Danek A, Lawden M. White matter abnormalities on MRI in neuroacanthocytosis. J Neurol Neurosurg Psychiatry 2004; 75(8): 1200-1.
VPS13D	Gauthier J, Meijer IA, Lessel D, Mencacci NE, Krainc D, Hempel M, et al. Recessive mutations in VPS13D cause childhood onset movement disorders. Ann Neurol 2018; 83(6): 1089-95. Seong E, Insolera R, Dulovic M, Kamsteeg EJ, Trinh J, Bruggemann N, et al. Mutations in VPS13D lead to a new recessive ataxia with spasticity and mitochondrial defects. Ann Neurol 2018; 83(6): 1075-88.
WILSON'S DISEASE (*ATP7B*)	Brugieres P, Combes C, Ricolfi F, Degos J, Poirier J, Gaston A. Atypical MR presentation of Wilson disease: a possible consequence of paramagnetic effect of copper? Neuroradiology 1992; 34(3): 222-4. Hitoshi S, Iwata M, Yoshikawa K. Mid-brain pathology of Wilson's disease: MRI analysis of three cases. J Neurol Neurosurg Psychiatry 1991; 54(7): 624-6. Kim TJ, Kim IO, Kim WS, Cheon JE, Moon SG, Kwon JW, *et al.* MR imaging of the brain in Wilson disease of childhood: findings before and after treatment with clinical correlation. AJNR Am J Neuroradiol 2006; 27(6): 1373-8. King AD, Walshe JM, Kendall BE, Chinn RJ, Paley MN, Wilkinson ID, *et al.* Cranial MR imaging in Wilson's disease. AJR Am J Roentgenol 1996; 167(6): 1579-84. Magalhaes AC, Caramelli P, Menezes JR, Lo LS, Bacheschi LA, Barbosa ER, *et al.* Wilson's disease: MRI with clinical correlation. Neuroradiology 1994; 36(2): 97-100.

	Pulai S, Biswas A, Roy A, Guin DS, Pandit A, Gangopadhyay G, *et al.* Clinical features, MRI brain, and MRS abnormalities of drug-naive neurologic Wilson's disease. Neurol India 2014; 62(2): 153-8. Sener RN. The claustrum on MRI: normal anatomy, and the bright claustrum as a new sign in Wilson's disease. Pediatr Radiol 1993; 23(8): 594-6.
WOODHOUSE SAKATI SYNDROME (*DCAF17*)	Abusrair AH, Bohlega S, Al-Semari A, Al-Ajlan FS, Al-Ahmadi K, Mohamed B, *et al.* Brain MR Imaging Findings in Woodhouse-Sakati Syndrome. AJNR Am J Neuroradiol 2018; 39(12): 2256-62. Bohlega SA, Alkuraya FS. Woodhouse-Sakati Syndrome. 2016 Aug 4. In: Adam MP, Ardinger HH, Pagon RA, et al., editors. GeneReviews® [Internet]. Seattle (WA): University of Washington, Seattle; 1993-2020. Available from: https://www.ncbi.nlm.nih.gov/books/NBK378974/

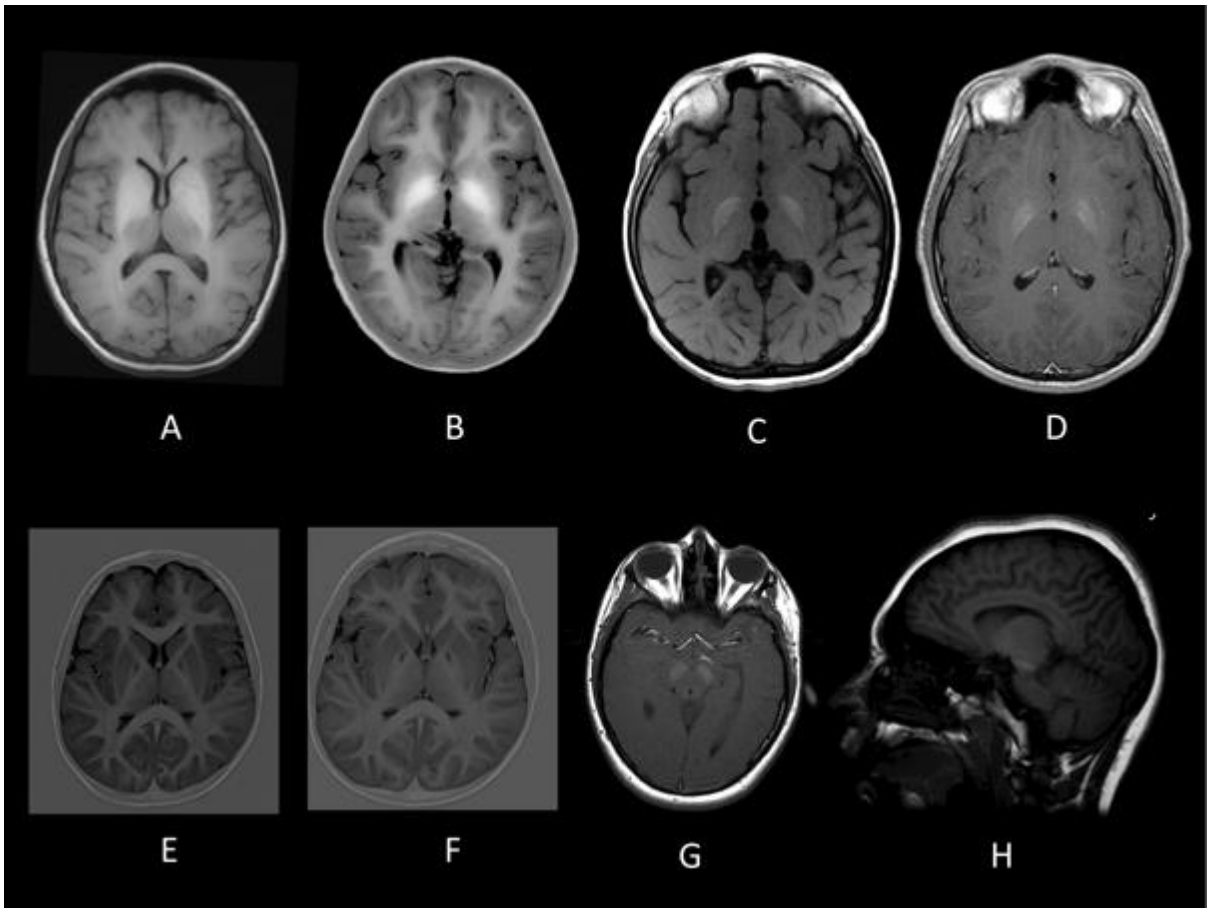

Supplementary figure 3. Axial (A-G) and sagittal (H) T1W MRI images of patients with bilateral basal ganglia MRI abnormalities to highlight the brighter signal change in disorders with genetic hypermanganesemia (A,B) compared to other disorders which are associated with brain iron accumulation or mimics. **A** – MRI of a 4-year-old boy with

hypermanganesemia associated with *SLC30A10* showing diffuse T1W hyperintensities in bilateral caudate, putamen and globus pallidus as well as diffuse but less intense T1W signal change diffusely in the white matter; **B** - MRI a 11-year-old girl with hypermanganesemia associated with *SLC39A14* showing T1W hyperintensities in bilateral globus pallidus as well as diffuse but less intense T1W signal change diffusely in the white matter; **C** – MRI of a 6-year-old girl with MPAN showing T1W hyperintensity in bilateral globus pallidus; **D** - MRI of a 2-year-old boy with fucosidosis showing T1W hyperintensity in bilateral globus pallidus; **E** – MRI of a 2-year-old girl with PKAN showing T1W hypointensity in bilateral ventral globus pallidus corresponding to T2W hyperintensity (the hyperintense part of the "eye of the tiger"); **F** – MRI of the same girl as in panel "E" at 5 years of age with specks of T1W hyperintensity in the centre of bilateral T1 hypointense regions in ventral globus pallidus; G and H – Axial (G) and Sagittal (H) MRI of a 5-year-old girl with BPAN showing T1W hyperintensity in bilateral substantia nigra

Abbreviations: MRI – Magnetic resonance imaging; T1W – T1-weighted; MPAN – Mitochondrial protein associated neurodegeneration; PKAN – Pantothenate kinase associated neurodegeneration; BPAN – Beta propeller protein associated neurodegeneration

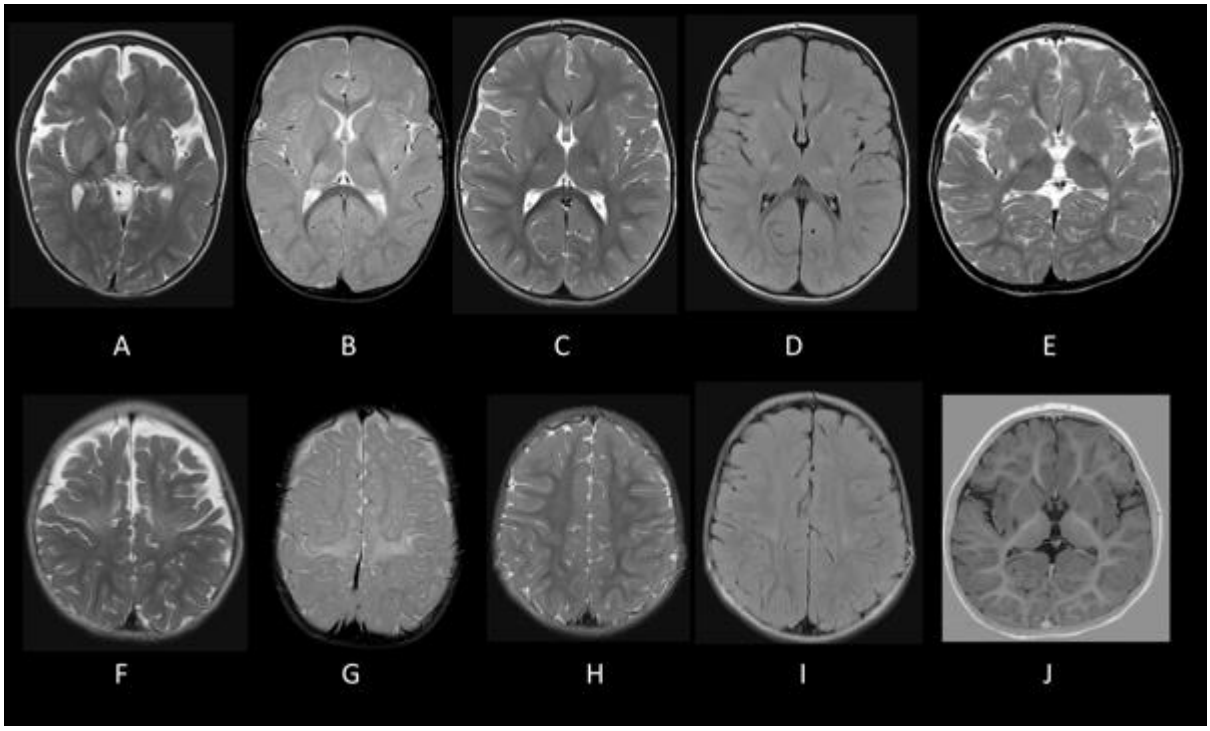

Supplementary figure 4. Axial (A-D, F-I) T2W, T2 FLAIR (Fluid attenuated inversion recovery) (E) and T1W (J) MRI images of children with cerebral palsy (CP) due to hypoxic ischaemic encephalopathy at term gestation. **A** – MRI at 3 years of age in a boy with CP showing T2W hyperintensity in bilateral putamina, corticospinal tracts in both internal capsules and ventrolateral thalami. Most of the putamina show signal change. There is also some frontal-temporal cortical atrophy; **B** – MRI of a 4 year old boy with CP showing T2W hyperintensity in bilateral dorsal putamina and ventrolateral thalami; **C** – MRI of a 3 year old girl with CP showing T2W hyperintensity in bilateral dorsal putamina and hyperintensity in ventrolateral thalami; **D** – MRI of the same patient as in panel "C" showing T2-FLAIR hyperintensity in bilateral dorsal putamina, corticospinal tracts in the internal capsurle and ventrolateral thalami; **E** – MRI of a 2 year old boy with CP showing prominent T2W hyperintensity in bilateral dorsal putamina and subtle hyperintensity in ventrolateral thalami; **F** – MRI of the same patient in panel "A" showing T2W hyperintensity in bilateral motor cortical regions as well as surrounding white matter and parasagittal white matter ; **G** – MRI of the same patient in panel "B" showing T2W hyperintensity in bilateral motor cortical

regions as well as surrounding white matter; **H** – MRI of the same patient in panel "C" showing very subtle T2W hyperintensity in bilateral motor cortical regions; **I** – MRI of the same patient in panel "D and H" with the subtle T2W hyperintensity now appearing clearing with parasagittal white matter hyperintensities ; **J** – T1W axial MRI image of the same patient in panel "E" showing hypointensities in the regions of the dorsal putamina corresponding to T2W hypointensity suggesting cystic degeneration.

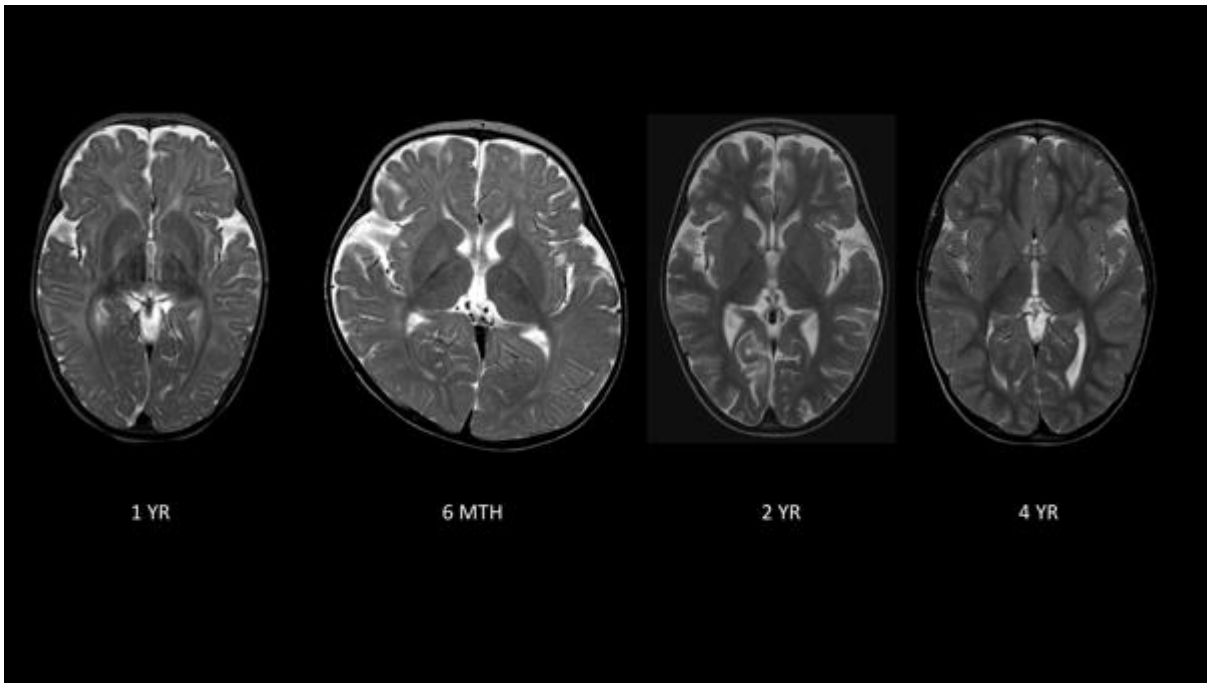

Supplementary figure 5. Axial T2W MRI images of children with kernicterus showing hyperintensities in bilateral globus pallidus at different ages (denoted below each image). The globus pallidus are normally more T2 hyperintense compared to the striatum in the first 2-3 years of life (on 1.5Tesla MRI scans). Distinguishing pathological hyperintensity may therefore be difficult as shown by the image at 2 years of age for the same patient whose pallidal hyperintensity was clearly prominent at 1 year of age (Ist image from left).

Supplementary table 7: Disorders reported with basal ganglia calcification*

PRIMARY FAMILIAL BASAL GANGLIA CALCIFICATION (FAHR'S DISEASE)
MYORG

PDGFB
PDGFRB
SLC20A2
XPR1
OTHER MONOGENIC DISORDERS REPORTED WITH BASAL GANGLIA CALCIFICATION
ADAR associated bilateral striatal necrosis
BETA PROPELLER PROTEIN ASSOCIATED NEURODEGENERATION (Gene: *WDR45*)#
CEREBRAL FOLATE DEFICIENCY (GENE: *FOLR1*)
CEREBRORETINAL MICROANGIOPATHY WITH CALCIFICATIONS AND CYSTS (GENES: *CTC1, STN1*)
COASY PROTEIN ASSOCIATED NEURODEGENERATION (Gene: *COASY*)
COCKAYNE SYNDROME (GENES: *ERCC6, ERCC8*)
COL4A1
DIHYDROPTERIDINE REDUCTASE DEFICIENCY (GENE: *QDPR*)
LIPOID PROTEINOSIS (GENE: *ECM1*)
RAB39B
PANTOTHENATE KINASE ASSOCIATION NEURODEGENERATION (Gene: *PANK2*)#
PETTIGREW SYNDROME (Gene: *AP1S2*)
POLYCYSTIC LIPOMEMBRANOUS OSTEODYSPLASIA WITH SCLEROSING LEUKOENCEPHALOPATHY (GENE: *TYROBP*)
SULFITE OXIDASE AND MOLYBDENUM COFACTOR DEFICIENCY
TRISOMY 21
VARIOUS MITOCHONDRIAL DISORDERS
OTHER DISORDERS THAT ARE REPORTED WITH (SECONDARY) BASAL GANGLIA CALCIFICATION
COELIAC DISEASE
INFECTIOUS SYNDROMES – BRUCELLOSIS, EPSTEIN BARR VIRUS, HUMAN IMMUNODEFICIENCY

VIRUS
LANGERHANS CELL HISTIOCYTOSIS
CARBON MONOXIDE AND LEAD POISONING
POST RADIATION AND POST CHEMOTHERAPY
SYSTEMIC DISORDERS OF CALCIUM AND PHOSPHATE METABOLISM HYPOPARATHYROIDISM, PSEUDOHYPOPARATHYROIDISM, PSEUDOPSEUDOHYPOPARATHYROIDSIM, HYPERPARATHYROIDISM, HYPOTHYROIDISM
SYSTEMIC LUPUS ERYTHEMATOSUS

** Calcification in the basal ganglia or other brain regions may sometimes, but not always appear as MRI signal change (T1W hyperintensity or hypointensity on T2W/susceptibility sensitive data sets) and may only be obvious on cranial CT scans.*

#DIsorders with brain iron accumulation where calcifications are also reported on ct scans in some patients

References for Supplementary table 7

Batla A, Bhatia KP. A new gene for Fahr's syndrome-PDGF-B. Movement disorders : official journal of the Movement Disorder Society 2014; 29(3): 307.

Donzuso G, Mostile G, Nicoletti A, Zappia M. Basal ganglia calcifications (Fahr's syndrome): related conditions and clinical features. Neurol Sci 2019; 40(11): 2251-63.

Dusi S, Valletta L, Haack TB, Tsuchiya Y, Venco P, Pasqualato S*, et al.* Exome sequence reveals mutations in CoA synthase as a cause of neurodegeneration with brain iron accumulation. American journal of human genetics 2014; 94(1): 11-22.

Giannandrea M, Bianchi V, Mignogna ML, Sirri A, Carrabino S, D'Elia E*, et al.* Mutations in the small GTPase gene RAB39B are responsible for X-linked mental retardation associated with autism, epilepsy, and macrocephaly. Am J Hum Genet 2010; 86(2): 185-95.

Giovannini D, Touhami J, Charnet P, Sitbon M, Battini JL. Inorganic phosphate export by the retrovirus receptor XPR1 in metazoans. Cell Rep 2013; 3(6): 1866-73.

Karin I, Borggraefe I, Catarino CB, Kuhm C, Hoertnagel K, Biskup S*, et al.* Folinic acid therapy in cerebral folate deficiency: marked improvement in an adult patient. Journal of neurology 2017; 264(3): 578-82.

Livingston JH, Stivaros S, van der Knaap MS, Crow YJ. Recognizable phenotypes associated with intracranial calcification. Dev Med Child Neurol 2013; 55(1): 46-57.

Nicolas G, Pottier C, Maltete D, Coutant S, Rovelet-Lecrux A, Legallic S*, et al.* Mutation of the PDGFRB gene as a cause of idiopathic basal ganglia calcification. Neurology 2013; 80(2): 181-7.

Sadana KS, Goraya JS. Intracranial Calcification in Down Syndrome. J Pediatr Neurosci 2018; 13(1): 120-1.

Shi CH, Zhang SY, Yang ZH, Yang J, Shang DD, Mao CY*, et al.* A novel RAB39B gene mutation in X-linked juvenile parkinsonism with basal ganglia calcification. Mov Disord 2016; 31(12): 1905-9.
Takashima S, Becker LE. Basal ganglia calcification in Down's syndrome. J Neurol Neurosurg Psychiatry 1985; 48(1): 61-4.

Teive HA, Pereira ER, Zavala JA, Lange MC, de Paola L, Raskin S*, et al.* Generalized dystonia and striatal calcifications with lipoid proteinosis. Neurology 2004; 63(11): 2168-9.

Tennison MB, Bouldin TW, Whaley RA. Mineralization of the basal ganglia detected by CT in Hallervorden-Spatz syndrome. Neurology 1988; 38(1): 154-5.

Tonduti D, Chiapparini L, Moroni I, Ardissone A, Zorzi G, Zibordi F*, et al.* Neurological Disorders Associated with Striatal Lesions: Classification and Diagnostic Approach. Curr Neurol Neurosci Rep 2016; 16(6): 54.

Wilson GR, Sim JC, McLean C, Giannandrea M, Galea CA, Riseley JR*, et al.* Mutations in RAB39B cause X-linked intellectual disability and early-onset Parkinson disease with alpha-synuclein pathology. Am J Hum Genet 2014; 95(6): 729-35.

Woody RC, Brewster MA, Glasier C. Progressive intracranial calcification in dihydropteridine reductase deficiency prior to folinic acid therapy. Neurology 1989; 39(5): 673-5.

Van Goethem G, Livingston JH, Warren D, Oojageer AJ, Rice GI, Crow YJ. Basal ganglia calcification in a patient with beta-propeller protein-associated neurodegeneration. Pediatr Neurol 2014; 51(6): 843-5.

Wang C, Li Y, Shi L, Ren J, Patti M, Wang T*, et al.* Mutations in SLC20A2 link familial idiopathic basal ganglia calcification with phosphate homeostasis. Nat Genet 2012; 44(3): 254-6.

Wong E, Dahl M. Basal ganglia calcification in idiopathic hypoparathyroidism. BCMJ 2013; 55(10): 462-5.

Basal ganglia MRI Study group:

Manoj P Menezes[1]

Sachin Gupta[1]

Christopher Troedson[1]

Sekhar Pillai[2]

Esther Tantsis[1]

Deepak Gill[1]

Carolyn Ellaway[3]

Simone Ardern Holmes[1]

Jayne Antony[1]

Kshitij Mankad[4]

Lucinda Carr[5]

Prab Prabhakar[5]

Pinki Munot[5]

Sanjay Bhate[5]

Paul Gissen[6]

Peter Clayton[6]

Karin Tuschl[6]

Louise Simmons[7]

Yanick Crow[8]

Troy Dalkeith[3]

Basal ganglia MRI Study group affiliations:

1. TY Nelson department of Neurology and Neurosurgery, the Children's Hospital at Westmead, Sydney, Australia
2. Department of Neurology, Sydney Children's hospital, Randwick, Sydney, Australia

3. Genetic Metabolic Disorders Service Sydney Children's Hospital Network, Sydney Australia, Disciplines of Genomic Medicine, and Child and Adolescent Health, Faculty of Medicine and Health, University of Sydney, New South Wales, Australia.
4. Department of Radiology, Great Ormond Street Hospital, London, UK
5. Department of Neurology, Great Ormond Street Hospital, London, UK
6. NIHR Great Ormond Street Hospital Biomedical Research Centre, London, UK.
7. Neurometabolic clinic, Birmingham Children's Hospital, Birmingham, UK
8. Centre for Genomic and Experimental Medicine, MRC Institute of Genetics and Molecular Medicine, University of Edinburgh, Edinburgh, UK.